Synthetic tools for optogenetic and chemogenetic inhibition of cellular signals

by

Stephanie Kainrath

April 2020

A thesis presented to the
Graduate School
of the
Institute of Science and Technology Austria, Klosterneuburg, Austria
in partial fulfillment of the requirements
for the degree of
Doctor of Philosophy

The dissertation of Stephanie Kainrath, titled Synthetic tools for optogenetic and chemogenetic manipulation of cellular signals, is approved by:

Supervisor:Harald Janovjak, IST Austria, Klosterneuburg, Austria

Signature: _____

Committee Member: Gaia Novarino, IST Austria, Klosterneuburg, Austria

Signature: _____

Committee Member: Martin Distel, St. Anna CCRI, Vienna, Austria

Signature: _____

Exam Chair:Johann Georg Danzl, IST Austria, Klosterneuburg, Austria

Signature: _____

signed page is on file

IST Austria Thesis, ISSN: 2663-337X

I hereby declare that this dissertation is my own work and that it does not contain other people's work without this being so stated; this thesis does not contain my previous work without this being stated, and the bibliography contains all the literature that I used in writing the dissertation.

I declare that this is a true copy of my thesis, including any final revisions, as approved by my thesis committee, and that this thesis has not been submitted for a higher degree to any other university or institution.

I certify that any republication of materials presented in this thesis has been approved by the relevant publishers and co-authors.

Signature: _____

Stephanie Kainrath

April 28, 2020

signed page is on file

Abstract

Proteins and their complex dynamic interactions regulate cellular mechanisms from sensing and transducing extracellular signals, to mediating genetic responses, and sustaining or changing cell morphology. To manipulate these protein-protein interactions (PPIs) that govern the behavior and fate of cells, synthetically constructed, genetically encoded tools provide the means to precisely target proteins of interest (POIs), and control their subcellular localization and activity *in vitro* and *in vivo*. Ideal synthetic tools react to an orthogonal cue, i.e. a trigger that does not activate any other endogenous process, thereby allowing manipulation of the POI alone.

In optogenetics, naturally occurring photosensory domain from plants, algae and bacteria are re-purposed and genetically fused to POIs. Illumination with light of a specific wavelength triggers a conformational change that can mediate PPIs, such as dimerization or oligomerization. By using light as a trigger, these tools can be activated with high spatial and temporal precision, on subcellular and millisecond scales. Chemogenetic tools consist of protein domains that recognize and bind small molecules. By genetic fusion to POIs, these domains can mediate PPIs upon addition of their specific ligands, which are often synthetically designed to provide highly specific interactions and exhibit good bioavailability.

Most optogenetic tools to mediate PPIs are based on well-studied photoreceptors responding to red, blue or near-UV light, leaving a striking gap in the green band of the visible light spectrum. Among both optogenetic and chemogenetic tools, there is an abundance of methods to induce PPIs, but tools to disrupt them require UV illumination, rely on covalent linkage and subsequent enzymatic cleavage or initially result in protein clustering of unknown stoichiometry.

This work describes how the recently structurally and photochemically characterized green-light responsive cobalamin-binding domains (CBDs) from bacterial transcription factors were re-purposed to function as a green-light responsive optogenetic tool. In contrast to previously engineered optogenetic tools, CBDs do not induce PPI, but rather confer a PPI already upon expression, which can be rapidly disrupted by illumination. This was employed to mimic inhibition of constitutive activity of a growth factor receptor, and successfully implement for cell signalling in mammalian cells and *in vivo* to rescue development in zebrafish. This work further describes the development and application of a chemically induced de-dimerizer (CDD) based on a recently identified and structurally described bacterial oxyreductase. CDD forms a dimer upon expression in absence of its cofactor, the flavin derivative F_{420}. Safety and of domain expression and ligand exposure are demonstrated *in vitro* and *in vivo* in zebrafish. The system is further applied to inhibit cell signalling output from a chimeric receptor upon F_{420} treatment.

CBDs and CDD expand the repertoire of synthetic tools by providing novel mechanisms of mediating PPIs, and by recognizing previously not utilized cues. In the future, they can readily be combined with existing synthetic tools to functionally manipulate PPIs *in vitro* and *in vivo.*

Acknowledgments

Back when I was in high school, I thought I might want to become a scientist. What started out as a vague idea, a desire to keep learning, discovering, challenging myself, eventually turned into a scientific career. And over the years, I sometimes had to stop for a moment and think back to those days, to realize that I am indeed exactly where I always wanted to be. Along with a feeling of accomplishment sometimes came a feeling of doubt, and the question of where to go from there. But that is the beauty of a scientist's trade: There are always questions to be answered, always new things to discover, and new skills to learn. Now, near the end of my PhD studies, I am thinking back to those days again, and how far I have come since being a child that collected caterpillars in the garden to raise them, since being an overly inquisitive high school student who pestered their biology teachers with questions, since being an undergrad, sometimes frustrated with their studies, but always motivated by that one desire – to keep learning. The past years of my life have been among the most exciting, most eventful and happiest, but certainly also most challenging. With this, I would like to say my thanks to the people who crucially contributed to me getting to this point.

To my supervisor Harald Janovjak, for his encouragement and support over the years, for his confidence in me and his support, the freedom to work independently while always being able to rely on his input, and providing me with opportunities to discover what I am passionate about and challenge myself to become a better scientist.

To Calin Guet and his group, for giving me a 'home away from home' when the Janovjak lab moved to Australia.

To my thesis committee member Martin Distel, for excellent collaborations, great scientific discussions, and support.

To the members of the Janovjak lab, past and present, for not just being great co-workers but also amazing friends. People say if you're passionate about your job it won't feel like work, but certainly the people you work with contribute to that feeling as well. Starting out in this lab as an undergrad, I always felt welcome and my input felt appreciated. Even on bad days, even when I felt like giving up, you were there to encourage me. You gave me confidence that I am in the right place and chose the right career path. Thank you.

To Eva, my sister in arms against reviewer #3 and the best Western Blot buddy, and Alex, the world's best housemate and the reason I didn't starve while living in Melbourne, for their unconditional support and friendship, and for helping me through tough times. I am endlessly happy to have found friends like you.

To my friends and colleagues at ARMI, who played a big role in making my year in Australia an exciting and fun experience. Special thanks to Mia and Renae, for being amazing friends and great festival company. You rock!

To my high school biology teachers, Susanne Tunner and Andrea Horvath, who encouraged me to ask questions and pursue my dream, even when others would get annoyed by my inquisitiveness.

To my grandmother, who taught me to see the beauty in all things and discover the world around me when I was a child, and who showed me that there's no shame it not always knowing the answer, as long as you have an idea where to look for it. To my parents, who supported me throughout all of this, encouraged me to pursue a career that makes me happy, and never pressured me to be something I am not. To my mother in particular, for giving me the freedom to choose my own path, but also being there for me when I got lost.

It has been an exciting few years, and as I reflect upon the way I have come and the road that still lies ahead, I am thankful for the support I have seen along the way, and excited about the challenges the future might hold.

About the Author

Stephanie Kainrath completed a Bachelor of Science in Medical and Pharmaceutical Engineering at the University of Applied Sciences IMC FH Krems in 2013, and joined IST Austria for a Master thesis internship in October 2014 while studying Molecular Medicine at the University of Vienna. In the group of Harald Janovjak, she worked on several projects to develop synthetic cell surface receptors.

In 2015 she joined the PhD program at IST Austria, and in January 2016 published the results of her research in *Angewandte Chemie International Edition.* In 2017 she received a DOC fellowship of the Austrian Academy of Sciences (ÖAW), became an associate member of the MolTag doctoral program finfanced by the Austrian Science Fund (FWF), and an associate member of the graduate program of EMBL Australia.

Throughout her studies, she has presented her work at various conferences, such as the ÖGMBT meeting in Graz, Austria, in 2016, the Fusion conference in Cancun in 2017, Mexico, and the GRC in Ventura, USA in 2018. From June 2018 to July 2019 she worked as a visiting scientist at the Australian Regenerative Medicine Institute in Melbourne, Australia, to continue her research on synthetic cell signalling.

List of Publications Appearing in Thesis

Kainrath S, Anotney J, Sturtzel C, Tailhades J, Cryle, M, Distel M, Jackson C, Janovjak H. A mycobacterial domain as a tool for chemically induced protein dissociation. (in preparation)

Kainrath S, Janovjak H. Optical control of receptor tyrosine kinases. *Methods in Molecular Biology* (accepted and soon to be published)

Kainrath S, Stadler M, Reichhart E, Distel M, Janovjak H. Green Light-Induced Inactivation of Receptor Signaling using Cobalamin-Binding Domains. *Angewandte Chemie International Edition*. 2017

Table of Contents

List of Figures

List of Tables

List of Abbreviations

AA	Amino acid
ABA	Abscisic acid
AbCID	Antibody-based chemically induced dimerization
AdoCbl	Adenosylcobalamin
AdoCbl	Adenosylcobalamin
Akt	Protein Kinase B (PKB)
AM	Acetoxymethyl
AP1510	Synthetic FKBP ligand
AP1903/AP20187	Synthetic FKBP ligands binding F36V mutant
AsLOV	LOV2 domain of phototropin of *A. sativa*
AtCRY2	Cryptochrome 2 of *A. thaliana*
ATP	Adenosine triphosphate
BD	Binding Domain
BG	O_6-benzylguanin
bisMTX	Homobifurcational MTX
BLUF	Blue light sensors using flavin adenine dinucleotide
BLUF	Blue Light Using FAD (domain)
BphP1	Bacterial phytochrome of *R. palustris*
BsYtvA	YtvA from *B. subtilis*
BV	Biliverdin IXα
CaMKIIα	Ca2+/calmodulin-dependent protein kinase Iiα
CarH	Bacterial repressor of caroteinoid synthesis operon
CarH	Chimeric antigen receptor
Cas9	CRISPR-associated protein 9
Casp9	Caspase 9
Casp9	Caspase 9
CBD	Cobalamin-binding domain
Cbl	Cobalamin
CCT/CCE	Cryptochrome C-terminus/CRY C-terminal extension
Cdc42	Cell division control protein 42 homolog
CIB1	Cryptochrome-interacting basic-helix-loop-helix
CIBN	Modified, minimal CIB1
CID	Chemically induced dimerization
CIP	Chemically induced proximity
CLICR	Clustering Indirectly Using CRY2
cm	Centimeter
CMV	Cytomegalovirus promoter
CMVtr	Truncated CMV
CoA	Coenzyme A
COP1	Constitutively photomorphogenic 1
Cph1	Cyanobacterial phytochrome of *Synechocystis* sp.
CPH1s	Codon optimized CPH1

Cre	Recombinase "causes recombination"
CREB	cAMP response element-binding protein
CRISPR	Endonuclease "clustered regularly interspaced short palindromic repeats"
CRY	Cryptochrome
CRY2phr	Modified, minimal CRY2
CRYolig	Modified, oligomerizing CRY2
CsA	Cyclosporin A
CT	C-terminus
CyP	Cyclophilin
Dab1	Disabled-1
DBD	DNA binding domain
dCas9	Catalytically inactive Cas9
DEX	Dexamethasone
DHFR	Dihydrofolate reductase
DMSO	Dimethyl sulfoxide
DNA	Deoxyribonucleic acid
DREADD	Designer Receptors Exclusively Activated by Designer Drugs
DTT	Dithiothreitol
ECD	Extracellular domain
EDTA	Ethylenediaminetetraacetic acid
EphB2	Ephrin type-B receptor 2
EtOH	Ethanol
ex/em	Excitation/emission
F_{420}	8-hydroxy-5-deazaflavin
FAD	Flavin adenine dinucleotide
Fas	FS-7-associated surface antigen
FDOR	Flavin/deazaflavin oxyreductase
FGFR1	Fibroblast Growth Factor Receptor 1
Firefly-AR	Firefly assay reagent
FK1012	Bivalent FK506 fusion
FK506	Tacrolimus
FKBP12	FK506-binding protein 12
F_M	FKBP F36M mutant
FMN	Flavin mononucleotide
FNR	plant ferredoxin-NADP+ reductase
FRB	FKBP12-rapamycin binding (domain)
FRP*	Modified FRB
GA	Gibberellin
GAF	cGMP phosphodiesterase/adenyl cyclase/Fhl1 domain)
GAI	Gibberellin insensitive
GEF	Guanine nucleotide exchange factor
GID1	Gibberellin insensitive dwarf1
GPCR	G-protein coupled receptors
GR	Glucocorticoid receptor

gRNA	Guide RNA
***GSK-3*β**	Glycogen synthase kinase-3 β
GyrB	DNA gyrase B subunit
h	Hour
HA	Haemagglutinin
hAGT	O_6-alkylguanine-DNA alkyltransferase
HaXS	HaloTag-SNAP-tag fusion
h-CTZ	h-Coelenterazine
HEK293	Human embryonal kidney cells
HTH	Helix-turn-helix
iCasp9	inducible Caspase 9
ICD	Intracellular domain
IgG	Immunoglobulin G
KD	Kinase domain
K_D	Equilibrium dissociation constant
K_i	Inhibitor constant
L	Liter
LACE	Light-activated CRISPR-Cas9 effector
LARIAT	Light-activated reversible inhibition by assembled trap
LED	Light emitting diode
LexA	Transcriptional repressor LexA
LITE	Light inducible transcriptional effectors
LitR	CarH homolog
LOV	Light-oxygen-voltage
loxP	DNA sequence recognized by Cre ("locus of crossing (x) over, P1")
LR	Luminescence ratio
LRP6	Low-density lipoprotein receptor-related protein 6
LSD	Light-sensing domain
LU	Luminescence units
m	Meter
m	Minute
MAPK	Mitogen activated protein kinase
mFGFR1	murine FGFR1
mg	Milligram
mL	Milliliter
mm	Millimeter
mM	Millimolar
MTHF	Methenyltetrahydrofolate
mTOR/FRAP	Mammalian target of rapamycin/FKBP12-rapamycin associated protein
MTX	Methotrexate
mV	mVenus
MxCarH	CarH of *M. xanthus*
MxCBD	CBD of MxCarH
myr	Myristoylation sequence

NADP+	Nicotinamide adenine dinucleotide phosphate
Ncap	NcVVD N-terminal cap
NcVVD	VIVID from *N. crassa*
NF-κB	nuclear factor 'kappa-light-chain-enhancer' of activated B-cells)
ng	Nanogram
nL	Nanoliter
nm	Nanometer
nM	Nanomolar
O/N	Overnight
p53	Phosphoprotein p53
PAS	PER-ARNT-SIM (domain)
PBS	Phosphate-buffered saline
PCB	phycocyanobilin
PDGFR	Platelet Derived Growth Factor Receptor
PDZ	PSD95-Dlg1-zo-1 (domain)
PEI	Polyethyleneimine
PHR	Photolyase Homology Region
Phy	Phytochromes
PHY	phytochrome specific PAS-related domain
PhyB	Phytochrome B
PI3K	Phosphatidylinositol 3 kinase
PIF	Phy-interacting factor
PIP_2	Phosphatidylinositol (4,5)-bisphosphate
PIP_3	Phosphatidylinositol (3,4,5)-trisphosphate
PLCγ	Phosphoinositide phospholipase Cγ
PLD	PAS-like domain
PLO	Poly-L-ornithine hydrobromide
POI	Protein of interest
PP2C	Protein phosphatase type 2C
PPI	Protein-protein interaction
pRap	Photocaged rapamycin
PTC124	Ataluren
PYR/PYL/RCAR	Pyrabactin resistance/PYR1-like/regulatory component of ABA receptor
PΦB	phytochromobilin
Rac1	"Ras-related C3 botulinum toxin substrate 1"
Raf	Serine/threonine-protein kinase ("Rapidly Accelerated Fibrosarcoma")
***Renilla*-AR**	*Renilla* assay reagent
RFU	Relative fluorescence units
RLU	Relative luminescence units
RNA	Ribonucleic acid
RsLOV	LOV domain from *R. sphaeroides*
RT	Room temperature
RTK	Receptor tyrosine kinase
s	Second

SDS	Sodium dodecyl sulfate
SH2	Src-homology 2 (domain)
SLF	Synthetic ligand of FKBP
Sos	Son of sevenless
sox32	Developmental gene "Sry-related HMG box 32"
Src	Proto-oncogene tyrosine-protein kinase Src
TALE	Transcription activator-like effector
tc	Tetracyclin
TCR	T-cell receptor
TetR	Tetracyclin repressor
Tiam	T-lymphoma invasion and metastasis-inducing protein-1
TMD	Transmembrane domain
TMP	Trimethoprim
Tris-Cl	Trizma hydrochloride
Trk	Tropomyosin kinase receptor
TrkC	Neurotrophin receptor tyrosine kinase C
Trp	Tryptophan
TtCarH	CarH of T. thermophilus
TtCBD	CBD of TtCarH
TULIP	Tunable light-inducible dimerization tags
Tyr	Tyrosine
UAS	Upstream activation sequence of Gal4
UV	Ultraviolet
UVR8	UV resistance locus 8
Vav2	Guanine nucleotide exchange factor VAV2
VfAU1-LOV	LOV domain from Aureochrome 1 of *V. frigida*
VP16	Herpes Simplex Virus VP16 transactivation domain
WASP	Wiskott-Aldrich Syndrome protein
Y3H	Yeast-three-hybrid
λ	Wavelength
µL	Microliter
µM	Micromolar
µW	Microwatt

Chapter 1: State of the art

1.1. Synthetic manipulation of protein-protein interactions

In all living systems, fundamental cellular processes are orchestrated by the collective action of proteins. Proteins can interact non-covalently in homomeric (between the same type of protein) or heteromeric (between different types of proteins) fashion, mediated via hydrophobic interactions, salt bridges and hydrogen bonds. Their interactions lead to assembly in complexes of dimers up to higher order oligomers, ultimately building complex molecular machines with distinct functions.

Through the formation of highly specific protein complexes at the right time and the right location within a cell protein-protein interactions (PPIs) are the core mechanism that regulates protein activity and function.[1] PPIs can be transient or stable. For example, the transient binding of extracellular ligands activates cell-surface receptors and triggers recruitment and activation of downstream signalling components that mediate cellular behavior and fate[2] and transient PPIs among transcription factors mediate DNA binding and gene expression.[3] The key initiator of apoptotic pathways, Caspase 9 (Casp9) is activated through homo-dimerization[4] while cell cycle checkpoint protein p53 requires assembly into a stable tetramer to bind DNA.[5] Cellular morphology also relies on PPIs. While the cytoskeleton is made up of a stable complex of interacting proteins, the dynamic reassembly of its components is necessary for motility[6] or for assembling the kinetochore complex pulling apart sister chromatids during cell division.[7]

One method to study such processes is through perturbation of one or more of the key components of interest. This can be achieved for example genetically through mutagenesis, or through chemical inhibition, and resulting changes in cell fate can be observed. However, to delineate the sequence and temporal dynamics in a complex series of events, such as a signalling cascade, often more precise means of manipulation are required. The need to manipulate PPIs and the molecular processes they control also arises in any system where growth or production rates shall be controlled, extending to applications for synthetic signalling circuits in biotechnology[8] and clinical applications, such as cell-based therapies and tissue engineering.[9,10]

Purely observational studies of protein function can be achieved through tagging, for example with a fluorescent protein that allows visualization of protein localization, or through short peptide tags that allow binding of small molecular dyes.[11,12] Chemical crosslinking can be employed to capture a ‘snapshot’ of interacting proteins, which can subsequently be analyzed through techniques such as affinity pulldown or mass spectrometry.[13] However, to achieve direct control over the function of a protein of interest (POI) synthetic tools can serve to manipulate protein-protein interactions. This can be either directly, through mediating the interaction of known binding partners or functional protein subunits, or through recruitment to or sequestering away from a site of action. In living systems, the use of genetically encoded tools to either visualize and track proteins, or dynamically and functionally influence their activity in order to understand and control their function, is collectively termed synthetic physiology.

PPIs are used by all domains of life, consequently protein domains mediating specific interactions in one organism can be harnessed as synthetic tools in other organisms. In general, synthetic tools are transgenes adapted from nature, often of bacterial or plant origin, and implemented in model systems ranging from single cells to vertebrates. An ideal synthetic tool must respond to an orthogonal cue, i.e. a trigger with minimal influence on any other endogenous process or component of the target organism. Distinguished by the nature of the trigger, two types of synthetic tools exist for the functional manipulation of PPIs, optogenetic and chemogenetic tools.

Optogenetic tools consists of light-sensing domains or photoreceptors, which can be fused to the POI. Illumination with a specific wavelength then triggers a conformational change in the photoreceptor, which induces or breaks protein interactions.[14] In chemogenetic tools, the conformational change is triggered by binding of a small molecule.[15] This chapter reviews the most common optogenetic and chemogenetic tools to manipulate intra-molecular PPIs.

1.2. Photoreceptors that manipulate PPIs

Light-sensing domains are abundant in nature and can absorb light of different wavelengths to trigger a conformational change, such as dimerization or oligomerization. In optogenetics, this characteristic is exploited by fusing a gene encoding a light-sensing domain to a target gene encoding a POI. Light can then be used as a highly precise cue to trigger conformational changes in the POI with spatial and temporal precision on a subcellular and millisecond scale.[16]

Light acts as an essential stimulus and energy source for all organisms. In microbes and plants, it regulates photo-induced movements and photomorphogenic responses, whereas in animals light mediates vision and entrainment of circadian rhythms.[17] Photoreceptor proteins have evolved in diverse biological systems to sense light over specific regions of the electromagnetic spectrum, including the ultraviolet, visible and near-infrared.[18] Photoreceptors that induce PPIs can be generally classified according to their light sensing moieties. Flavin-binding photoreceptors sense blue light through a riboflavin derivative and can be subdivided in cryptochromes, proteins containing light-oxygen-voltage (LOV) sensing domains, and blue light sensors using flavin adenine dinucleotide (BLUF).[19,20] Photoreceptors sensing green light using the vitamin B12 derivate AdoCbl (adenosylcobalamin) have been discovered in the past decade.[21,22] [23] Phytochromes sense red and far-red light using tetrapyrroles as their co-factor,[23] and UV light photoreceptors sense UV-B light through a cluster of tryptophan residues.[24]

Notably, the light-activated tools based on photoreceptors described here are complementary to existing optogenetic methods that rely on light-induced allosteric changes within a single protein, such as light-activated ion channels and pumps to hyper- and depolarize neurons,[25,26] regulate G-protein signalling[27] and light-responsive enzymes, e.g. the GTPase Rac[28] and adenylyl cyclases,[29] hence these will not be discussed here.

1.2.1. LOV domains

LOV (Light-Oxygen-Voltage) domains are small protein domains that bind flavin mononucleotide (FMN) or flavin adenine dinucleotide (FAD) as light-sensing cofactor and act as blue-light responsive photoreceptors in plants, bacteria and fungi.[30] First discovered in plants, LOV domains act as tandem sensory domains in phototropins to mediate rapid, light induced changes in phototropism, chloroplast and leaf movements and stomatal opening.[19] In the ZEITLUPE family of proteins they regulate slower light responses such as circadian clock entrainment and flowering.[31] while in aureochromes, they regulate morphogenesis.[32] LOV domains have also been found in fungi and bacteria, structurally and functionally regulating a variety of output domains.[30,33]

In the dark, LOV domains bind their flavin cofactor non-covalently. Blue light ($\lambda max \approx 450nm$) absorption results in the formation of a covalent adduct between the C4a carbon of the flavin chromophore and a conserved cysteine residue of LOV.[18] The domains revert back to their dark state by thermal decay of the C4a adduct, or alternatively by UV-light induced cleavage. Whereas LOV domains of plants exhibit adduct state lifetimes on the order of seconds, some bacterial and fungal LOV domains exhibit substantially extended lifetimes that range from hours to days.[34]

The structural changes upon photoexcitation depend on the individual LOV domain. Generally LOV domains adopt a canonical PER-ARNT-SIM (PAS) fold, with a C-terminal helix denoted Jα, packed against a β-scaffold core that binds the flavin cofactor. Upon illumination, the Jα helix unfolds to unblock an associated effector domain, such as the kinase in phototropin.[35-37] The LOV domain of YtvA from *B. subtilis* (BsYtvA) exists as a dimer, mediated by two Jα helices forming a coiled-coil and exposing the β-scaffold core. Illumination results in rotational movement between the helices in a 'scissor-like' fashion.[38] In VIVID from *N. crassa* (NcVVD), the N-terminal region is flanked by an additional α-helix and β-strand, referred to as Ncap, that docks against the core. Photoexcitation of NcVVD induces dimerization.[39] In auroechromes, both N-terminal A'α and C-terminal Jα helix are involved in mediating structural changes upon illumination. Structural rearrangements within the flavin binding core translate to undocking of both helices, which results in intra- or inter-protein dimer formation.[40,41]

Detailed studies of the photochemistry and structure of LOV domains have subsequently enabled mutations to alter lifetime kinetics of LOV domains and structural changes undergone upon illumination.[42] Combined with their abundance in nature across plants and fungi, their use of an endogenous cofactor and their small size, LOV domains make excellent optogenetic tools that have been employed for a variety of different applications.

Light-induced homodimerization of NcVVD has been harnessed to generate a light-induced gene expression system based on GAL4-UAS, termed LightOn. GAL4 is a dimeric transcriptional activator that specifically recognizes UAS (upstream activation sequence), originally from yeast. Removal of the GAL4 dimerizing domain and replacement with NcVVD gave rise to a light-regulated transcriptional activator.[43,44] The system has since been used to regulate expression of a variety of target genes, in particular to enable dynamic control over

transcription factors with oscillatory behavior. For example, LightOn was used to control activity of AscI1, a transcription factor involved in neuronal fate determination,[45] and to tune dynamic expression of components of Notch signalling.[46,47] In combination with a chemically induced transcriptional activation system based on TetR, induced by its ligand tetracyclin (tc), LightOn was used for combinatorial, dual-input synthetic transcription regulation in mammalian cells and in mice.[48,49] Gene expression has also successfully been manipulated with a fusion of NcVVD to LexA of E.coli, termed LEVI. LexA is a transcriptional repressor, therefore illumination and dimerization of the NcVVD domain results in DNA binding and repression of a target gene. Since the system works inverse to LightOn it is referred to as LightOff.[50]

Mutations of the dimerization interface of NcVVD has further led to the development of a selectively hetero-dimerizing pair of photoswitches termed Magnets.[51] The system has successfully been employed for a variety of purposes, from control of gene expression in *E. coli*[52] to control of heterotrimeric G protein signalling,[53] to light induced-reconstitution of split proteins, giving rise to optogenetic Cre-loxP[54] and CRISPR-Cas9 systems.[55] Recently, Magnets were used to regulate viral polymerases and control proliferation of oncolytic viruses *in vitro* and *in vivo*.[56]

In contrast to the above mentioned LOV domains, LOV2 domain of phototropin 1 of *Avena sativa* (AsLOV) does not undergo dimerization but Jα helix unfolding. This has been employed as the key mechanism in the TULIP (tunable light-inducible dimerization tags) system, where an engineered cognate PDZ domain can only interact upon illumination, effectively creating a hetero-dimerization tool.[57]

The LOV domain from *Rhodobacter sphaeroides* (RsLOV) has been suggested to exist as a dimer in the dark that dissociates upon illumination.[58] This property was exploited in a screen of domain-insertions in dCas9, a catalytically inactive variant of the endonuclease Cas9 that can be used as RNA-guided DNA-binding protein, and can be employed to recruit transcriptional repressors or activators. While only moderate control over transcriptional activity could be achieved by illumination, the study revealed temperature-sensitive behavior of RsLOV.[59]

EL222 is a bacterial transcription factor employing a photosensory LOV domain and helix-turn-helix (HTH) motif for DNA binding. In the dark, LOV occludes the HTH domain, and prevents dimerization and DNA binding. By fusion of different transactivation domains, EL222 has been employed to control transcription in mammalian cells[60] and in zebrafish for tight spatial and temporal control of developmental sox32 and Nodal genes, as well as CRISPR/Cas9 activity.[61]

An algal LOV domain from aureochrome 1 of *Vaucheria frigida* (VfAU1-LOV) has been identified in a screen as a mediator of homo-dimerization, and successfully been employed as a tool for light induced signalling of fused receptor tyrosine kinases (RTKs). In this approach, VfAU1-LOV was fused C-terminally to a kinase domain with N-terminal membrane anchor instead of the endogenous ligand binding domain, creating a receptor that uniquely responds to light instead of its cognate ligand. Interestingly, not all LOV domains screened were capable of mimicking active signalling states with high induction and low background signals,

compared to a chemically induced receptor, indicating that the lifetime of the photoexcited state has to be comparable to the lifetime of the endogenous ligand-receptor complex.[62] VfAU1-LOV was subsequently also used to induce dimerization between Nodal receptors in Zebrafish and elucidate the role of this signalling pathway in cell fate speciation during gastrulation.[63] This highlights the usefulness of expanding the optogenetic toolbox to include various domains with different kinetics and modes of interaction.

Other LOV domains that do not form homo-or heterodimers but undergo intra-protein conformational changes have also found variety of applications. For example, BsYtva was employed for light-regulation of gene expression via a fused histidine kinase[64,65] or TetR domain.[66]

1.2.2. Cryptochromes

Cryptochromes (CRY) are photoreceptors that sense blue light ($\lambda_{max} \approx 450$ nm) via a bound flavin cofactor. Although first identified in *Arabidopsis thaliana* mutant screens as regulators of flowering in response to day-length[67] they have since been found responsible for the entrainment of the circadian clock in plants and animals. Among animal CRYs, there are two functionally distinct types. Type I CRYs act as circadian photoreceptors in Drosophila and other insects. Type II CRYs are light-irresponsive, and serve as transcriptional repressors in mouse, human and other vertebrates. Some animals, such as zebrafish and monarch butterflies, possess both.[68] CRY2 from *Arabidopsis thaliana* (AtCRY2) is the best studied CRY to date.[69,70] Endogenously, it interacts with ubiquitin ligase COP1 (constitutively photomorphogenic 1),[71] transcriptional regulator CIB1 (cryptochrome-interacting basic-helix-loop-helix)[72] and has also been shown to interact with the photoreceptor PhyB (Phytochrome B)[73] upon blue illumination.

Structurally, AtCRY2 contains a characteristic PHR (Photolyase Homology Region) domain of about 500 AA, which is implicated in light sensing, and a distinctive cryptochrome C-terminus (CCT or CCE, for CRY C-terminal extension) which is implicated for its signalling function.[71,74] CRYs bind two chromophores: FAD and the pterin derivative 5,10-methenyltetrahydrofolate (MTHF). FAD is bound non-covalently to the PHR and functions as the primary light sensor, whereas MTHF is proposed to harvest and transfer additional light energy to the FAD chromophore from the near-UV region (370-390nm).[75]

The PHR domain and the CCT are proposed to form a closed or inactive conformation in darkness. Blue light sensing by the PHR domain would then trigger a conformational change in the CCT to produce an open or active conformation that initiates signalling. However, studies suggest that a contributing factor might involve the ability of cryptochrome to bind ATP (adenosine triphosphate). ATP binds close to the flavin cofactor at the PHR domain and ATP binding is reported to both increase the yield and prolong the lifetime of the signalling state.[76,77]

Many optogenetic applications of CRY rely on its well-studied hetero-interaction with endogenous binding partner CIB1. Early work employed CRY2 and CIB1 to reconstitute a split Cre recombinase and Gal4 transcriptional activator, and allowed precise control over protein

expression levels in a light-dose dependent fashion.[78] Later, an approach employing split Cre recombinase fused to CRY2/CIBN (see below) achieved light-control of cell differentiation and tissue development *in vivo* in mice[79] CRY2/CIB1 was also used to reconstitute split Gal4 and LexA for transcriptional control in yeast,[80] zebrafish[81] and *Drosophila*.[82]

A second generation hetero-dimerizer system uses only minimal components of CRY2 and CIB1, effectively reducing the size of these tools, as well as photocycle mutants to achieve longer or shorter complex lifetimes. Variants of this system, often generally referred to as CRY2phr and CIBN, have been shown to provide tight control over activity when employed to reconstitute split Gal4, LexA-VP16 and a Cre recombinase.[83]

The LITE (Light inducible transcriptional effectors) system was generated as an optogenetic two-hybrid system based on TALEs (transcription activator-like effectors), a group of versatile DNA binding domains. Upon illumination, a fusion of CIB1 to a desired effector domain, such as a transcription factor or histone modifier, is recruited to a DNA-bound TALE-CRY2 fusion.[84] In the LACE system (light-activated CRISPR-Cas9 effector) a CIBN-dCas9 fusion was used for light-induced recruitment of transcriptional activators fused to CRY2. Notably, since dCas9 can be combined with different gRNA (guide RNA) sequences, the system provides easily adaptable control over a variety of target genes.[85]

A particularly interesting application of optogenetics is direct light-control of cellular signalling events. The dynamics of complex signalling cascades and interplay of different pathway components can often only be delineated and understood by spatially and temporally precise manipulation. In several of these applications, one component, usually CIB1/CIBN, is anchored to a membrane to allow light-induced recruitment of an effector to a target site via CRY2. Photo-activated Akt (also known as PKB, Protein Kinase B) was generated by fusing Akt to CRY2phr and membrane-anchoring CIBN. Illumination causes translocation of Akt-CRY2 to the membrane where Akt is activated and subsequently induces downstream MAPK/ERK (mitogen activated protein kinase/ extracellular signal-regulated kinase) signalling.[86]

The spatial precision of light application was also exploited to locally and dynamically induce lipid signalling directly at the membrane. A phosphatase controlling PIP_2 (phosphatidylinositol (4,5)-bisphosphate) and PIP_3 (phosphatidylinositol (3,4,5)-trisphosphate), or PI3K (phosphatidylinositol 3 kinase) was fused to CRY2 for local recruitment to membrane-tagged CIBN upon illumination, to rapidly control membrane ruffling and dissect the temporal kinetics of phosphatidylinositol signalling.[87] In a similar approach, light—activated recruitment of PI3K was used to specifically and locally induce PIP_3 production in neurite outgrowths, which was found to be sufficient to trigger filopodia and lamellipodia formation.[88] With CIBN anchored to the cell membrane, soluble CRY2 fused to Raf1, a serine/threonine protein kinase, was also used to activate MAPK/ERK signalling and was employed to stimulate neurite outgrowth in PC12 cells.[89] The spatial precision of light application was also exploited to elucidate dynamics of cell contractility in developing *Drosophila* larvae by locally manipulating PIP_2 levels in live embryos during mesoderm invagination.[90]

CRY2 has been shown to form photobodies upon illumination in plants[69,74] and this propensity to oligomerize has been harnessed for light-induced clustering of target proteins. Through a fusion of LRP6 (Low-density lipoprotein receptor-related protein 6) to CRY2, the β-catenin pathway was put under light-control. Rac1 GTPase activity was also activated by forced oligomerization.[91]

The propensity for homo- or hetero-interactions of CRY2 depend on the fusion proteins and presence in a restricted 2D environment, such as the membrane, or freely diffusing in the cytosol.[92] In one approach, CRY2 was fused to Trk (Tropomyosin kinase) receptor and light induced activation of MAPK signalling. This approach did not require the use of a CIB-fused interaction partner, as membrane anchored CRY2 was found to homo-interact upon illumination.[93] Similarly, CRY2 fused to FGFR1 (Fibroblast Growth Factor Receptor 1) allowed light-induction of MAPK signalling purely through homo-interaction of CRY2.[94] Fusion of CRY2 to TrkC (neurotrophin receptor tyrosine kinase C) critically contributed to revealing the temporal dynamics of TrkC signalling, where stimulation at lower light powers lead to MAPK/ERK and Akt signalling, while higher power leads to activation of PLCγ (Phosphoinositide phospholipase Cγ) and CREB (cAMP response element-binding protein) signalling.[95]

Homo-oligomerization of a CRY2-Raf fusion activated downstream signalling events, while hetero-dimerization of two isoforms of Raf fused to CRY2 and CIBN respectively led to the finding that a kinase-dead form of Raf can act as a scaffold and still enhance signalling despite lacking kinase activity.[96] Homo-oligomerization of CRY2 alone was also harnessed to design CLICR (Clustering Indirectly Using CRY2). In this system, soluble CRY2 is equipped with a binding domain (BD) of interest, recognizing a cognate, membrane-localized protein such as a transmembrane receptor. Upon illumination, clusters of CRY2 form that present several BDs. Recruitment to the membrane via the cognate binding partners then induces clustering of the receptors as well and inducing signal activation. This approach was employed to activate endogenous FGFR1 and PDGFR (Platelet Derived Growth Factor Receptor) via SH2 (Src-homology 2) domains which act as adaptor proteins for downstream signaling components. Clustering of SH2-CRY2 fusions activated signaling without a necessity to introduce transgenic variants of the receptors themselves.[97]

In the LARIAT (Light-Activated Reversible Inhibition by Assembled Trap) system, oligomerization of CRY is exploited for light-induction of protein clusters to trap and inactivate target proteins. The native oligomerization domain of CaMKIIα (Ca^{2+}/calmodulin-dependent protein kinase Iiα) was replaced with CIB1 and co-expressed with CRY2. Upon illumination, CRY2 oligomerizes and binds CIB1, thereby causing formation of CaMKIIα oligomers. By anchoring CRY2 to the membrane, a fusion of CIB1 to Vav2, an activator of Rho GTPases. Illumination induced trapping of Vav2-CIB1 in clusters and allowed local disruption of lamellipodia formation.[98]

The initial property of CRY2 to oligomerize in solution is further enhanced in a mutant termed CRYolig. This variant of CRY2 assembles into higher order oligomers, that were used for light-induced disruption of clathrin-mediated endocytosis and actin polymerization.[99] CRYolig has since been used in a number of further studies, for example to induce assembly of an

oligomeric $Ca2^+$ membrane channel,[100] in a modified LARIAT system to disrupt mitosis and cell polarity in *Drosophila* larvae[101] and for the assembly of enzyme clusters to create compartmentalized, synthetic organelles.[102] Local light-induction of a Dab1, a key regulator of synaptic plasticity, via CRYolig was used to mimic clustering by its cognate interaction partner Reelin, circumventing previous limitations of chemical- and expression based approraches.[103] CRYolig has also successfully been applied *in vivo* in pyramidal neurons of mice, to show that EphB2, a regulator of synaptic transmission, can enhance fear-conditioning memory formation.[104] These applications highlight the importance of optogenetic tools for applications where spatial and temporal precision of activation is indispensable to elucidate the effect of a cellular process.

The abundance and diversity of optogenetic experiments designed based on CRY2/CIB(N) is a testament to the versatility of this tool. Notably, the two different modes of CRY2 interactions – homo-oligomerization or hetero-dimerization with CIBN – and the implementation in a membrane-bound or soluble fashion make it a versatile tool for a variety of interactions and applications.

1.2.3. Phytochromes

Phytochromes (Phy) are photoreceptors and generally mediate organismal responses to light in the environment. Originally discovered in plants, where they act in concert with phototropins and cryptochromes to mediate photomorphogenesis and entrainment of the circadian clock, they are also found in cyanobacteria, proteobacteria and fungi.[23,105] Phys act as red/far-red light sensors via the linear tetrapyrrole chromophore phytochromobilin (PΦB) in plants, phycocyanobilin (PCB) in cyanobacteria and biliverdin IXα (BV) in eubacteria and fungi.[106]

Structurally, phytochromes act as homodimers of two 120kDa protomers, comprising an N-terminal photosensory and cofactor-binding domain consisting of PLD (PAS-like domain), GAF (cGMP phosphodiesterase/adenyl cyclase/FhlI domain) and PHY (phytochrome specific PAS-related domain), and C-terminal regulatory domain, usually with histidine kinase activity.[106] Endogenously, plant phytochromes interact with transcription factors, such as COP1 and PIFs (Phy-interacting factors).[107]

The photocycle of Phys is reversible, with red-light ($\lambda \approx 670$ nm) absorption converting Phy from its P_r state to a far-red ($\lambda \approx 730$ nm) absorbing state P_{fr}.[108] Generally, photon absorption results in cis-to-trans isomerization within the chromophore, leading to reorientation of the PHY domain and altering the hairpin contact between PHY and GAF, which results in structural changes along the dimerization surface.[106,109]

One of the first described optogenetic tools making use of light-induced PPIs employs PhyB and PIF6 of *Arabidosis thaliana*. The Gal4 DNA binding domain (DBD) and Gal4 activating domain fused to PhyB and PIF respectively were used for optogenetic control of transcription in *S. cervisiae*. Notably, while the process was inducible by red light it was also rapidly reversible by far red illumination to interrupt transcription. Furthermore, a dose-response effect depending of light intensity was demonstrated.[110]

Hetero-dimerization between PhyB and PIF has since been used in a vast number of further applications. A light-induced conditional protein splicing system was generated from fusion of PhyB and PIF3 to a split intein, a protein domain that undergoes autocatalytic excision and fusion of flanking polypeptides.[111] In *E. coli*, GTPase Cdc42 fused to PhyB was employed for light induced interaction with effector WASP (Wiskott-Aldrich Syndrome protein) fused to PIF3, to control actin assembly.[112] Light-dependent trapping of biomolecules from biomaterials has recently been achieved by fusing a short PIF-based tag sequence to a target molecule, and equipping PhyB with a biotinylation motiv, which allows immobilization on an agarose-polymer.[113]

Fused to the TetR repressor domain for DNA targeting and Herpes Simplex Virus VP16 transactivation domain the system was used to induce gene expression in mammalian cell layers with spatial precision.[114] This approach was also successfully employed to regulate gene expression in Tobacco protoplasts and moss. Since plants need light to grow, optogenetic approaches to control plant signals are challenging to implement, as white light exposure would continuously activate the target process. However, due to the far-red reversion, the PhyB-PIF system can be kept in an 'off' state by supplementation with far-red light.[115]

In a number of approaches, mammalian cell signalling was regulated using PhyB/PIF. Rho-family GTPases Rac1, Cdc42 and RhoA were controlled by fusion of the GEF (guanine nucleotide exchange factors) Tiam to PhyB and upon illumination recruited to membrane-bound PIF6, and allowed local and rapidly reversible manipulation of cell morphology.[116]

In the Opto-SOS system, PhyB is anchored to the membrane, and PIF6 fused to SOS which is an activator of the MAPK/ERK pathway. Notably, the fast reversion by far red light allows dynamic and temporally highly precise control over signalling activity and has revealed intensity and frequency gating of downstream signalling pathways.[117] PI3K activity was regulated similarly by modulating protein localization with PhyB-PIF.[118]

The previously herein reviewed optogenetic applications of blue-light sensing cryptochromes all relied on CRY2 of *A. thaliana*. Interestingly, PhyB has been found to interact with CRY1 to form dark promoted complexes that can be disrupted by stimulation of either PhyB with red, or CRY1 with blue light. PhyB-CRY1 has been successfully employed to regulate transcription in yeast.[119] while the endogenous function of this interaction remains to be elucidated.[120]

An engineered binding partner for bacterial phytochrome BphP1 was used for red-light controlled transcription regulation and chromatin modification. Notably, due to the red-light sensitivity of BphP1 with minimal overlap to blue wavelengths, this system could be implemented for spectral multiplexing experiments in combination with a LOV-domain based system for tri-directional protein targeting.[121]

The cyanobacterial Phytochrome Cph1 from *Synechocystis* sp. has been shown to undergo homo-dimerization.[122] Naturally Cph1 is a light sensing histidine kinase, and its sensory domain was fused with various enzymes to regulate their activity, e.g. bacterial histidine kinase,[123] phosphodiesterase,[124] and adenylate cyclase.[125]

The characteristic of Cph1 to form homo-dimers was further exploited to generate optogenetic RTKs that undergo dimerization upon red illumination. Notably, due to the spectral distance to commonly available fluorescent proteins, this allowed the implementation of a dual fluorescent reporter system with minimal excitation and emission overlap. Furthermore, red light penetration through tissue allowed *ex vivo* transdermal activation of these receptors up to 10mm depth.[126]

One drawback of the PhyB-PIF system is that PCB and PΦB are orthogonal molecules not found in animals, hence the cofactor has to be supplemented in applications in animal systems. One approach to circumvent this is to implement a transgenic biosynthesis pathway. In mammalian cells, the expression of bacterial and plant ferredoxin-NADP+ reductases (FNR) allowed intracellular synthesis of sufficient PCB from the endogenous precursor heme to operate PhyB-PIF.[127]

1.2.4. Adenosylcobalamin-binding photoreceptors

Recently, a new class of bacterial photoreceptor that employs adenosylcobalamin (AdoCbl), a vitamin B12 derivative, as light-sensing chromophore has been characterized.[128,129] AdoCbl was originally implicated in radical-based enzyme reactions,[130] and the novel function of AdoCbl as light sensor critically expands the list of known chromophores. In the LitR/CarH photoreceptor family, light causes the photolysis of the cofactor and this reaction mediates light-dependent gene expression.[22,131] Homologs of LitR/CarH exist widely in non-phototrophic bacteria , but the best characterized photoreceptors are from *Myxococcus xanthus* (MxCarH) and *Thermus thermophilus* (TtCarH).[22,131,132] In these organisms, CarH controls the light-induced expression of carotenoids, which are used as a defense mechanism against photo-oxidative damage.

The structure of dark state CarH is a dimer-of-dimers type tetramer. Each monomer of CarH has a modular structure with one N-terminal DNA binding domain followed by a C-terminal light-sensing domain (cobalamin-binding domain or CBD). In the tetramer, the four light-sensing domains together form a central core and the DNA-binding domains are displayed on the surface. Two light-sensing domains assemble in a dimer in a head-to-tail orientation and two such head-to-tail dimers form the tetramer. Notably, wild-type CarH lacking the DNA-binding domain is still capable of tetramer formation. Upon ultraviolet, blue or green illumination, the photosensitive Co-C bond of AdoCbl is disrupted, which leads to disassembly into monomers.[21,128]

CBDs have been harnessed to engineer green-light responsive optogenetic tools in mammalian and plant cell lines as well as zebrafish. Through fusion of CBD to the kinase domain of a receptor tyrosine kinase, which is activated by dimerization, downstream signalling was activated in the dark, and disrupted upon green illumination. This green-light responsive receptor has been employed to mimic a constitutively active signal leading to developmental defects in zebrafish embryos, which was conditionally rescued by light.[133] This work will be discussed in greater detail in Chapter 3 of this thesis.

CBDs also present a suitable tool for optogenetic applications in plants due to their green-wavelength sensitivity, which avoids cross-talk to endogenous plant photoreceptors. The CBD of CarH and the cognate DNA operator sequence CarO from *T. termophilus* have been successfully employed to engineer a light-sensitive transcription system that is functional in mammalian cell lines and Arabidopsis protoplasts. A key challenge of this approach is the delivery of the AdoCbl cofactor, as Vitamin B12 is not endogenous to plants. While the cofactor was readily taken up by cultured protoplasts, this could potentially be a limiting factor for applications in whole plants.[134]

The particular photochemistry of AdoCbl cleavage upon photoexcitation does not produce a 5'-dAdo radical but instead a 4',5'-anhydroadenosine, thereby limiting cytotoxic effects upon illumination.[129] This feature was exploited for another application, where an AdoCbl dependent, light responsive hydrogel was engineered by stitching together CBDs into polymeric protein complexes via SpyTag-SpyCatcher peptide linking. The material was successfully used to encapsulate fibroblasts and mesenchymal stem cells. which causes the gel to liquify and encapsulated material to be released.[135]

1.2.5. Others

BLUF (Blue Light Using FAD) domains are small (100-140 AA) protein domains containing a flavin chromophore and undergo their photocycle upon blue or UV-A illumination.[19,136] They are widely used in bacteria to mediate photosynthetic gene expression (AppA in *Rhodobacter sphaeroides*[137]), phototaxis and general mobility (PixD of *Synechocystis*,[138] BlsA of *A. baumannii*[139] and PAC of *E. gracilis*[140]) and biofilm formation (Bluf/YcgF in *E. coli*[141] and PapB in *R. plaustris*[142]).

A rapid characteristic 10 nm red shift within nanoseconds upon photoexcitation is common to BLUF domains, while their reversion kinetics to the dark state vary from a few seconds to several minutes,[143,144] physiologically reflecting their differential roles as low or high light intensity sensors. The photocycle is best characterized in AppA. Generally, photon absorption involves conserved Tyr or Trp residues in the flavin pocket and rearrangement of H-bonds that translate to structural changes in the C-terminal helices of the protein, which affect interaction of BLUF domains and their effectors.[145]

PixD has been employed as an optogenetic tool to regulate transcription by controlled aggregation of a dominant-negative transcription factor. PixD forms a complex with PixE and serves as a light intensity sensor for phototaxis.[146] The crystal structure of PixD shows assembly of a decameric complex consisting of two stacked pentameric rings, with two monomers of PixE binding on each face.[147] Light excitation dissociates the complex into PixD monomers and dimers.[148] A fusion of a dominant negative mutant Ntl transcription factor to the PixD-binding portion of PixE resulted in PixD/PixE-Ntl complex formation in the dark, inhibiting repressor activity of Ntl until illumination dissociates the complex.[143]

UV-light sensing photoreceptor UVR8 (UV resistance locus 8) differs from other known photoreceptors due to the striking absence of a prosthetic chromophore to absorb light. Instead, a group of specific Trp residues are employed for photoreception.[19,149]

The prototypical UVR8 from *Arabidopsis thaliana* has been extensively characterized structurally and photochemically. In *Arabidopsis*, it mediates the production of proteins for DNA repair[150] and UV-absorbing phenolic compounds that act as "sun-screen".[151] Beside stress responses, UVR8 regulates photomorphogenic and phototropic mechanisms, and circadian clock entrainment.[24]

In the dark state, UVR8 forms a dimer of two donut-shaped protomers, stacked face-to-face. In the dimer interface, three Trp residues are positioned close together forming the so-called "triad", and there are two such triads per dimer forming a "pyramid" with one Trp of the opposing monomer. *In vivo* and *in vitro* mutational studies in combination with far-UV circular dichroism and florescence spectroscopy showed that Trp285 and Trp233 act as the principal UV-B chromophore of UVR8.[19,149,152-154] From functional experiments it is known that the C-terminal domain is important for interaction with its endogenous binding partner COP1 (constitutively morphogenetic 1). UV-B illumination results in dimer dissociation, allowing subsequent interaction with COP1.[155]

The independence of a cofactor and the assembly of a dimer in the dark that can be disrupted upon illumination makes UVR8 an interesting potential synthetic tool, but the short wavelength of activation light in the UV range poses a risk of phototoxicity and limits its applications to date. In one case, UVR8-COP1 has been employed as an optogenetic tool in mammalian U2OS cells by fusion of the transcription activation domain (AD) of NF-κB to UVR8 and the DNA-binding domain of GAL4 to COP1. The dimeric UVR8-complex is localized to the cytoplasm until illumination breaks it into monomers. UVR8 can interact with DNA-bound COP1 and translocate to the nucleus where the NF-κB AD can induce transcription of a target gene. However, even upon illumination by short pulses of UV-B light DNA damage responses were detectable.[156]

UVR8 has also been employed to generate a light-induced secretion system. In this approach, UVR8 dimerization in the dark causes retention of a fused protein in the endoplasmic reticulum, until illumination triggers trafficking and secretion to the plasma membrane of neuronal cells, with a minor decrease in cell viability observed upon several seconds of illumination with UV-B light.[157]

1.3. Chemogenetics tools to manipulate PPIs

Chemogenetics generally refers to applications of small, engineered molecules binding to genetically encoded protein domains or peptide sequences. Similar to optogenetics, chemogenetic approaches have been extensively used to orthogonally regulate molecular processes *in vitro* and *in vivo* to observe and manipulate cell behavior.[15]

Compared to light, the use of a chemical trigger has reduced temporal and spatial precision due to diffusion and association/dissociation kinetics, but facilitates sustained and systemic

manipulation of processes. Additionally, chemogenetics do not require the use of any kind of illumination hardware. Light delivery into deeper tissue can prove challenging, and as such diffusing molecules can be of particular interest for applications in larger organisms, thereby providing potential for clinical applications in humans.[158]

Chemogenetic methods have found broad application in neuroscience, where genetically engineered GPCRs (G-protein coupled receptors), commonly called DREADDs (Designer Receptors Exclusively Activated by Designer Drugs) are paired with designer molecules for targeted manipulation of neuronal activity.[159,160] Together with tools for dynamic tracking (e.g. small fluorescent dyes that recognize an engineered peptide 'tag'[161] and obtaining static 'snapshots' of interacting protein complexes (e.g. chemical cross-linking[13]), they provide important means to understand cellular processes and events. Artificial assemblies of protein scaffolds with catalytically active molecules to generate so-called semi-synthetic enzymes can be considered another, application-driven avenue of chemogenetics.[162]

Complementary to these methods, several chemogenetic tools are specifically designed for functional mediation by mediate PPIs between two or more POIs through chemically induced dimerization (CID) or more generally, chemically induced proximity (CIP).[163]

1.3.1. FK506-binding protein

The most widely used chemogenetic tools for targeted induction of PPIs are based on FKBP12 (FK506-binding protein 12). FKBP12 is a small (108 AA) peptidyl-prolyl isomerase originally identified as an immunophilin in human and named after its ability to bind FK506 (also known as Tacrolimus), a potent immunosuppressant.[164] FK506 exhibits its function through binding to FKBP (K_i = 200nM) which creates a binding interface for calcineurin, a phosphatase implicated in T cell signalling, consequently leading to immunosuppression.[165]

Due to its immunosuppressive potential, *in vivo* application of FK506 can potentially lead to toxic effects.[166] In a seminal study, dimeric FK506 variants were synthesized, ultimately giving rise to several compounds termed FK1012, which retained FKBP12 binding and induced dimerization, but did not interact with calcineurin, and retained good cell permeability.[167] Second generation FK1012 compounds were developed to have shorter linker lengths and higher affinity.[168] Subsequently, a range of fully synthetic FKBP ligands was developed[169] and further modified to tune binding kinetics, ultimately giving rise to a compound termed AP1510.[170,171] AP1903 and the closely related AP20187 present further improved 'bumped' versions of AP1510, which were developed to selectively interact with a F36V-mutant of FKBP.[172]

The FKBP system in combination with homo-dimerizing compounds has since found a plethora of applications. For example, FK1012 was used for activation of a synthetic T-cell receptor (TCR) that lacked its endogenous ligand binding domain but was instead equipped with a cytosolic FKBP12 domain that allowed chemically induced dimerization.[167] Notably, this approach used three tandem fusions of FKBP, which potentially results in oligomerization, as each repeat of the domain might interact with another receptor. A synthetic Fas receptor

employing FKBP in a similar fashion was activated by FK1012 *in vivo* in mice thymocytes.[173] The system is also useful to control subcellular localization of proteins. Targeted membrane localization of POIs via one fused and one membrane bound domain have been employed to manipulate cell signalling. For example, a study on Src-like kinases showed that dimerization via FK1012 alone is insufficient for their activation, but recruitment to the membrane via FKBP activated downstream signalling components.[174] In a similar approach, Sos was recruited to the membrane to activate Ras signalling.[175]

Structural analysis of another mutant of FKBP employing an F36M mutation, termed F_M, showed that it was capable of forming dimers in the absence of ligand. In cells, several copies of F_M were required to mediate interaction of fused POIs, resulting in higher order oligomer aggregates. These could rapidly be dissolved upon addition of synthetic FKBP ligands, however even the most potent compound AP22542 had to be applied at 100 times higher concentration than previously reported binding affinities for the wild type.[176]

Another natural ligand for FKBP is rapamycin (also known as sirolimus). Upon binding to FKBP, the rapamycin-FKBP complex binds the FRB (FKBP12-rapamycin binding) domain of mTOR (mammalian target of rapamycin, also known as FRAP, FKBP12-rapamycin associated protein) with high affinity ($K_D < 1nM$).[177] FKBP-FRAP heterodimerization was used to elucidate whether endoplasmic reticulum and Golgi membranes remain distinct during mitosis. Indeed, an FKBP-tagged Golgi enzyme did not dimerize with an ER-anchored FRAP during mitosis.[178] The hetero-interaction of FKBP and FRAP was also used to re-constitute split transcription factors to regulate gene expression, endowing control over circulating levels of human growth hormone from transgenic cells implanted in mice.[179]

As mTOR is a fundamental regulator of cell growth, a critical concern of applications of rapamycin is the potential of undesired off-target inhibition of endogenous mTOR.[180] Modified variants of rapamycin, termed rapalogs, have been designed to contain 'bumps' that sterically prevent binding to FRB but allow binding to a complementary mutant FRB*.[181] In one application, FKBP12 and FRB* were used for hetero-dimerization of TGF-β receptors via rapamycin and rapamycin derivatives, and showed that TGFBR2 interacts with TGFBR1 and induces its phosphorylation.[182] In a screen of several rapalogs and a panel of FRB mutants, several compounds were identified that allowed selective control over individual FRBs, opening the avenue for tandem experimental designs where CID of more than one target is controlled.[183] A modified, photocaged rapamycin termed pRap was demonstrated to allow regulation of heterodimerization with high spatial and temporal precision upon irradiation with UV light (365 nm).[184]

The hetero-interaction of FKBP12 and FRB has also been purposefully exploited in an approach that harnessed endogenous FKBP12. In an *in vivo* approach in mice, the endogenous *GSK-3*β (glycogen synthase kinase-3 β) was fused to FRB*, causing destabilization and loss of function. Upon treatment with a rapalog, *GSK-3*β-FRB* would interact with endogenous FKBP12, which stabilized its expression levels and rescued activity.[185]

In another important application of FKBP12, Dexamethasone (DEX), a glucocorticoid receptor (GR) ligand, was fused to FK506 to create a bivalent ligand capable of inducing hetero-dimerization of GR and FKBP12. This was utilized in a pioneering yeast-three-hybrid (Y3H) screen combining a ligand with the yeast-two-hybrid system. GR was fused to a DNA binding domain ('hook'), binding of DEX-FK506 ('bait') subsequently recruited FKBP12-bound transcriptional regulators ('fish').[186] The system was subsequently applied in a high-throughput genetic screen for enzymes, where the chemical linker between DEX and FK506 was replaced with a target bond. Cleavage of the bond resulted in disruption of transcription, providing a direct readout of enzymatic activity.[187]

Collectively, the chemically induced homo- and hetero interactions of FKBP and its mutants have been used for a vast number of studies *in vitro* and *in vivo*. Notably, the FKBP system is also used in clinical applications in conjunction with adoptive T-cell therapy. Through the development of iCasp9, an inducible Caspase 9 kill-switch responding to AP1903, apoptosis of transgenic cells can be induced to prevent unwanted malignant effects or potentially aberrant cells.[188,189]

1.3.2. Dihydrofolate reductase

Another system for CID is based on dihydrofolate reductase (DHFR) from *E. coli* and methotrexate (MTX). DHFR is an important metabolic enzyme that converts dihydrofolate to tetrahydrofolate in a crucial step of thymine synthesis. Originally used as a chemotherapeutic in clinical applications, MTX acts as a competitive inhibitor of DHFR that binds with high affinity and thereby inhibits DNA synthesis.[190]

Early generation of homobifurcational versions of MTX termed bisMTX allowed dimerization of DHFR in solution.[191] Since then, MTX fusion molecules have found wide application in Y3H screens, similar to the previously described DEX-F506 fusion. For example, MTX-SLF (synthetic ligand of FKBP) fusions were used for hetero-dimerization of DHFR and FKBP[192,193] MTX-DEX fusions were successfully employed for hetero-dimerization of DHFR and GR.[194-197]

In another approach, MTX was fused to O_6-benzylguanin (BG), the ligand of hAGT (O_6-alkylguanine-DNA alkyltransferase). When fusing hAGT with the DNA binding domain LexA, treatment with MTX-BG results in the recruitment of DHFR fused to a transcriptional activator and allowed to control transcription in yeast. Notably, hAGT catalyzes covalent attachment to its ligand, hence this system for CID is irreversible.[198]

One concern for *in vivo* applications of DHFR-based CID is the immunosuppressive and cytotoxic effect of MTX.[199] TMP (trimethoprim) is a ligand of bacterial DHFR that shows no affinity for mammalian DHFR, and is therefore expected to show limited toxicity and high orthogonality in mammalian cell lines. A TMP-SLF conjugate was developed which was capable of hetero-dimerizing DHFR and FKBP12, and was successfully employed to control transcription in yeast and glycosylation in mammalian cells.[200]

1.3.3. Phytohormones

Phytohormones are signalling hormones that regulate a variety of processes in development and growth in plants.[201] These molecules provide interesting opportunities for CID and CIP in animal systems, where they are expected to act orthogonally to endogenous proteins.

Abscisic acid (ABA) is a key regulator of plant stress responses, growth and development, and endogenously interacts with a family of receptors termed PYR/PYL/RCAR (pyrabactin resistance/PYR1-like/regulatory component of ABA receptor) to neutralize activity of PP2C (protein phosphatase type 2C).[202] The availability of structural data of ABA complexed with several of its receptors sparked the development of an ABA-induced system for hetero-dimerization of complementary surfaces of PYL1 (PYL_{CS}, 176 AA) and ABI1 (ABI_{CS}, 297 AA). The system was successfully employed to regulate gene expression and subcellular localization, and further implemented in tandem with the FKBP-FRB system to show full orthogonality.[203] ABA has also been modified to be photocaged, giving rise to a light-controlled CID system responsive to 365 nm UV light.[204]

Gibberellins (GAs) are important for plant growth and flowering, but also found in algae and fungi.[205-207] While not all gibberellins have known biological activity, it has been shown that GA_3 binds to GID1 (Gibberellin insensitive dwarf1) and subsequently recruits GAI (gibberellin insensitive).[208,209] GA_3-induced hetero-dimerization of GAI (151 AA) and GID1 (172 AA) has been successfully employed for membrane targeting of Tiam1 and subsequent induction of Rac signalling. Notably, GA_3 originally exhibited limited cell permeability, and was modified by esterification with an acetoxymethyl (AM) group to improve cellular uptake.

The GA_3-AM system was then successfully combined with rapamycin and FKBP-FRB for induced translocation of two fluorophores, demonstrating orthogonality of the two systems.[210] This property was further exploited to design a Boolean-logic gated Rac signalling circuit in mammalian cells.[211] In an impressive study combining GA_3, ABA and rapamycin-based CIDs, a panel of activatable recombinases was generated. The combination of these different systems allowed independent and precise chemical and light-induced control of activity.[212] This example illustrate the importance of expanding the chemogenetic toolkit with novel compounds and domains that exhibit orthogonality to existing systems.

1.3.4. Others

While not directly inducing PPIs, the chemogenetic toolbox contains various methods for tagging proteins for recognition by a labelling domain. The SNAP-tag (182 AA) is based on a modified hAGT protein.[213] It is conventionally used for tagging proteins with small fluorescent dyes, but has been employed for complementation assays. The SNAP tag can be functionally split, and by fusing to two POIs their interaction will re-constitute the tag and allow labelling.[214] The development of a variant of the SNAP tag termed CLIP, which recognizes a different small chemical binding partner, further complements the method by enabling multi-protein labelling.[215]

While SNAP and CLIP are mainly used for labelling and dynamic tracking of PPIs, a heterodimerization system based on HaloTags and SNAP-tags , termed HaXS, has successfully been employed to induce PPIs and control subcellular protein localization.[216] In addition, the previously described fusion of SNAP-FKPB via a heterobifurcational ligand[176] allows to imagine tri experimental designs in which complementation of a split SNAP protein precedes forced dimerization with FKBP or a HaloTag.

The immunomodulatory compound cyclosporin A (CsA) is structurally related to FK506/rapamyin, and binds the protein cyclophilin (CyP). Modified CsA was used to activate a chimeric receptor consisting of CyP fused to the Fas receptor, to initiate cell death *in vitro*.[217]

The bacterial repressor TetR has recently been modified for chemically-induced hetero-dimerization. Endogenously, TetR regulates expression of tc resistance genes in bacteria. Tc-induced expression of target genes has found wide applications in eukaryotic systems.[218] In a recent approach, split TetR repressors could be reconstituted by addition of tc, allowing targeted control of transcription. As of yet, the system has not been applied to control dimerization of other POIs.[219]

Another interesting, recently developed CID system is based on antibodies (AbCID). Through binding of the drug ABT-737, an epitope for an engineered antibody is created on the surface of BCL-xL. In a proof-of-principle application the system was used to control transcription via dCasp9 and reconstitute a split CAR (chimeric antigen receptor). Since ABT-737 is a clinically approved drug, AbCIDs have potential for clinical applications in cell-based therapies.[220]

In another approach, coumermycin, a coumarin derivative antibiotic, was used for CID of the bacterial DNA gyrase B subunit (GyrB). In a transcriptional application, the GyrB activator was fused to a repressor-binding domain, and application of coumermycin recruited a transactivator. Notably, by applying novobiocin, an coumermycin antagonist, transcription was interrupted again.[221]

1.4. Current limitations

Synthetic tools employing optical and chemical triggers to manipulate PPIs have found wide applications, from basic research to the clinic. The variety of optogenetic applications reviewed here illustrate how the spatial and temporal precision of optogenetic tools can provide insight into fast, dynamic processes such as oscillatory gene activity and complex inter- and intra-cellular signalling networks, and how combinations of systems from the opto- and chemogenetic toolbox allow the design of complex synthetic circuits for precise control of cellular behavior.

Rapid and reversible induction of signalling pathway components using optogenetics have crucially contributed to understanding signalling dynamics relying on intensity, logic gating and oscillations.[45-47,118] Local activation of signalling is of particular relevance to approaches related to cell polarity and morphology.[89,90,93,222]

Background activity in the dark/inactivated state, and a maximum activation level similar to an endogenous response are desirable to recapitulate endogenous signalling events faithfully. Work on optogenetic RTKs employing different LOV domains has showcased the necessity to consider activated state lifetime as a crucial factor to mimic cellular signalling.[62]

Mutations allow the tuning of LOV domain kinetics by altering the lifetime of their activated states. [42] A yeast transcriptional assay comparing CRY2/CIP, the TULIP system and PhyB/PIF has illustrated differences in light sensitivity and strength of induction of these systems.[223] While further comparative studies of optogenetic tools are highly desirable, this implies that some fundamental knowledge on the process to be manipulate is a prerequisite to design a functional optogenetic tool to control it.

Light delivery into tissues is a major challenge for optogenetic applications *in vivo*. To an extent, red-light sensing tools based on PhyB/PIF can be activated even in deeper tissue levels.[126] Two-photon excitation partially circumvents the problem of activating blue-light sensing tools by applying red-shifted illumination. Coincidental absorption of two photons of double the wavelength normally required for excitation can lead to excitation of a chromophore in a single event, however the process is stochastically rare and hence high photon flux is required to achieve it.[224]

Another special consideration when using combinations of optogenetic tools is the potential overlap of stimulating light, additionally complicated when a fluorescent readout is desired. While blue-light sensing protein domains have been harnessed for optogenetic applications for over a decade, the more recent application of red-sensitive phytochromes for homodimerization has enabled the design of multi-color optogenetic screens. [126] The discovery of the green-light responsive CBDs provides additional potential for optogenetic experiments, by closing a previous gap in the spectrum of optogenetic tools, and providing a novel modality of interaction – a non-covalently linked protein complex that can be disrupted.[133,134] Notably, there is currently no such tool available in the chemogenetic toolkit.

Chemogenetic tools rely on the delivery of a small molecule trigger which is subject to pharmacodynamic limitations such as diffusion and cellular uptake, and *in vivo* pharmacokinetics. Tools based on mammalian protein domains or from organisms implicated in pathogenesis in animals further pose a risk of crosstalk to endogenous proteins. Clinically approved drugs as targets are interesting due to their known pharmacology, but by nature will not act orthogonally *in vivo.*

While optogenetic tools provide the spatial and temporal precision to manipulate a target process with high fidelity, e.g. with a precise pulse of laser light, chemogenetic tools are of particular interest for processes that shall be influenced over longer periods of time. Much work has been done to optimize existing chemogenetic tools and ensure specificity and minimal cross-talk to endogenous cellular components, such as the generation of FKBP mutants and synthetic ligands and novel approaches have been developed that directly combine existing chemogenetic tools for new applications, e.g. through the creation of hetero-bifurcational molecules. However, these approaches limit the combinatorial potential of using these tools to manipulate different processes in the same system in tandem.

Continued expansion of the repertoire of synthetic tools is desirable to enable combined experimental designs in which several processes shall be influenced and monitored in parallel. In this work, the general design of optogenetic experiments to manipulate cellular signalling will be discussed in Chapter 2. The engineering and application of green-light sensing cell surface receptors employing CBDs will be presented in Chapter 3, followed by a novel synthetic tool for chemically-induced de-dimerization described in Chapter 4. These tools crucially expand the synthetic toolkit and shall in the future facilitate tandem experimental designs, applications with fluorescent readouts, and applications in which a desired PPI shall be disrupted rather than induced.

Chapter 2: Design and application of light-regulated receptor tyrosine kinases

2.1. Introduction

Receptor tyrosine kinases (RTKs) are cell surface receptors that are activated by a wide variety of growth factors, cytokines and hormones. They couple to important downstream signalling pathways, such as the mitogen activated protein kinase/extracellular signal-regulated kinase (MAPK/ERK) pathway, the phosphatidylinositol 3-kinase pathway, and phospholipase C. These pathways are tightly linked to cell survival, proliferation and differentiation, making RTKs important players in development, tissue homeostasis and disease.[225] The signalling networks downstream of RTKs are orchestrated by a variety of mechanisms, such as variability in receptor-ligand binding affinity and complex lifetime, and intracellular feedback loops.[226,227] The complexities in RTK signalling become apparent when they are disrupted in degenerative diseases and cancer [228,229] and can be challenging to delineate using conventional pharmacological methods.[14,225,230]

Light-regulated RTKs (termed Opto-RTKs) are RTKs that were re-engineered for applications in optogenetics and can be activated or inactivated by light instead of their cognate biological or synthetic ligands.[93,231,232] Light is an orthogonal cue that allows the manipulation of cellular processes with high spatial and temporal precision, and is thus uniquely suited for the dissection of complex and dynamic signalling networks.[14,230]

The seminal studies of the group of Won Do Heo[93,232] and our group[231] have resulted in a flurry of approaches in which different RTKs[126,133,232-234] and also enzyme receptors of other families[222,235,236] have been controlled by light. In these studies, the receptors have been combined with light-sensing domains (LSDs) that alter their oligomerization state in a light-dependent manner, e.g., through dimerization or oligomerization reactions, thereby mimicking the endogenous activation mechanism of many RTKs. In the first engineering approach, an LSD is directly fused to the receptor (Figure 1 a, I and II), whereas in the second approach, an LSD is fused to a protein that binds to the RTK (Figure 1 a, III).[233] Full-length receptors modified with LSDs in either of these approaches will retain ligand binding capabilities and will therefore respond to both ligands and light (Figure 1 b). To endow more stringent control, the extracellular domain (ECD) and transmembrane domain (TMD) of a receptor can be removed, truncating it to the kinase domain (KD) and C-terminus (CT) so that it is exclusively controlled by light. In this case, the KD of the receptor is commonly anchored directly to the membrane *via* a short myristoylation (myr) sequence.[126,133,222,231,232,234,235] Alternatively, the TMD and ECD can be replaced with those of the p75 receptor (a low affinity nerve growth factor receptor) to serve as an orthogonal transmembrane anchor.[231,237] In other examples, the intracellular portion of a receptor (KD and CT) was expressed in soluble form, and LSDs were employed to achieve membrane recruitment and subsequent clustering.[234] or heterodimerization between two different receptor types. [235] Table 1 and Figure 1 c-d summarize the LSDs employed in our group and the corresponding Opto-RTKs.

Table 1: LSDs employed in Opto-RTKs generated in our group. λ_{max} designates the optimal wavelength for activation (and reversal in the case of CPH1s), λ_{safe} refers to (a) wavelength(s) that will not activate the LSD and thus is safe for handling of cells expressing the domain or for imaging. LOV domains (e.g., VfAU1-LOV) and CBDs (e.g., MxCBD or TtCBD) do not absorb light above the indicated λ_{safe}, whereas the λ_{safe} of phytochromes (e.g., CPH1S) lies between two absorbance peaks and thus high intensity light from a broad band source may elicit some response. Asterisks designate exogenous cofactors that have to be supplied to cells.

	VfAU1-LOV	CPH1S	MxCBD / TtCBD
λ_{max} (nm)	470	660 / 730	545
λ_{safe} (nm)	>520	500	>600
Cofactor	Flavin mononucleotide (FMN)	Phycocyanobilin (PCB)*	Adenosyl-Cobalamin (AdoCbl)*
Reference	32,231	14,122,126	128,133

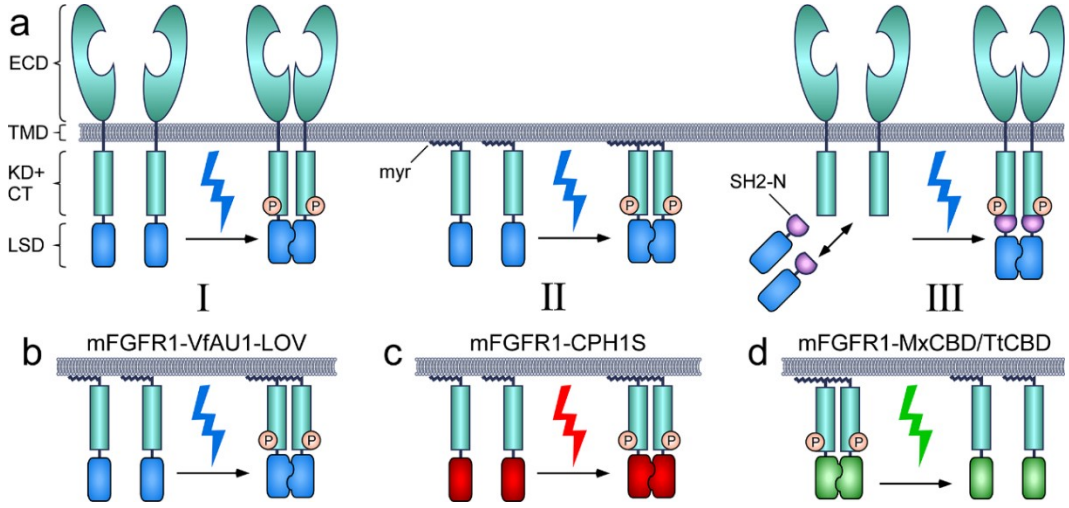

Figure 1: Approaches to engineer Opto-RTKs. (a) An LSD can be directly fused to the CT of the full-length receptor or of a truncated receptor lacking the ECD and TMD. Alternatively, the LSD can be tethered to a protein that interacts with the receptor CT. (b-d) In these examples, the KD and CT of the murine fibroblast growth factor receptor1 (mFGFR1) is linked to the membrane via a myr anchor. (b) The LOV domain auf Aureochrome 1 of *V. frigida* (VfAU1-LOV) dimerizes upon blue light stimulation. (c) The sensory domain of phytochrome 1 (CPH1S) of *Synechocystis* sp. dimerizes upon red light stimulation. (d) The cobalamin-binding domains (CBDs) of *M. xanthus* (MxCBD) or *T. thermophilus* (TtCBD) form a constitutive receptor complex that breaks upon green light stimulation.

Here, we present methods for the optical control of canonical cell signalling pathways *ex vivo* using Opto-RTKs. The protocol covers the assessment of activity of prototypical Opto-RTKs following transient transfection in HEK293 cells. We describe appropriate controls that allow benchmarking the light-induced signal of an Opto-RTK and serve to exclude unspecific effects of expression or light, and to verify if receptor dimerization by light is sufficient to activate the signal (Table 2). Transfecting a range of DNA amounts for Opto-RTKs and controls then allows determining ideal conditions for minimum unspecific background signalling and a maximum signal-to-background ratio.

We further describe a quantitative reporter gene assay, as well as preparation of samples for semi-quantitative assessment of Opto-RTK temporal properties using the WB technique. The methods presented here are geared towards the use of receptors developed in our group, but we reason that similar considerations should be taken into account when using other light-regulated enzyme receptors.

Table 2: Control vectors and technical controls to evaluate signalling activity of an Opto-RTK in cell-based experiments. All controls should be performed under light and dark conditions.

	Type of Control	Description
transgenes	FKBP domain fusion	• Fusion of the KD and CT to an engineered FKBP (FK506 binding protein) domain, which can be forced to homodimerize by addition of the small chemical ligand AP20187 [238] • To test if the receptor can be activated by forced dimerization and to benchmark signaling levels of an induced receptor
	Fc (IgG) domain fusion	• Fusion of the KD and CT to the Fc fragment of an IgG antibody, which forces constitutive dimerization [133] • To benchmark signaling levels of a constitutively dimeric receptor
	KD and CT only	• Monomeric, membrane anchored isolated KD and CT • To benchmark unspecific background signaling levels of the transfected receptor as a "baseline"
	dimerization-deficient receptor	• Mutation in the KD that blocks dimerization, e.g., R577E in full length mFGFR1 [239] • To show that the observed signal relies on receptor dimerization and not an unspecific, cell-autonomous effect of the LSD or light
	KD mutation	• Mutation in the KD that eliminates kinase activity, e.g., Y653F/Y654F in mFGFR1 [240] • To show that the observed signal requires catalytic activity in the Opto-RTK and is not an unspecific, cell-autonomous effect of the LSD or light
	photo-insensitive LSD	• Mutations in the LSD or absence of exogenous cofactor to prohibit photocycle • To show that the observed signal requires photoactivation of the LSD in the Opto-RTK and is not an unspecific, cell-autonomous effect of the LSD or light
other	change in stimulation light	• Stimulation with a wavelength that the LSD domain does not respond to (e.g., see Table 1) • To show that the observed signal requires photoactivation of the LSD in the Opto-RTK and is not an unspecific, cell-autonomous effect of the LSD or light
	mock transfection	• Transfection with empty plasmid vector (not containing Opto-RTK gene) • To show that transfection and illumination have no effect

2.2. Materials

2.2.1. Cell culture and transfection

1. Purified plasmid DNA for transfection: reporter plasmid (*see* **Note 1**) and optogenetic receptor construct (*see* **Note 2**).

2. Cell culture facility equipped with a laminar flow hood, water bath (37 °C), incubator (37 °C, 5% CO_2), and cell counting chamber.

3. HEK293 cells cultured according to the provider's recommendation in 75 cm^2 tissue culture flasks.

4. D10 medium: Dulbecco's modified essential medium (DMEM) supplemented with 10% fetal bovine serum (FBS) and 1% penicillin/streptomycin (P/S), sterile filtered and stored at 4 °C.

5. D5 medium: DMEM supplemented with 5% FBS, sterile filtered and stored at 4 °C.

6. COI0.5 medium: CO_2 independent medium (COI) supplemented with 0.5% FBS and 1% P/S, sterile filtered and stored at 4 °C.

7. Opti-MEM I reduced serum medium (Thermo Fisher Scientific).

8. Phosphate-buffered saline (PBS) without Ca^{2+} and Mg^{2+}.

9. 0.25% Trypsin-EDTA solution.

10. Polyethyleneimine (PEI) transfection reagent: Completely dissolve PEI to a final concentration of 1 mg/mL (typically, using a total volume of 100 ml) in ultra-pure H_2O (adjusted to pH 2.0 with HCl) then bring pH to 7.0 with NaOH. Aliquot and store at -80 °C for up to one year. Once thawed, keep at 4 °C for up to one month [241].

11. Poly-L-ornithine hydrobromide (PLO) solution at 4 mg/mL in ultra-pure H_2O.

12. Black or white walled, clear flat-bottom polystyrene 96 well plates for reporter gene assay or 35 mm polystyrene dishes for analysis by WB (*see* **Note 3**).

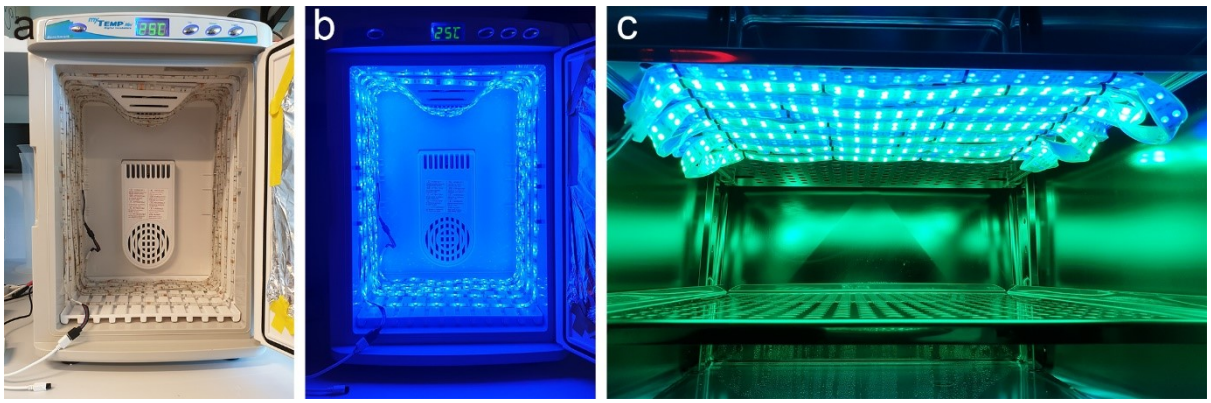

Figure 2: Set-up of customized incubators for illumination. (a) A Benchmark Scientific MyTemp Mini incubator was repurposed for optogenetic experiments by equipping it with two strips of 3528 SMD LEDs (for a total of 250 LEDs).(b) The maximum light intensities achieved with this setup are ~330 µW/cm^2 for blue, 130 µW/cm^2 for red and 170 µW/cm^2 for green light. (c) A cell line incubator with CO_2 supply and humidification was equipped with waterproof 5050 SMD LEDs. A 5 m strip (600 LEDs) was cut in two 2.5 m halves which can be connected to power supplies individually. The strips were attached to the bottom of the metal shelf and affixed with cable ties. The set-up enables dual-color optogenetic experiments, e.g., simultaneous blue and green illumination. The maximum intensity when using both strips with the same color is ~2,100 µW/cm^2 for blue, 760 µW/cm^2 for red and 820 µW/cm^2 for green light.

2.2.2. Light activation and reporter readout

1. Small illumination incubator (*see* Note 4) (Figure 2 a,b).

2. RGB LED strips (SMD 5050 LEDs, 5 m length, 60 LEDs/meter, spray water shielding) with power supply, remote control and dimmer (*see* Note 5).

3. Digital thermometer with probe on a wire.

4. Optical power meter (e.g. Sanwa LP-1) capable of measuring light in the 400 to 900 nm range.

5. Plate reader capable of measuring luminescence and/or fluorescence.

2.2.3. Luciferase assay buffers and stock solutions [242]

1. Lysis buffer: 100 mM Tris-Cl, 40 mM Tris-base, 75 mM NaCl, 3 mM $MgCl_2$, 0.25% Triton X-100. Store at room temperature (RT).

2. *Renilla* salts buffer: 45 mM Na_2EDTA, 30 mM $Na_4O_7P_2$, 1.425 M NaCl. Store at RT.

3. Firefly assay stock solutions: Dissolve reagents in ultra-pure H_2O unless otherwise indicated. Prepare aliquots of 500 mM dithiothreitol (DTT, 300 µL aliquots), 10 mM coenzyme A (CoA, 600 µL aliquots), 100 mM adenosine 5'-triphosphate disodium salt (ATP, 45 µL aliquots), 80 mg/mL luciferin free acid (in lysis buffer, 52.5 µL aliquots). Store aliquots at -80 °C for up to several months.

4. *Renilla* assay stock solutions: Dissolve and prepare aliquots of 10 mM Ataluren (PTC124, in DMSO, 60 µL aliquots), 2 mM h-Coelenterazine (h-CTZ, in EtOH + 1% HCl, 50 µL aliquots). Store aliquots at -80 °C for up to several months.

5. 3x Firefly assay reagent (Firefly-AR): Combine one of each stock aliquot (DTT, CoA, ATP, luciferin free acid) with 9 mL lysis buffer. Store at -20 °C for up to several weeks.

6. 3x *Renilla* assay reagent (*Renilla*-AR): Combine one of each stock aliquot (PTC124, h-CTZ) with 9.9 mL *Renilla* salts buffer. Store at -20 °C for up to several weeks.

2.2.4. WB sample preparation

1. RIPA buffer: 150 mM NaCl, 1% Triton X-100, 0.1% SDS, 50 mM Tris-Cl pH 8.0, 0.5% sodium deoxycholate, protease inhibitor cocktail. Keep at 4 °C for up to several weeks, or in aliquots at -20 °C for up to one year.

2. Cell scrapers.

3. Microcentrifuge, chilled (4 °C).

4. 4x Laemmli loading buffer: 40% glycerol, 240 mM Tris-Cl pH 6.8, 8% SDS, 0.04% bromophenol blue. Store aliquots at -20 °C and add 5% β-mercaptoethanol fresh before use.

2.3. Methods

2.3.1. Preparation of plates and dishes

1. Perform cell culture under sterile conditions in a laminar flow hood. Disinfect tools and containers with media and reagents by spraying their outside with 70% EtOH followed by wiping them down with a clean paper towel and placing them in the hood.

2. Coat the wells of a 96 well plate or 35 mm dishes with PLO with 70 µL PLO solution per well or 1 mL PLO solution per dish and incubate for 3 h at 37 °C or overnight at 4 °C.

3. Remove PLO solution and wash once with 100 µL PBS per well or 2 mL PBS per dish and allow to air dry for a few minutes.

2.3.2. Transient reverse transfection

This section describes the reverse transfection of HEK293 cells in clear-bottom 96 well plates for reporter gene assays or in 35 mm dishes for WB. In reverse transfections, cells are seeded and transfected in a single step by adding the cells to wells containing the transfection mix (*see* **Note 6**).

1. Warm trypsin solution, PBS, D5, D10 and Opti-MEM I in the water bath to 37 °C.

2. Prepare a master mix by combining sufficient Opti-MEM I (24 µL per well or 237.5 µL per dish) and PEI (1 µL per well or 12.5 µL per dish) for each condition that will be tested. Let stand at RT for 5 min.

3. In individual microcentrifugation tubes, combine Opti-MEM I and DNA for each condition to a total volume of 25 µL per well or 250 µL per dish (*see* **Note 7** for further information about DNA amounts).

4. Add Opti-MEM I-PEI mix to each Opti-MEM I-DNA mix 1:1. Mix by pipetting up and down a few times. Incubate 20 min at RT.

5. In the meantime, remove the tissue culture flask with HEK293 cells from the incubator and aspirate medium.

6. Add 10 mL of PBS and rock the flask back and forth to gently wash the cells.

7. Aspirate PBS and add 1 mL of trypsin solution. Let stand at RT for 1 min or until cells are fully detached. Gently tap against the side of the flask a few times to facilitate detachment.

8. Add 5 mL of D5 to stop trypsinization, gently pipette up and down with a serological pipette 5 times to resuspend cells and detach clumps.

9. Transfer cells to a 15 mL centrifugation tube and spin down at 500 xg for 3 min.

10. Aspirate medium and gently resuspend the cell pellet in 5 mL fresh D5.

11. Transfer 1 mL cell suspension to a new culture flask with 9 mL D10 for future passaging after 2-3 days.

12. Count the cells using a counting chamber and dilute to 500,000 cells/mL in D5.

13. Add 50 µL of Opti-MEM I-DNA-PEI mix to each well or 500 µL to each dish.

14. Add 100 µL of the cell suspension for a final 50,000 cells to each well, or 2 mL for a final 10^6 cells to each dish. Place the plates or dishes in the cell culture incubator.

15. After 6h, change medium to pre-warmed COI0.5 (*see* **Note 8** for further instructions on cofactor supplementation). Proceed immediately to Section 3.3 for reporter gene assays, or Section 3.4 for WB sample preparation.

2.3.3. Light stimulation and reporter gene assay

1. Adjust the temperature inside the light incubator to ensure that it is at or slightly below 37 °C while LEDs are on, and adjust light intensity using the dimmer and power meter (*see* **Note 9**).

2. The steps in light stimulation depend on whether light-activated or light-*in*activated receptors are studied. For light-activated receptors (e.g., mFGFR-VfAU1-LOV), wrap both the 'light' and 'dark' plate in foil to keep them in the dark during cell starving overnight. The next morning, unwrap one plate and place both plates in an incubator equipped with LEDs for 6-8 h depending on the reporter of choice (and **Note 10**). For light-inactivated receptors (e.g., mFGFR-MxCBD or -TtCBD), wrap only the 'dark' plate in foil and immediately place both plates in the light incubator for 16 h/overnight (O/N) illumination.

3. After light stimulation, aspirate medium from all wells.

4. For fluorescent reporters, add 50-100 µL of PBS and read fluorescence in a plate reader (*see* **Note 11**).

5. For luciferase reporters, dilute 3x Firefly-AR to 1x with H_2O. Add 60 µL 1x Firefly-AR per well and immediately read luminescence in a plate reader.

6. If in addition a *Renilla* viability reporter is used, add 30 µL 3x Renilla-AR (for a final 1x concentration) per well on top of to the luciferase assay reagent and read luminescence in a plate reader.

2.3.4. Light stimulation and sample preparation for WB analysis

This section covers the sample preparation for SDS-PAGE and WB analysis with a focus on the special considerations when handling samples from cells that were transfected with Opto-RTKs. The analysis of the samples can then be performed according to any general protocol, depending on available equipment and the specific signalling pathway of interest.

1. Following medium change after transfection, wrap the dishes in foil individually and keep in the dark O/N. Both light-activated and light-inactivated receptors are treated the same because no transcriptional reporter is employed here.

2. The next day, stimulate cells in the dishes for desired amounts of time in a light incubator (*see* **Note 12**).

3. Immediately after stimulation, place dishes on ice.

4. Wash cells with 1 mL ice-cold PBS by pipetting against the wall of the dish, gently tilting the dish and aspirating from the edge without disturbing the cell layer.

5. Add 180 µl ice-cold RIPA buffer, scrape cells and transfer them to pre-chilled microcentrifugation tubes. From here on, keep cells on ice.

6. Spin down at 4 °C at 20,000 rpm for 20 min.

7. Transfer supernatant to fresh, pre-chilled tubes. Discard the pellet.

8. Mix 90 µL sample with 30 µL 4x Laemmli buffer.

9. Denature proteins at 95 °C for 5 min. After this step, samples can be frozen and stored at -20 °C for several days.

10. Spin down at 10,000 rpm for 1 min.

11. Load duplicate gels with 30 µL of each sample per well (*see* **Note 13**) and proceed to perform SDS-PAGE and WB. The remainder of the samples can be frozen as backup and stored at -20 °C for several days.

2.4. Notes

1. Transcriptional reporters are available commercially, from researchers or through non-profit plasmid depositories such as Addgene.org. The choice of reporter plasmid will depend on the interrogated signalling pathway and preferred readout. For instance, a serum response element driven reporter is suited for analysis of the MAPK/ERK pathway. Luciferase reporters provide robust luminescence readouts. For fluorescent reporter proteins, the wavelength used to excite the Opto-RTK should not overlap with the excitation of the reporter fluorophore, otherwise illumination may bleach the reporter and reduce the signal. Careful choice of LSD and reporter allows the design of dual-color fluorescent assays with minimal wavelength overlap.[126] Choosing two different reporter systems can allow multiplexing to investigate more than one pathway or to use one signalling and one viability reporter, e.g., a pathway-activated firefly luciferase and a constitutively expressed *Renilla* luciferase.

2. A strong promoter, such as the cytomegalovirus (CMV) promoter, can potentially lead to overexpression of the receptor. A consequence of overexpression is high baseline activity, also for corresponding control vectors (e.g., receptor without the LSD), resulting in a requirement for low vector amounts in transfections. A truncated version of the CMV promoter (CMVtr) can be useful to titrate expression levels.[126,133,243] As a rule of thumb, shorter, myristoylation-anchored constructs are at higher risk of being overexpressed, making CMVtr a suitable choice. P75-anchored or full-length constructs are larger proteins that

require shuttling through the ER and Golgi network to the secretory pathway, and generally benefit from expression under the stronger full-length CMV promoter.

3. For luminescence assays, opaque/white bottom well plates can be used. Cell-culture grade plates for adherent cell culture are often pre-treated to facilitate cell attachment and thus do not require pre-coating with PLO.

4. To stimulate cells in dishes, plates, as well as whole animals (e.g., zebrafish and *Drosophila*) with light, we repurpose consumer grade incubators, e.g., designed for reptile breeding or as mini-fridges, which feature cooling/heating (but no CO_2 control). The LEDs can then simply be taped to the walls in parallel turns. Waterproof LED strips can be mounted in conventional cell line incubators with CO_2 control and humidification (Figure 2).

5. To control light intensity, the remote control provided with the LED strips can be used. However, many commercial LED strips achieve reduced intensity through frequency modulation (rapid flickering not visible to the human eye) rather than by reducing the power output. To lower intensity with continuous illumination, a dimmer should be used, or alternatively light absorption filters (e.g., neutral density filter foils obtained from the photography industry).

6. Alternatively, cells can be forward transfected by seeding at a slightly lower density (e.g., 30,000 cells per well for 96 well plates) in D5, incubating O/N and adding the transfection mix to them on the next day. In some cases, this can improve cell viability and transfection efficiency.

7. DNA amount and cell number can be scaled by surface for larger assay formats. For 96 well plate format, we use a maximum of 250 ng DNA with 1 µg PEI (1 µL of 1 mg/ml stock) per well. Our standard transfection to detect MAPK/ERK pathway consists of 150 ng pluc, 10 ng Elk trans-reporter (PathDetect System, Agilent Technologies), 10 ng *Renilla* viability reporter and up to 30 ng receptor DNA per well. In initial studies with a new receptor, we test DNA amounts ranging from 0.1 ng to 30 ng, also in combination with strong and weak promoters (*see* **Note 2**). DNA amounts for transfection and duration of stimulation can vary depending on the reporter gene assay. Generally, it is recommended to follow the plasmid supplier's requirements and protocols. For reporter gene assays, prepare all transfections in duplicate on two plates (one sample plate will be illuminated, the other will be the dark control). For WB, transfect cells in 35 mm dishes with a maximum of 2.5 µg receptor DNA and 12.5 µg PEI. Prepare one dish for each sample or point in a time course (e.g., dark control, 1 min illumination, 5 min illumination, 5 min illumination followed by 5 min dark recovery).

8. Depending on LSD, supplementation with an exogenous cofactor may be necessary. For CBDs, cells can be grown in the presence of 10 µM AdoCbl for 1-2 passages before transfection for reporter gene assays, for WB the cofactor can be supplemented to the starve medium after transfection. The cofactor and supplemented cells should be handled under red light (650nm) to minimize bleaching. For CPH1s, add 10 µM PCB to the starve medium. PCB is extremely light sensitive and both the cofactor and supplemented cells should be handled exclusively under green light (550 nm) to avoid bleaching of the isolated cofactor and

activation of the receptor. Not all suppliers of PCB provide material of high quality and testing of PCB from multiple suppliers is required.

9. Light intensity impacts receptor responses. We generally utilize 200 µW/cm^2 as an initial starting value for reporter gene assays employing an SRE luciferase reporter but CPH1s has been shown to be activated by intensities as low as 6.2 µW/cm^2.[126] For CBDs, varying light intensity allows to titrate the receptor signal.[133] Light intensities can be measured with power meters, some of which may not be equipped with spectral analysis properties or filters to allow the direct measurement of different colors of light. In such cases, a conversion factor may have to be applied. Refer to the manufacturer's specifications for details.

10. In our experience, 6-8 h stimulation is sufficient to obtain a readout for most reporter plasmids. Continuous illumination for up to 16 h (O/N) with red, green or blue light of 200 µW/cm^2 intensity has no significant impact on HEK293 cell viability. Other cell types might be sensitive to light exposure. In such cases, a pulsing regime (e.g., 15 sec on, 45 sec off) might be preferable. A short pulse of light is sufficient to activate light sensing domains and they will remain dimerized for up to several minutes (VfAU1-LOV, CPH1s).

11. For fluorescent readouts, note that many commercial well plates exhibit autofluorescence, e.g., 384-well plates that we previously applied (Cat Nr. #3712, Corning) upon excitation with light <500 nm. The excitation and emission wavelengths for fluorescent reporter readout may have to be optimized to detect signals.[244]

12. An example for a time course of light activation would be to place one dish each in the light for 0 min (dark control), 5 min, 15 min, 30 min and 30 min light followed by 60 min dark. After WB analysis, these time points give an indication over signalling activity on the minute to hour timescale.

13. We recommend performing WB analysis in duplicate blots to be able to stain against total target protein and against phosphorylated protein (e.g., pErk and total Erk when testing for the MAPK/ERK pathway). In both cases, include an antibody against a housekeeping protein (e.g., vinculin) as an internal standard. For quantification, determine the intensity of each band relative to internal standard for its respective lane. Then determine the ratio of phospho-protein to total protein for each individual sample.

Chapter 3: Engineering and characterization of a green-light inhibited RTK

3.1. Introduction

The optogenetic revolution has enabled spatially and temporally precise control over molecular processes, cellular signals, and animal behavior by employing microbial or plant photoreceptor domains capable of light-controlled inter- or intramolecular interactions. The diversity of the current domain repertoire allows blue light- or red light-induced formation of protein complexes[245]: light-oxygen-voltage-sensing (LOV) domains and phytochromes (PHY) homodimerize, [44,246] PHY and cryptochromes (CRY) heterodimerize with accessory proteins[78,116] and CRY also oligomerize.[91] Blue or red light-induced unbinding of stable complexes spontaneously formed in the dark has been observed in LOV domains in vitro [58], for PHY and CRY in yeast screens,[119] and developed into optogenetic tools for LOV domains and engineered fluorescent proteins.[247,248] In general, none of the currently used photoreceptor domains are maximally responsive to green light - a notorious “blind spot” in optogenetic experiments (Figure 3). Here, we employ cobalamin (vitamin B12)-binding domains (CBDs) for dark-promoted membrane receptor interactions that are dissociated by green light, and apply them to regulate signaling pathways in human cells and development in zebrafish embryos.

Functional, photochemical and structural information for CBDs of CarH of *Myxococcus xanthus* and *Thermus thermophilus* and the related LitR of *Streptomyces coelicolor* and *Bacillus megaterium* have emerged in recent years and represent an active area of photobiology research[21,128,129,131,132,249,250] (Figure 3 a and b). These transcription factors act as light-sensitive repressors of carotenoid synthesis. Their relatively small CBDs (~200 amino acids in length) mediate assembly as a dimer-of-dimers in the dark and dissociate into monomers upon green illumination after photolytic cleavage of the 5’-deoxyadenosylcobalamin (AdoCbl) cofactor (Figure 4, Figure 5).[128] AdoCbl is a form of cobalamin also synthesized in mitochondria of eukaryotic cells.[251] In mammals, cobalamins are required for red blood cell formation, neural function, protein and DNA synthesis, and no adverse effects are associated with excess cobalamin intake in healthy individuals.[252-254] These properties prompted us to explore CBDs for dark-promoted, green light-disrupted signaling in mammalian cells.

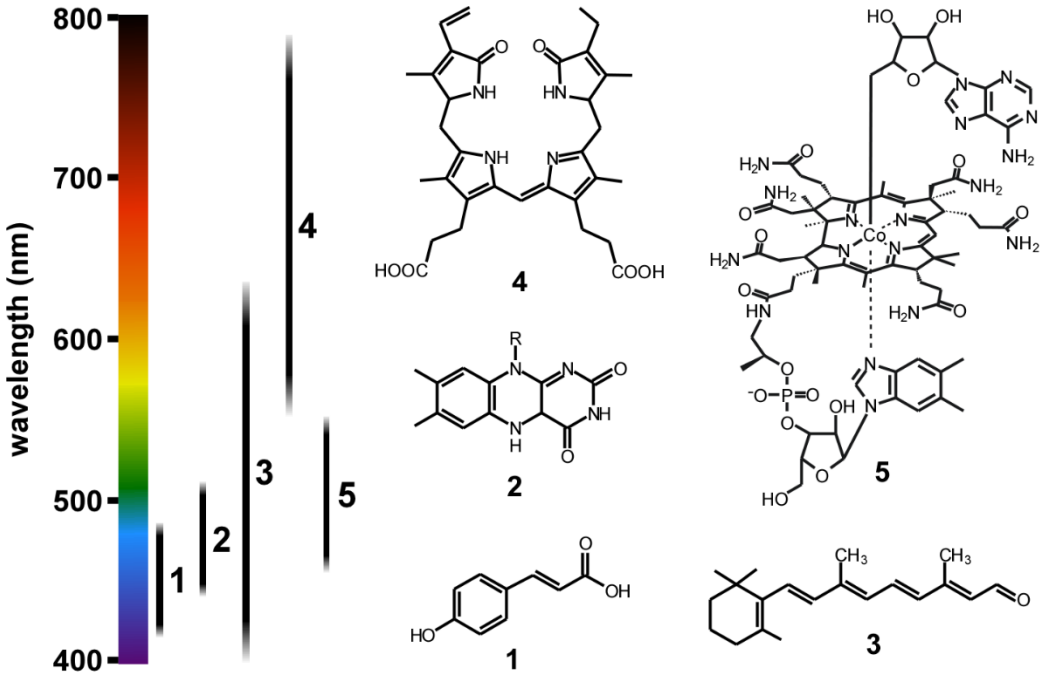

Figure 3: Chromophores of main photoreceptor classes (1: *p*-coumaric acid, 2: flavins, 3: retinal, 4: tetrapyrroles, 5: AdoCbl).

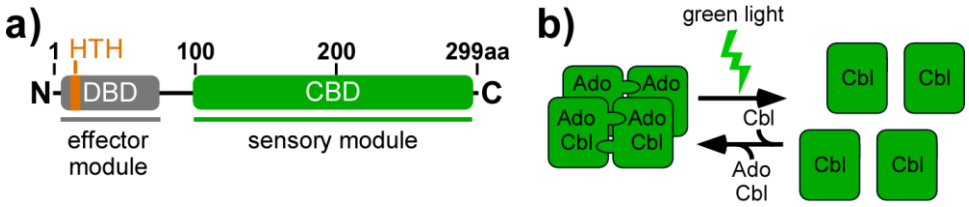

Figure 4: Domain structure and assembly of CarH. a) CarH with light-sensitive CBD and DNA binding domain (DBD; HTH: helix-turn-helix motif), drawn to scale representing CarH of *M. xanthus*. c) In the dark, CBDs with bound AdoCbl assemble into tetramers. Upon illumination, the 5'deoxyadenosyl-group is cleaved and the complex dissociates.

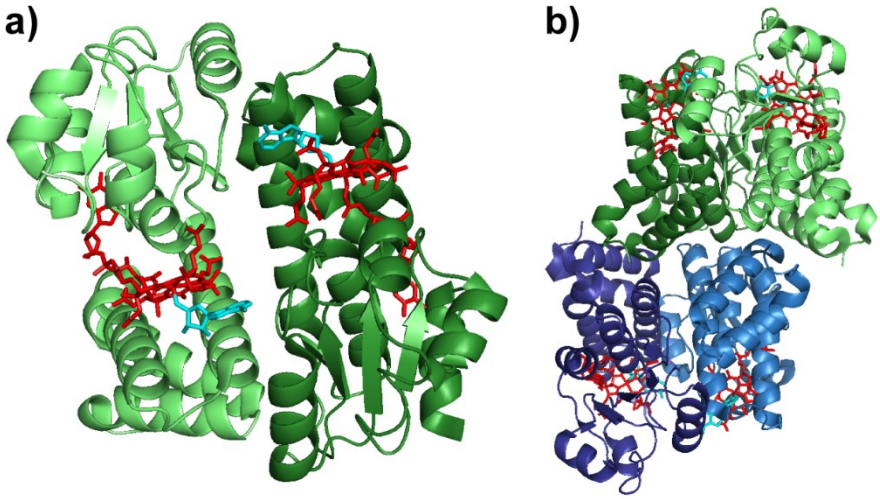

Figure 5: Assembly of TtCBD crystal structure.[128] a) Head-to-tail dimer with bound AdoCbl (corrin ring and 5'-hydroxyadenosyl group are colored in red and cyan, resp.). b) Tetramer of two head-to-tail dimers.

3.2. Methods

Unless stated otherwise, all chemicals were obtained from Sigma-Aldrich (Vienna, Austria).

3.2.1. CarH CBDs

CBDs of CarH of *M. xanthus* (MxCBD; residues 94 to 299 of NCBI GenBank sequence CAA79965.2) and *T. thermophilus* (TtCBD; residues 80 to 285 of NCBI GenBank sequence WP_038030370.1) were obtained as synthetic gene fragments with mammalin optimization (H. sapiens) following the recommendation of the manufacturer (Integrated DNA Technologies, Leuven, Belgium) (Table 3). CBDs were amplified using PCR (oligonucleotides 1-4, Table ***4***) with overhanging recognition sequences for AgeI and XmaI restriction enzymes.

3.2.2. mFGFR1 fusion proteins

CBDs were inserted into a previously described mFGFR1 expression plasmid in pcDNA3.1(-)[62] using restriction enzymes and ligation. For a positive control construct, the Fc portion of human IgG1 (IgG; residues 230 to 461 of NCBI GenBank sequence KU951249.1 with an additional Cys to Ser substitution) was amplified using PCR (oligonucleotides 5 and 6, Table ***4***) from human cDNA and inserted into the same construct. The construct contains an N-terminal myristoylation (MYR) membrane anchor and a C-terminal hemagglutinin (HA)-epitope. The CMV promoter of the plasmid was truncated as previously described[255] using inverse PCR (oligonucleotides 7 and 8, Table ***4***) followed by blunt end ligation to allow more precise adjustment of expression levels in transient transfection experiments. Point substitution R195E in mFGFR1-MxCBD and mFGFR1-TtCBD, H497A in mFGFR1-TtCBD, E499H in mFGFR1-MxCBD (numbered relative to the start codon of the fusion receptors) were introduced using site-directed mutagenesis PCR (oligonucleotides 9-14, Table ***4***). The charge inversion substitution (R577E in full length mFGFR1; R195E in fusion receptors) prevents formation of a functionally essential, asymmetric kinase domain dimer in FGFR1[239] and was used as a probe for dimer formation during receptor signalling. All constructs were verified by DNA sequencing. Protein sequences are summarized in Table 5.

3.2.3. Cell culture

HEK293 cells were maintained in DMEM supplemented with 10 % FBS, 100 U/ml penicillin and 0.1 mg/ml streptomycin. For luciferase assays, medium was supplemented with AdoCbl or CNCbl (10 µM final concentration; 10 mM stock concentration in water adjusted to pH 5.5 with HCl[256] and stored at -20°C in small aliquots in the dark). Cells were kept in supplemented medium for at least two passages prior to experiments, and cofactor supplemented medium and cells were kept in the dark to avoid cofactor bleaching.

3.2.4. Incubators for illumination

For illumination of cells, desktop temperature incubators (PT2499; ExoTerra/HAGEN, Holm, Germany or Nordfrost #49340, Schortens, Germany) were equipped with 300 RGB light-emitting diodes. Light intensity was controlled with a dimmer and measured with a power meter (PM120VA, Thorlabs, Dachau, Germany or LP1, Sanwa, Sanwa Electric Instrument, Tokyo, Japan). Intensities were 200 µW cm^{-2} for blue light ($\lambda \approx 470 \pm 5$ nm), 170 µW cm^{-2} for green light ($\lambda \approx 530 \pm 5$ nm) and 14 µW cm^{-2} for red light ($\lambda \approx 630 \pm 5$ nm) for experiments in cells, and 180 µW cm^{-2} for green light ($\lambda \approx 530 \pm 5$ nm) for experiments in zebrafish.

3.2.5. MAPK/ERK pathway activation (luminescence)

Activation of the MAPK/ERK pathway was assessed with the PathDetect Elk1 trans-Reporting System (Agilent, Vienna, Austria) containing firefly luciferase and an expression plasmid encoding Renilla luciferase as internal standard. Experiments were conducted in 96-well clear bottom plates coated with poly-L-ornithine. 5 x 10^4 HEK293 cells per well from untreated, AdoCbl, or CNCbl supplemented cultures were transfected with 245 ng DNA and 1000 ng polyethylenimine (PEI; Polysciences, Hirschberg an der Bergstrasse, Germany) per well (200 ng trans-activator, 10 ng trans-reporter, 10 ng RL standard, and 25 ng receptor fusion protein) in CO_2-independent medium (Gibco/Life Technologies, Vienna, Austria; supplemented with 5 % FBS, 2 mM L-glutamine, 100 U/ml penicillin, and 0.1 mg/ml streptomycin). Six h after transfection, medium was changed to CO_2-independent reduced serum starve medium (0.5 % FBS), and cells were incubated for another 14 h under the respective light/dark conditions. Luciferase expression was assessed with a homemade dual-luciferase assay reagent.[257] Firefly and Renilla luminescence were measured separately in a microplate reader (Synergy H1, BioTek, Winooski, VT) and the two signals were divided to yield luminescence ratio (LR). For light intensity dependence, cells were incubated with illumination through one, two, or three layers of a neutral density filter foil (transmission for one layer was 0.78) for 6 h after medium change before luciferase quantification.

3.2.6. MAPK/ERK pathway activation (immunoblotting)

1 x 10^6 HEK293 cells were transfected with 2.5 µg receptor in 35 mm dishes or 6 well plates coated with poly-L-ornithine. 6 h after transfection, medium was changed to CO_2-independent reduced serum starve medium (untreated, AdoCbl, or CNCbl supplemented). After 20 h in starve medium, cells were illuminated for different time intervals with LEDs. Following treatment, cells were washed with ice-cold PBS and lysed on ice in 250 µl lysis buffer (150 mM NaCl, 1 % TritonX-100, 0.1 % SDS, 0.5 % sodium deoxycholate, 50 mM Tris, complete protease inhibitor (Roche, Vienna, Austria), pH 8.0) per dish. Lysates were shaken for 30 min at 4°C and centrifuged for 20 min at 12000 rpm at 4°C. 30 µl lysate per lane were separated by SDS-PAGE and electro-blotted onto PVDF membranes. Blots were incubated with primary antibodies (HA #12158-67001, dilution 1:500, Roche; or Phospho-FGF Receptor (Tyr653/654) #3471, dilution 1:330, pERK1/2 #9101, dilution 1:1000, Cell Signaling Technology Leiden, Netherlands; ERK 2 (K-23) sc-153, dilution 1:1000, Santa Cruz

Biotechnology, Dallas, Texas, US) in blocking solution (5 % milk powder in TBST) overnight at 4°C. Secondary antibody (goat anti-rabbit IgG(H+L)-HRP conjugate, goat anti-rat IgG(H/L)-HRP, dilution 1:10000, Biorad, Vienna, Austria) was applied for 2 h at 20°C and blots were developed with Clarity™ Western ECL Substrate (Biorad).

3.2.7. Immunoblot quantification

Phosphorylated FGFR and total receptor levels for three to four biological replicates were quantified after immunoblotting on separate membranes using Image Studio Lite software (LI-COR Biosciences, Bad Homburg, Germany). For each blot, total protein amounts were normalized to the highest detected value, and the ratio of phosphorylated to total protein was calculated. Phosphorylated protein ratios were then normalized by setting the value of the dark condition (0 min illumination) to 1. The mutant receptor mFGFR1-MxCBD-E499H could not be quantified, due to overall faint bands. Phosphorylated Erk 2 levels quantified with this method showed no recovery within the investigated timeframe.

3.2.8. Fluorescent fusion proteins, expression, and viability testing

CBDs were inserted into a previously described expression plasmid in pcDNA3.1(-)[62] that contains the fluorescent protein mVenus (mV)[258] followed by a glycine- and serine-rich linker and a BspEI restriction site. A previously described mV-FKBP fusion protein was used as positive control.[62] 5 x 10^4 HEK293 cells were transfected with 25 ng expression plasmid. Expression was assessed using mVenus fluorescence in the microplate reader 30 h after transfection. For viability testing, cells were incubated for 2 h with thiazolyl blue tetrazolium bromide (0.5 mg/ml) followed by lysis with 70 µl acidic isopropanol (0.1 N HCl). Absorbance measurements were taken at 570 nm with 620 nm reference in the microplate reader. Fluorescence microscopy images were recorded on a digital microscope (EVOS FL, Peqlab, Erlangen, Germany) 30 h after transfection.

3.2.9. Animals and analysis of development

mFGFR1-MxCBD and mFGFR1-IgG were subcloned into the pCS2+ expression vector using PCR and the EcoRI and XbaI restriction enzymes. Experiments in zebrafish were performed by Manuela Stadler, St. Anna Children's Cancer Research Institute, Vienna. Zebrafish *(Danio rerio*) were maintained at standard rearing conditions[259,260] and according to the guidelines of the local authorities under licenses GZ:565304/2014/6 and GZ:534619/2014/4. Zebrafish embryos were injected with 1 nl of 13 ng/µl mFGFR1-IgG or mFGFR1-MxCBD with or without 25 µM AdoCbl at the one-cell stage using injection capillaries (glass capillaries pulled with a needle puller; P-97, Sutter Instruments, Novato, CA) mounted onto a micromanipulator (World Precision Instruments Inc., Berlin, Germany) and connected to a microinjector (FemtoJet 4i, Eppendorf, Hamburg, Germany). Injections of AdoCbl were performed using a filter passing red light (106-Primary Red Lee Colour Filter; Thomann, Burgebrach, Germany) on the injection stage and dimmed light. After injection, zebrafish were kept in petri dishes at

28°C. Green illumination was performed using LEDs (see above). To keep zebrafish embryos in the dark, petri dishes were wrapped in aluminum foil. Images of zebrafish embryos were recorded using a stereomicroscope (M125 with LAS software, Leica Microsystems, Wetzlar, Germany). Embryos were divided in four different groups according to their phenotype and counted.

3.3. Results

3.3.1. Cobalamin supplementation and CBD expression

We first verified that cobalamin supplementation is well tolerated using human embryonic kidney 293 (HEK293) cells as a model system. We did not observe reduced cell viability after incubation with AdoCbl or cyanocobalamin (CNCbl, a widely manufactured precursor) at a final concentration of 10 µM for 24 h (Figure 6 a); 10 µM corresponds to a typical concentration for cofactor application[116,246]). We next tested if CBDs can be expressed robustly and without cytotoxicity by fusing synthetic gene fragments encoding the 618 bp long CBDs of *M. xanthus* (MxCBD) and *T. thermophilus* (TtCBD), codon-optimized for expression in human cells[246], to the bright yellow fluorescent protein mVenus (mV), to quantify domain expression.[62] CBD levels were comparable to a robustly expressing human FK506 binding protein (FKBP) domain (Figure 6 b) with no obvious cytotoxicity or protein aggregation (Figure 6 c, Figure 7).

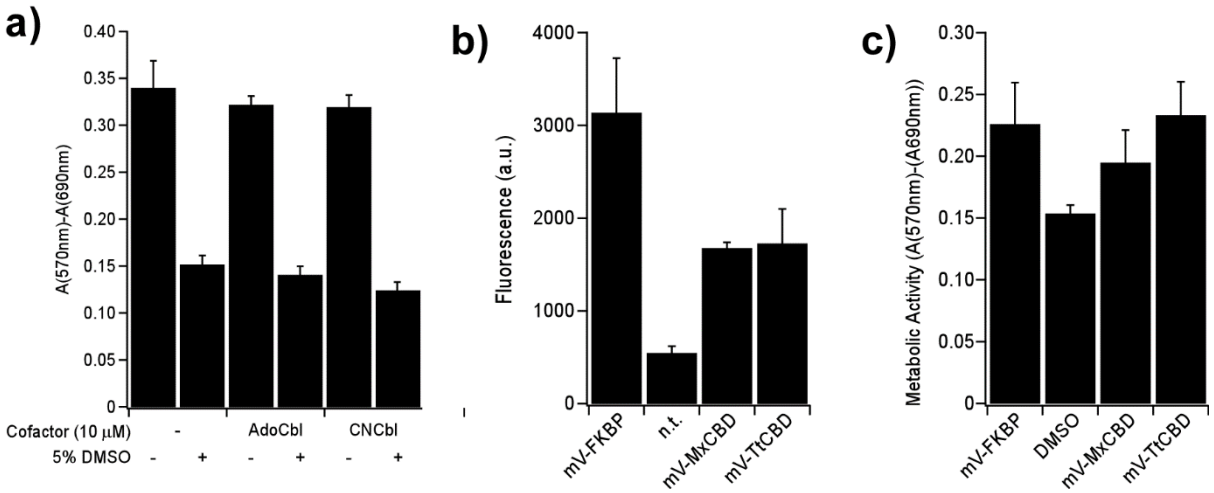

Figure 6: Expression testing of mV-MxCBD and mV-TtCBD fusions in dependence of supplementation. a) Viability (metabolic activity) of HEK293 cells treated with AdoCbl or CNCbl for 24 h. DMSO was applied as a positive control with reduced viability. b) Fluorescence intensity of mV tagged MxCBD, TtCBD, or FKBP expressed in HEK293 cells and not transfected cells (n.t.) as negative control. c) Metabolic activity of HEK293 cells expressing mV-MxCBD, mV-TtCBD, or mV-FKBP and a 5 % DMSO treated control with reduced viability. Shown are mean values ± SEM for three independent experiments each performed in triplicate.

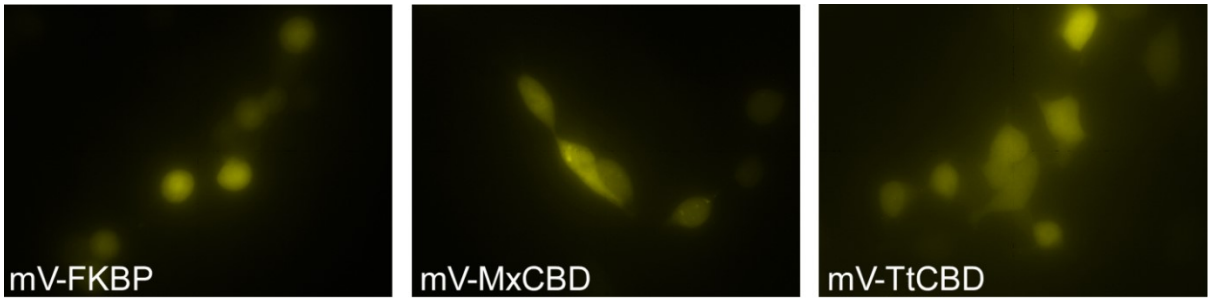

Figure 7: Representative fluorescence microscopy images for mV-FKPB, mV-MxCBD, and mV-TtCBD.

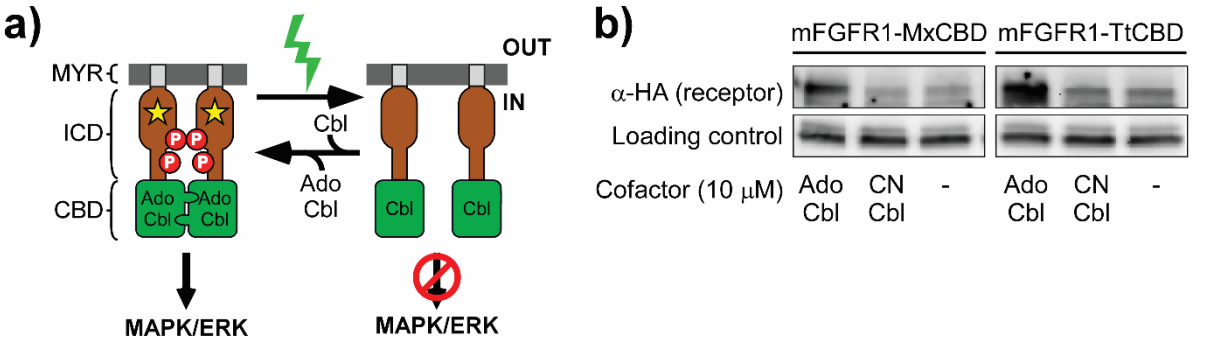

Figure 8: Schematic of mFGFR1-CBD receptor fusions and expression levels in dependence of supplementation. a) CBDs were fused to the ICD of mFGFR1 to engineer green light-inactivated receptors. b) Expression of mFGFR1-MxCBD and mFGFR1-TtCBD in HEK293 cells supplemented with AdoCbl or CNCbl.

3.3.2. CBD mediated light-dependent activity of a receptor tyrosine kinase

We next tested light-induced dissociation of a CBD fusion protein complex. Complex formation upon ligand binding is the functional mechanism underlying receptor tyrosine kinase (RTK) activation, leading to signalling events such as mitogen-activated protein kinases/extracellular signal-regulated kinase (MAPK/ERK) signalling.[261] To control RTK interaction we fused MxCBD and TtCBD to the C-terminus (where chemical oligomerization domains or fluorescent proteins were incorporated previously without perturbation of receptor function) of the intracellular domain (ICD) of murine fibroblast growth factor receptor 1 (mFGFR1, a prototypical RTK) (Figure 8 a).[238,262] We replaced the N-terminal ligand binding and transmembrane domains by a myristoylation (MYR) anchor[62,238] to render them solely regulated by the CBD, and further incorporated a C-terminal hemagglutinin (HA-)epitope. Interestingly, we found that fusion proteins expressed more efficiently in HEK293 cells supplemented with AdoCbl compared to CNCbl or no supplement (Figure 8 b) suggesting that the cofactor aids in protein expression. This was not observed for mV fusion proteins, likely reflecting a difference in expression yield and stability of the fluorescent protein and receptor ICD (compare Figure 9 to Figure 6 b).

Next, we quantified the capability of mFGFR1-MxCBD and mFGFR1-TtCBD to regulate the MAPK/ERK signalling pathway using a luciferase reporter gene assay (Figure 10). For both fusion receptors in the dark, we observed induction comparable to a constitutively dimerized receptor (mFGFR1-IgG; see Supporting Information for details). Induction required AdoCbl, in

line with observations that the cofactor is required for domain interaction.[21] Upon green illumination, we observed decreased pathway activity comparable to unsupplemented or untransfected cells, demonstrating light-induced dissociation of receptor complexes. While the two fusion receptors generally behaved similar, we noticed that blue light reduced activity of the TtCBD fusion receptor, but not of mFGFR1-MxCBD, to similar levels as green light. Control experiments showed that receptor dimerization is required for signalling (determined using a charge inversion substitution (R195E, see Supporting Information for details). Furthermore, illumination with different light intensities allowed to tune signalling activity to intermediate levels (Figure 11). Collectively, these results demonstrate that green light effectively inhibits the activity of mFGFR1-CBD receptors and that AdoCbl is required for complex formation in the dark.

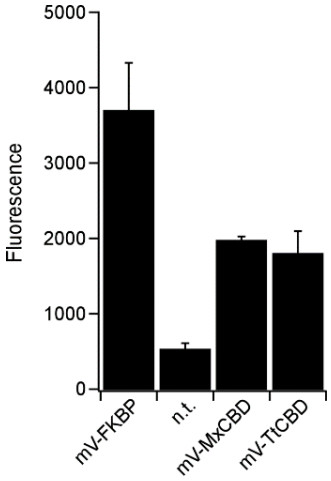

Figure 9: Fluorescence intensity recorded on HEK293 cells expressing mV-FKPB, mV-MxCBD, or mV-TtCBD in medium supplemented with AdoCbl (10 μM, 24 h). Experiments were performed as for data shown in Figure 1 d. Not transfected cells (n.t.) are the negative control. Shown are mean values ± SEM for three independent experiments each performed in triplicate.

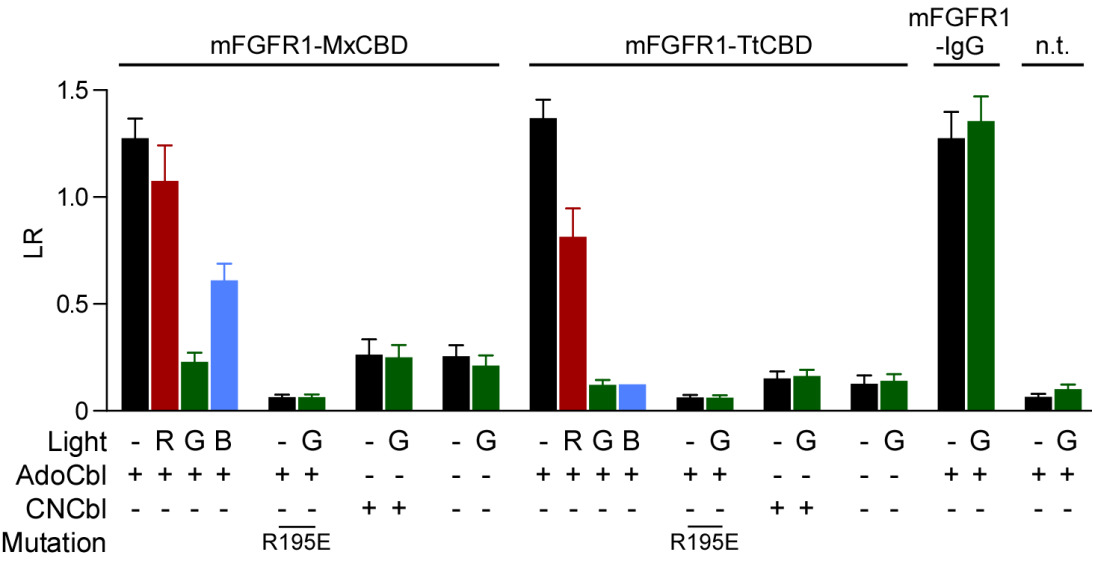

Figure 10: Activation of the MAPK/ERK pathway by mFGFR1 fused to MxCBD, TtCBD and controls. (LR: luminescence ratio) by mFGFR1 fused to CBDs or the Fc domain of IgG1 (IgG) and not transfected cells (n.t.) in response to red (R; λ = 670 ± 5 nm, I = 14 μW cm^{-2}), green (G; λ = 545 ± 5 nm, I = 170 μW cm-2) or blue (B; λ = 470 ± 5 nm, I = 200 μW cm^{-2}) light. Shown are mean values ± SEM for three to twelve independent experiments each performed in triplicate.

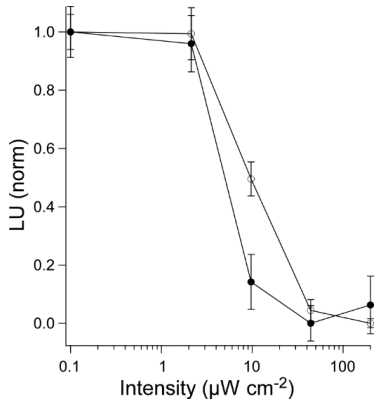

Figure 11: Light intensity dependence of green light-induced inactivation of MAPK signaling. Experiments were performed as for data shown in Figure 10 and data were normalized to highest and lowest responses. Closed symbols: mFGFR1-MxCBD. Open symbols: mFGFR1-TtCBD. Shown are mean values ± SEM for three independent experiments each performed in triplicate.

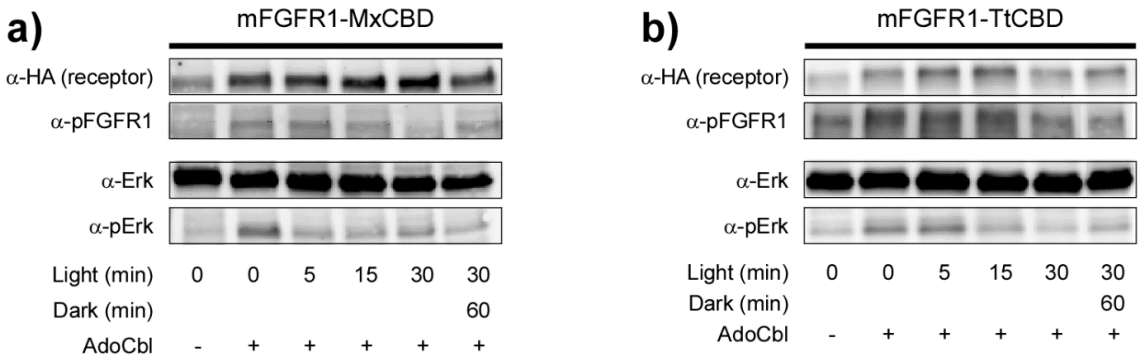

Figure 12: Temporal kinetics of inactivation of mFGFR1-MxCBD and mFGFR1-TtCBD. Phosphorylation of Erk and mFGFR1-MxCBD (a) or mFGFR1-TtCBD (b) in response to green light (0 to 30 min and after 60 min dark recovery, λ = 545 ± 5 nm, I = 170 µW cm^{-2}).

3.3.3. Temporal precision of light-induced signalling inhibition

We also explored temporal precision of light-induced receptor and downstream signaling inactivation. Using immunoblotting, we confirmed that receptors and the downstream signaling protein Erk are phosphorylated in the dark in the presence of AdoCbl, with phosphorylation decreasing to baseline levels (comparable to unsupplemented cells) within 5 min of green illumination for Erk and 30 min for mFGFR1. This result also indicates that dissociated receptors remain phosphorylated without downstream signal propagation. We also investigated recovery of phosphorylation upon cessation of illumination. When placed in the dark for 60 min after 30 min illumination, mFGFR1-MxCBD phosphorylation recovered to 86% of the original value, whereas no recovery was observed for mFGFR1-TtCBD (Figure 12 a and b, Figure 13 a and b). We investigated the molecular mechanism underlying this difference, which we hypothesized to reflect the ability of CBDs for cofactor exchange. For TtCBD, it was shown that the corrin ring of AdoCbl forms a stable adduct with a histidine residue (H132; in full length CarH) preventing release of bleached cofactor from its binding pocket.[128] Indeed, substitution of this residue in mFGFR1-TtCBD (H497A) allows recovery of phosphorylation (Figure 13 c and Figure 14; substitution of the corresponding glutamate residue in mFGFR1-MxCBD to a histidine (E499H) diminished activity preventing detailed analysis). Thus the CBDs can provide reversible or irreversible optical control of protein complex dissociation.

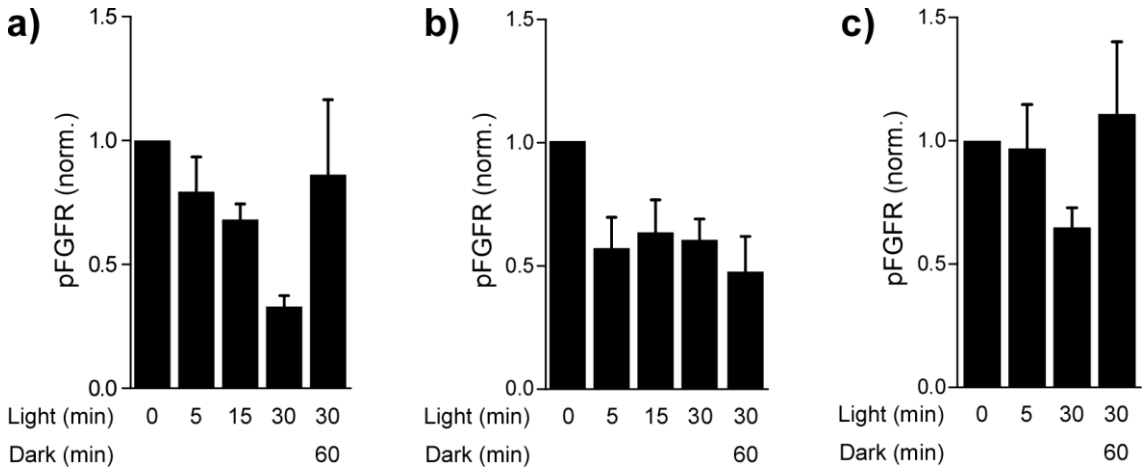

Figure 13: Quantification of immunoblot data. Receptor phosphorylation in HEK293 cells transfected with mFGFR1-MxCBD (a), mFGFR1-TtCBD (b) or mFGFR1-TtCBD-H497A (c) was quantified by band intensity. Shown are mean values ± SEM for three to four independent experiments.

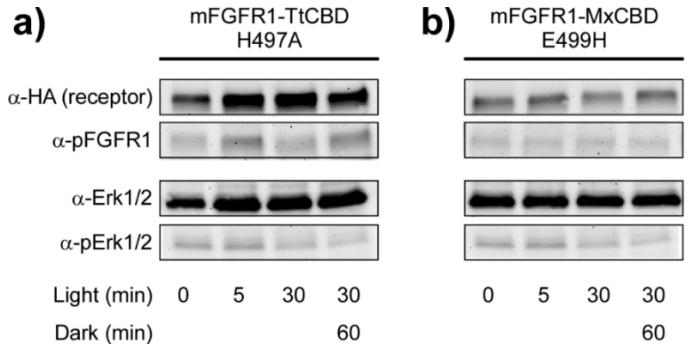

Figure 14: Temporal kinetics of inactivation of CBD mutants. Phosphorylation of Erk and mFGFR1 in HEK293 cells transfected with mFGFR1-TtCBD with H497A substitution (a)) or mFGFR1-MxCBD with E499H substitution (b)) in reponse to green light (5 or 30 min) and after dark recovery (60 min).

3.3.4. Light-dependent manipulation of zebrafish embryogenesis

To assess the potential of CBDs for optogenetics in vertebrates, we chose to employ mFGFR1-MxCBD to manipulate zebrafish (*Danio rerio*) embryogenesis, as FGF is an important signalling axis during vertebrate development.[263,264] We first investigated if mFGFR1 is functional in zebrafish. Transient overexpression of the constitutively active mFGFR1-IgG caused developmental malformations such as caudalization of the brain and formation of a secondary axis, similar to constitutively active zebrafish FGFR1[263] (Figure 15 a and b). We next confirmed that injection of AdoCbl and mFGFR1-MxCBD alone did not negatively impact animal development (Figure 15 c and d). To demonstrate light control over mFGFR1-MxCBD signalling, we raised animals injected with receptor and AdoCbl either in the dark or in green light (λ = 545 ± 5 nm, I = 180 µW cm^{-2}). In the dark they showed malformations comparable to animals injected with mFGFR1-IgG, suggesting a similar constitutively active mode of action, whereas embryos treated with green light did not show any abnormalities, demonstrating that mFGFR1-MxCBD signalling can be turned off by green light *in vivo* (Figure 15 e and f). These results indicate that MxCBD is functional in a vertebrate model organism and mFGFR1-MxCBD promises temporal control to investigate consequences of aberrant FGF signalling during targeted periods of development.

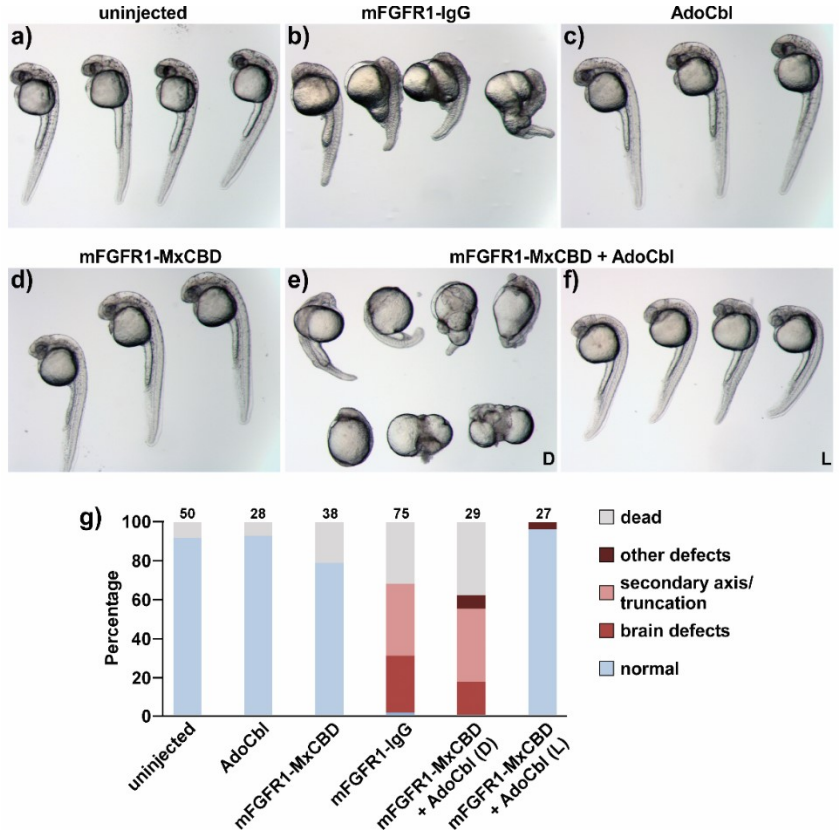

Figure 15: Light-dependent rescue of embryonic phenotypes of constitutively active mFGFR1 signalling. Embryos were a) uninjected or injected at the one cell stage with b) constitutively active mFGFR1-IgG (13 pg plasmid), c) AdoCbl (50 fmoles), d) mFGFR1-MxCBD (13 pg plasmid), e) mFGFR1-MxCBD (13 pg plasmid) and AdoCbl (25 fmoles) raised in the dark (D), and f) mFGFR1-MxCBD (13 pg plasmid) and AdoCbl (25 fmoles) raised in green light (L, 545 $\pm$ 5 nm, I = 180 μW cm^{-2} from 1 to 24 hpf). Images were recorded at 24 (a,c,d) and 30 hpf (b,e,f). g) Quantification of phenotypes (numbers denote number of embryos).

3.4. Discussion

Optogenetics and photopharmacology provide spatio-temporally precise control over protein interactions and protein function in cells and animals. Optogenetic methods sensitive to green light and for breaking protein complexes are not broadly available but would permit multichromatic experiments of previously inaccessible biological targets. Here, we repurposed cobalamin (vitamin B12)-binding domains of bacterial CarH transcription factors for green light-induced receptor dissociation. We show that CBDs allow dissociation of protein complexes by green light. Dark-promoted activation of mFGFR1-CBDs in human cells and zebrafish embryos resulted in constitutively active signalling and abnormal phenotypes that were abolished by green light. Generation of such signals with conventional optogenetic tools would require constant illumination with risk of bleaching, phototoxicity, and a necessity to track animals. We showed that green light abolished receptor activity either reversibly or irreversibly and with potential for multichromatic experiments. CBDs critically expand the repertoire of photoreceptor domains in optogenetics, and will enable new approaches for cell-based and animal studies.

Chapter 4: Engineering and characterization of a chemically inhibited de-dimerizer

4.1. Introduction

PPIs are a core mechanism that underlies the regulation of a wide range of cellular processes. For instance, non-covalent, transient binding of protein domains mediates protein localization, enzymatic activity, recognition of extracellular signals and downstream transduction, as well as regulation and initiation of transcription via transcription factors and chromatin modifiers.[265] In order to understand the link between binding events and cell and organism-wide functional outcomes, genetically encoded synthetic biology tools have been developed that facilitate both the observation as well as direct manipulation of PPIs.[15] Chemogenetic tools utilize small molecules as triggers, which can be applied for prolonged periods of time and can spread systemically in organisms, and optogenetic tools recognize light as trigger, which is beneficial for fast and precise control of PPIs.

Among existing chemogenetic tools, the small protein FKBP (FK506 binding protein) is commonly used to induce homo-dimerization or hetero-dimerization with its native binding partner FRB.[167] Both domains are endogenous in humans, and consequently both application of FKBP/FRB binding drugs, such as rapamycin[181] as well as introduction of FKBP as a transgene itself[266] can result in undesired cross-talk. Consequently, a repertoire of rapalogues for heterodimerization and SLFs (synthetic ligands of FKBP) for homodimerization have been developed to target FKBP with high specificity.[15,267] The F36V mutation was introduced in FKBP to further reduce the affinity to FRB and facilitate induction of homo-interaction.[172,268,269]

In another system for chemically-induced hetero-dimerization methotrexate *(*MTX) or trimethoprim (TMP) have been combined with dexamethasone (DEX) into hetero-bifurcational molecules to allow dimerization of DHFR and glucocorticoid receptor (GR).[196,197] MTX and TMP have also been combined with SLF[192,194,200,270,271] to induce formation of dimers or small oligomers, while SLF fused to the dye Congo Red can fuse FKBP to dimers or small oligomers of the Aβ peptide involved in Parkinson's disease to prevent their aggregation. [272] FKBP has also found clinical application, through fusion to Caspase 9 (Casp9), to create a chemically inducible "kill switch" for cell therapy.[189,273]

The small plant phytohormone S-(+)-abscisic acid (ABA) serves as a hetero-dimerizer for a pair of plant-derived protein domains PYL1 and ABI1.[203] This system has successfully been employed *in vivo* in mice to study the dynamics of histone modifications.[274] A derivative of the phytohormone gibberellin has also been employed for chemically-induced hetero-dimerization, and has found application in tandem experimental designs with rapamycin/FKBP.[210]

Recent methodologies employing FKBP alone or with hetero-bifunctional fusions of SLF and other small molecules, showcase further powerful implementations of chemically induced dimerization. They have collectively been used in dozens of studies and groups *in vitro* and *in vivo* for a variety of purposes, such as investigation of signalling dynamics,[275-277] to control

protein expression,[278] to target histone modification[274] and nuclease activity[279] and to control split fluorescent protein assembly.[280]

While these methods are well characterized and established to *induce* interaction of target proteins, tools capable of *disrupting* PPIs with the same high fidelity are much less available. An F36M mutant of FKBP was employed for ligand-reversible aggregation. While the crystal structure of the mutant shows formation of an anti-parallel dimer, at least three sequential copies of the gene are required to induce significant interaction of a fused protein in cell based assays, and proteins with more than three copies are prone to aggregation into higher order oligomers of unknown stoichiometry.[176,281]

The fast reversible chemical dimerizer rCD1 is a modified SLF with a bimodal binding capability. In this system, a POI (protein of interest) is tagged with an FKBP domain, and upon addition of rCD1 can be recruited to a SNAP-tagged protein partner, e.g. for targeted localization or translocation.[282] FK506 competes with rCD1 for binding to FKBP, and can be added to quickly release the POI from the SNAP-tagged interaction partner.[283] Whereas both FKBP domain and SNAP tag are well characterized, using them for the rCD1 system prevents their use on other POIs in tandem experimental designs. The system consists of four components – FKBP, SNAP and two competing ligands with differential binding kinetics - additionally complicating transgene design, in particular for homo-interactions.

Among the synthetic biology toolbox, tools to break non-covalently linked dimers or oligomers of known stoichiometry are still lacking, but desirable for controlling cellular events where an initially formed PPI shall be disrupted, such as extinction of a signalling pathway, or conditional suppression of an otherwise constitutive process. An ideal chemogenetic tool to control PPIs should be well characterized in its structure and modality of interaction, react to a molecule that is well-tolerated and orthogonal to endogenous signals, and be applicable *in vitro* and *in vivo* without toxicity.

Here, we present a novel synthetic tool for chemically induced dissociation based on the mycobacterial flavin/deazaflavin oxyreductase (FDOR) MSMEG_2027. FDORs are a large superfamily of structurally related bacterial enzymes involved in heme degradation, biliverdin reduction, fatty acid modification, and quinone reduction, and utilize flavin cofactors. MSMEG_2027 from *Mycobacterium smegmatis* has been shown to endogenously function as a quinone reductase and binds F_{420}, a flavin derivative exclusively synthesized by bacteria and archea, with high specificity.[284-286] We utilized novel structural insights about the protein in presence and absence of its cofactor, to design a chemogenetic tool that functions as a chemically induced de-dimerizer (CDD). We employ the CDD to induce constitutive activity in an important prototypical receptor for cell growth and survival (Fibroblast Growth Factor Receptor1 (FGFR1)) and show specific signalling inhibition by F_{420} treatment in mammalian cells.

4.2. Methods

4.2.1. CDD synthetic gene

A synthetic gene fragment, termed CDD, encoding residue 2 to 140 of MSMEG_2027 (nitroreductase family deazaflavin-dependent oxidoreductase of *M. smegmatis*, UniProt A0QU01) was obtained with mammalian codon optimization (*H. sapiens*) following the manufacturer's recommendation (Bioneer, Daejeon, Korea) (Table 3). The fragment was amplified using PCR with overhanging recognition sequences for restriction enzyme ClaI (oligonucleotides 15 and 16, Table 4), or AgeI and XmaI (oligonucleotides 17 and 18, Table 4).

4.2.2. mVenus, FGFR1 and Casp9 fusion proteins

For expression and viability testing, 2027 was inserted into the AgeI restriction site of a previously described expression plasmid in pcDNA3.1(-)[62] that contains the fluorescent protein mVenus (mV)[258] followed by a glycine- and serine-rich linker and a BspEI restriction site. A previously described mV-FKBP fusion protein was used as positive control. [62]

To generate chimeric, de-dimerizing receptors, CDD was subcloned into a plasmid encoding the ligand binding and transmembrane domains of p75 (low affinity nerve growth factor receptor) and the kinase domain of murine FGFR1 in a pcDNA3.1(-) backbone (termed p75_FGFR1). CDD was inserted at a ClaI restriction site previously introduced between the signaling peptide of p75 and the start of the extracellular domain through inverse PCR (oligonucleotides 19 and 20, Table 4), yielding CDD_FGFR1.

Point substitution R599E (numbered relative to the start codon of the fusion receptor) was introduced in CDD_FGFR1 using site-directed mutagenesis PCR (oligonucleotides 21 and 22, Table 4). The charge inversion substitution (R195E in full length murine FGFR1; R599E in our fusion receptor) prevents formation of a functionally essential, asymmetric kinase domain dimer in FGFR1[239] and was used as a probe for dimer formation during receptor signaling. The resulting construct was termed CDD_FGFR1_R599E.

As a positive control construct, the Fc portion of human IgG1 (residues 230 to 461 of NCBI GenBank sequence KU951249.1 with an additional Cys to Ser substitution) was amplified from human cDNA using PCR (oligonucleotides 23 and 24, Table 4) and inserted into p75_FGFR1 at an AgeI restriction site C-terminally of the mFGFR1 kinase domain. The resulting construct yields a covalently linked receptor dimer that acts as a constitutively active signaling complex[263] termed FGFR1_IgG. All constructs were verified by DNA sequencing. Protein sequences are summarized in Table 5.

4.2.3. Cell culture and transfection

HEK293 cells were maintained in full medium (DMEM supplemented with 10 % FBS, 100 U/ml penicillin and 0.1 mg/ml streptomycin) at 37 °C in a humidified incubator with 5% CO_2. All transfections were carried out in transfection medium (DMEM supplemented with 5 % FBS)

using PEI (Polysciences, Hirschberg an der Bergstrasse, Germany) as previously described.[287] Experiments were conducted in 96-well clear bottom plates coated with poly-L-ornithine.

4.2.4. Fluorescent fusion proteins, expression, and Resazurin viability testing

For F_{420} toxicity testing, 5 x 10^4 HEK293 cells were seeded per well and after 6 h were treated with medium supplemented with 10% vehicle or F_{420}. A positive control was treated with 10% DMSO. For expression and domain toxicity testing, 5 x 10^4 HEK293 cells were transfected with 100 ng expression plasmid encoding mVenus fusions. Expression was assessed using mVenus fluorescence in a microplate reader 30 h after transfection. Viability was assessed as metabolic activity using Resazurin.[288] Cells were incubated for 1 h with Resazurin (0.01 mg/ml), and fluorescence of the metabolic product Resorufin was read at ex/em 540/590 nm in a microplate reader. Fluorescence microscopy images were recorded on a digital microscope (Nikon Eclipse Ti-S) 30 h after transfection.

4.2.5. F_{420} Uptake

To measure F_{420} uptake, 50.000 HEK293 cells were seeded per well, after 6 h washed with DPBS and treated with Leibovitz (L-15) medium supplemented with 10% vehicle or F_{420}. After 16 h, cells were washed with DPBS and lysed in 40 µL lysis buffer (36 mM Tris-Cl, 14 mM Tris-Base, 25 mM NaCl, 1 mM $MgCl_2$, 0.08 % Triton-X in H_2O). A standard curve of 0.3 – 30 µM F_{420} in lysis buffer was prepared in empty wells, and ex/em 430/480 was measured in a microplate reader (CLARIOstar Plus, BMG Labtech). The standard curve was used to correlate the measured relative fluorescence (RFU) to n (number of F_{420} molecules per well), e.g. 40 µL lysis buffer containing 30 µM F_{420} corresponds to 1200 pmol. Linear regression of standards and quantification of unknowns was performed in GraphPad Prism. Cellular concentration of F_{420} was determined with respect to the theoretical volume of all cells in the well. An exemplary calculation is presented in the following. 6.13 pmol were measured in the lysate of 50000 cells treated with + 10 µM F_{420} (average of three replicate wells in three experimental runs). This corresponds to $1.2 \cdot 10^{-4}$ pmol or $1.2 \cdot 10^{-16}$ mol per cell. The volume of a HEK293 cell, assuming a diameter of 15 µm,[289] is 1767 μm^3, or $1.77 \cdot 10^{-15}$ L. From $1.2 \cdot 10^{-16}$ mol per $1.77 \cdot 10^{-15}$ L we determine a cytosolic concentration of $6.94 \cdot 10^{-2}$ mol/L or 69 mM.

4.2.6. MAPK/ERK pathway activation (luminescence)

Activation of the MAPK/ERK pathway was assessed with the PathDetect Elk1 *trans*-Reporting System (Agilent, Vienna, Austria) containing firefly luciferase. In brief, 5 x 10^4 HEK293 cells per well were transfected with 213 ng DNA (200 ng *trans*-activator, 10 ng *trans*-reporter, 3 ng receptor) and 1000 ng PEI per well. After 6 h transfection medium was changed to starve medium (0.5 % FBS) with 10% vehicle (Tris-Cl pH 7.5), F_{420} (concentration as indicated) or 10 µM FMN (flavin mononucleotide), FAD (flavin adenine dinucleotide) or FO (a metabolic precursor of F_{420}). Cells were incubated for another 16 h, and luciferase expression was

assessed with a homemade dual-luciferase assay reagent.[242] Luminescence was measured in a microplate reader (CLARIOstar Plus, BMG Labtech).

4.2.7. *In vivo* toxicity testing in zebrafish

Animal experiments were performed my Catarina Sturtzel, St. Anna Children's Cancer Research Institute, Vienna. Zebrafish (*Danio rerio*) were maintained at standard rearing conditions[259,260] and according to the guidelines of the local authorities under licenses GZ:565304/2014/6 and GZ:534619/2014/4. F_{420} intracellular toxicity *in vivo* in zebrafish embryos was determined by injecting 1 nl of F_{420} dissolved in ultrapure water. Injections were performed at the one-cell stage using injection capillaries (glass capillaries pulled with a needle puller; P-97, Sutter Instruments, Novato, CA) mounted onto a micromanipulator (World Precision Instruments Inc., Berlin, Germany) and connected to a microinjector (FemtoJet 4i, Eppendorf, Hamburg, Germany). After injection, zebrafish were kept in petri dishes at 28°C. Viability was assessed 24 h and 48 h after injection and live and dead embryos counted. Images of zebrafish embryos were recorded using a stereomicroscope (M125 with LAS software, Leica Microsystems, Wetzlar, Germany).

4.3. Results

4.3.1. Expression of MSMEG_2027 in eukaryotic cells

The crystal structure of MSMEG_2027 revealed that the protein exists as a dimer in absence of its cofactor F_{420}.[290] The N-terminal loop of one domain threads into the cofactor binding pocket of another, resulting in a parallel, head-to-head dimer. In presence of the ligand, the cofactor blocks the pocket and the protein exists in a monomeric state. These features of MSMEG_2027 suggested it as a suitable candidate for a chemically induced de-dimerizer (CDD), a novel synthetic tool that can be fused to a protein of interest to mediate dimer-formation and allow induction of breakage into monomers. However, prokaryotic enzymes of this family have not been harnessed for synthetic biology applications before.

We first evaluated whether MSMEG_2027 can be expressed in eukaryotic cells which are the target of many synthetic biology protein domain control tools. For this, we fused the mammalian codon optimized MSMEG_2027 gene (see Supplementary information for details) with a fragment encoding the small fluorescent protein mVenus in a mammalian expression vector followed by transient transfection into HEK293 (human embryonal kidney) cells. mVenus serves as a marker to quantify expression and visualize localization or clustering, and HEK293 cells were chosen because they represent a common model system for *in vitro* studies. We fused mVenus N or C-terminally to the domain because we suspected the implication of the N-terminal loop in dimerization could potentially impact expression and clustering of the domain in the cytosol. mVenus fused to FKBP was used as a control, due to its similar size and wide application in synthetic systems. We found that both N- and C-terminally fused MSMEG_2027 express efficiently and uniformly throughout the cytosol (Figure 16 a, Figure 17).

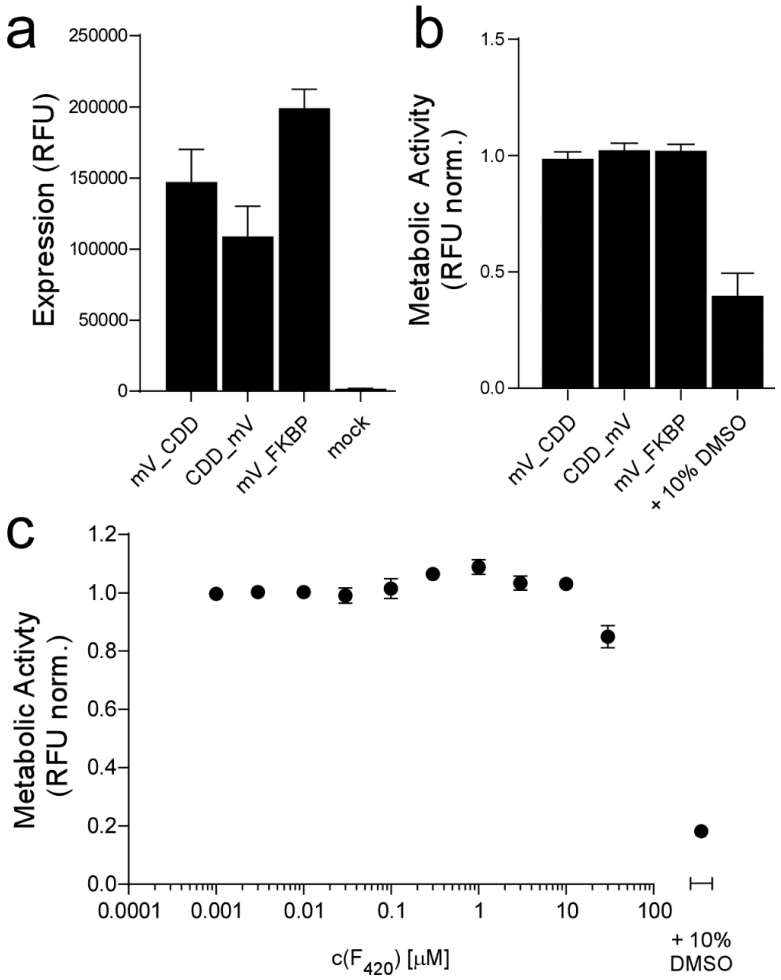

Figure 16: Expression efficiency and viability testing of CDD fusions and F_{420} treatment. a) Expression efficiency (measured as RFU = relative fluorescence units) of N- or C-terminally mVenus (mV)-tagged CDD in HEK293 cells compared to mV-tagged FKBP expressing and mock transfected cells. b) Viability (measured as metabolic activity) of HEK293 cells expressing mV-tagged CDD and FKBP, compared to a 10% DMSO treated control with reduced viability, normalized to mock transfected condition. c) Viability (measured as metabolic activity) of HEK293 cells upon 24 h treatment with F_{420}, compared to a 10% DMSO treated control. Mean values ± SEM for three independent experiments, each performed in triplicate, are given.

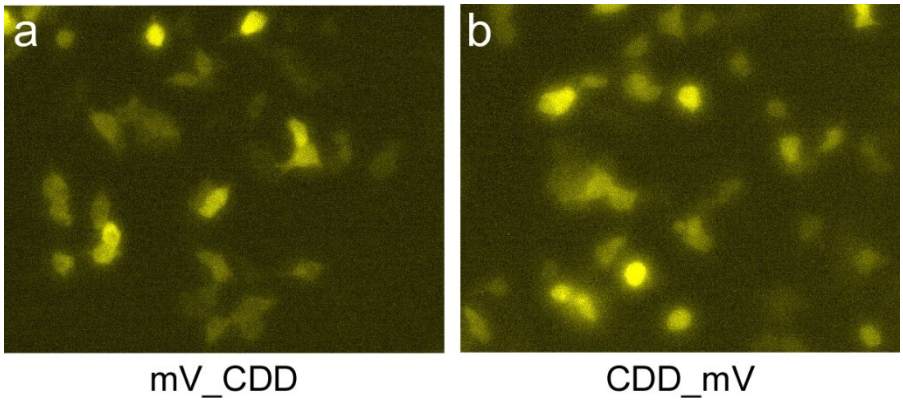

Figure 17: Representative fluorescence microscopy images of HEK293 cells expressing mV_CDD and CDD_mV.

We next validated that intracellular expression of MSMEG_2027 does not impact cell viability. Viability was assessed as metabolic activity through conversion of resazurin to resorufin as in our previous work on synthetic tools.[126,231,287] 24 h after transfection, cells transfected with mVenus-tagged MSMEG did not show reduced resorufin values compared to mVenus-tagged FKBP suggesting that there is no negative effect of MSMEG expression (Figure 16 b).

4.3.2. Cofactor F_{420} treatment and uptake

F_{420} is a 5-deazaflavin compound that serves as a rare catalytic cofactor in redox reactions in some bacteria and archaea.[285] Although the similarity to related cofactors is limited, we verified that F_{420} does not exhibit toxicity in eukaryotic cells, e.g. by interfering with critical flavin dependent processes. Indeed, treatment with F_{420} for 24h was well tolerated and did not impact metabolic activity, which we used as a measure for viability (compared to a vehicle treated control) (Figure 16 c). We chose 10-30 µM as a working concentration for all subsequent experiments.

To test the potential for an *in vivo* application, we also tested for lethality of F_{420} in zebrafish embryos. Up to 10 µM of compound led to no significant decrease in viability or developmental defects five days after injection at the one cell stage (Figure 18).

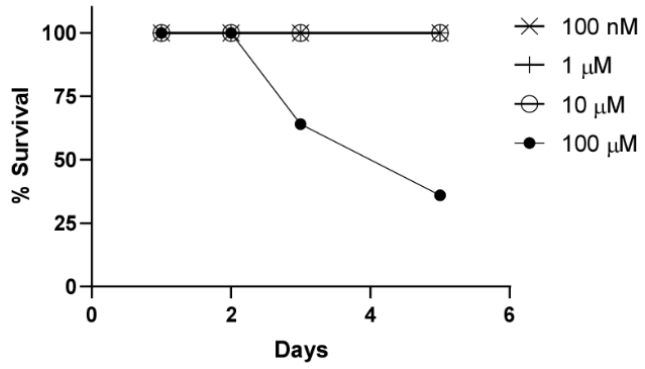

Figure 18: Survival of embryos following injection of varying concentrations of F_{420} at the one cell stage (n = 17).

Use of MSMEG and F_{420} would be most powerful if both inside and outside of cells, and we therefore tested uptake of F_{420} into HEK293 cells. Taking advantage of the characteristic fluorescence (ex/em 420/475 nm) of the compound, we established a fluorescent assay for uptake quantification. We first determined the detection limit of F_{420} in solution in a plate reader and found a linear relationship between 4–1200 pmol of compound and fluorescence emission (Figure 19 a, see section 4.2.5 for example calculation). We then incubated HEK293 cells with F_{420} at varying concentrations. After 24 h, we quantified F_{420} both in the supernatant and cell lysate and detected millimolar intracellular concentrations of F_{420} upon treatment with micromolar concentrations of the cofactor (Figure 19 b). This high intracellular concentration, and the large size and polarity of F_{420} which likely do not permit passive diffusion through the membrane, indicate that F_{420} is subject to active uptake, possibly via a flavin-transporter. Compared to cellular concentration of other flavins, F_{420} is taken up with high efficiency, while the highly specific affinity of MSMEG_2027 to F_{420} ensures orthogonality of the system even in the presence of cellular FMN and FAD. [284,291]

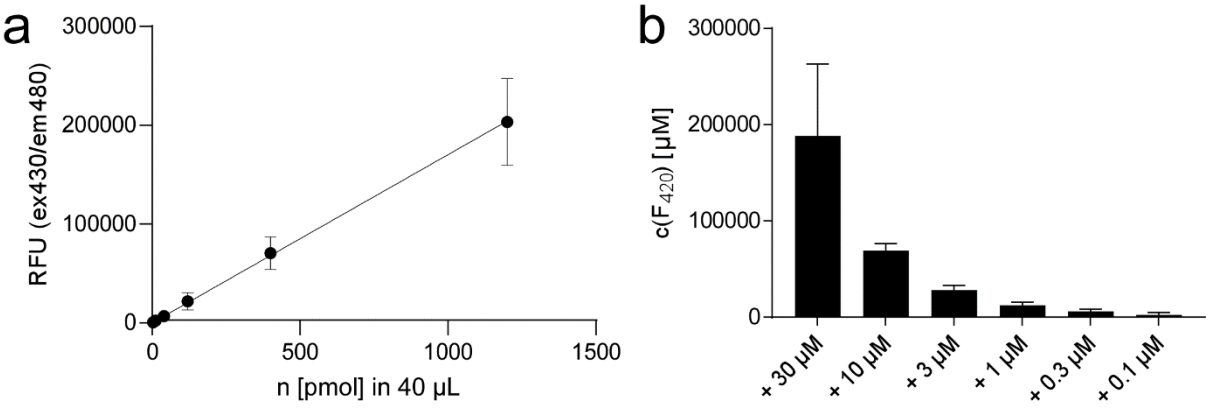

Figure 19: Quantification of F_{420} uptake. a) Representative standard curve for F_{420} quantification in lysis buffer, demonstrating a linear relationship between F_{420} content and fluorescence. b) Cytosolic concentration of F_{420} measured from cell lysate after 24 h of treatment as indicated. Data shown as mean ± SEM for three independent experiments, each performed in triplicate.

4.3.3. MSMEG_2027 induced activity and F_{420}-induced release of a kinase receptor

To demonstrate applicability of MSEMG_2027 as a chemically induced de-dimerizer (CDD), we created a fusion receptor for chemically induced signalling inhibition. Fibroblast Growth Factor Receptor 1 (FGFR1) is a prototypical Receptor Tyrosine Kinase (RTK). It has been previously shown that FGFR1 and other RTKs are activatable by forced dimerization[94,126,167,231,238,287] and their roles in development and disease make them interesting targets for synthetic manipulation.[292] Our chimeric receptor CDD_FGFR1 consists of an N-terminal fusion of CDD to the intracellular domain of the murine FGFR1 kinase domain (KD) and C-terminus with phosphorylation sites, via p75, which serves as a transmembrane anchor and renders the receptor irresponsive to its endogenous ligand FGF.[293]

We hypothesized that attachment of CDD to FGFR1 will result in formation of a constitutive dimer upon expression, which should manifest through activation of the MAPK/ERK pathway

and should be disrupted by the addition of F_{420} (Figure 20 a). Indeed, in HEK293 cells CDD_FGFR1 activated the MAPK/ERK pathway to a similar extent as a constitutively active control receptor (FGFR1_IgG). In a next step, we tested that this activity is inhibited by addition of F_{420} and we observed that signalling of CDD_FGFR1 was reduced to levels comparable of a purely monomeric control receptor (p75_FGFR). As a probe for dimer formation during receptor signalling, we employed a charge inversion substitution (R499E numbered form the start of the construct, see Methods) in the FGFR1 kinase domain that prevents formation of a functionally essential, asymmetric dimer.[239] Indeed, CDD_FGFR1_R499E does not activate the MAPK/ERK pathway (Figure 20 b), illustrating that activity of CDD_FGFR1 is a specific effect of receptor dimerization through the CDD, and can efficiently be abolished by addition of F_{420}.

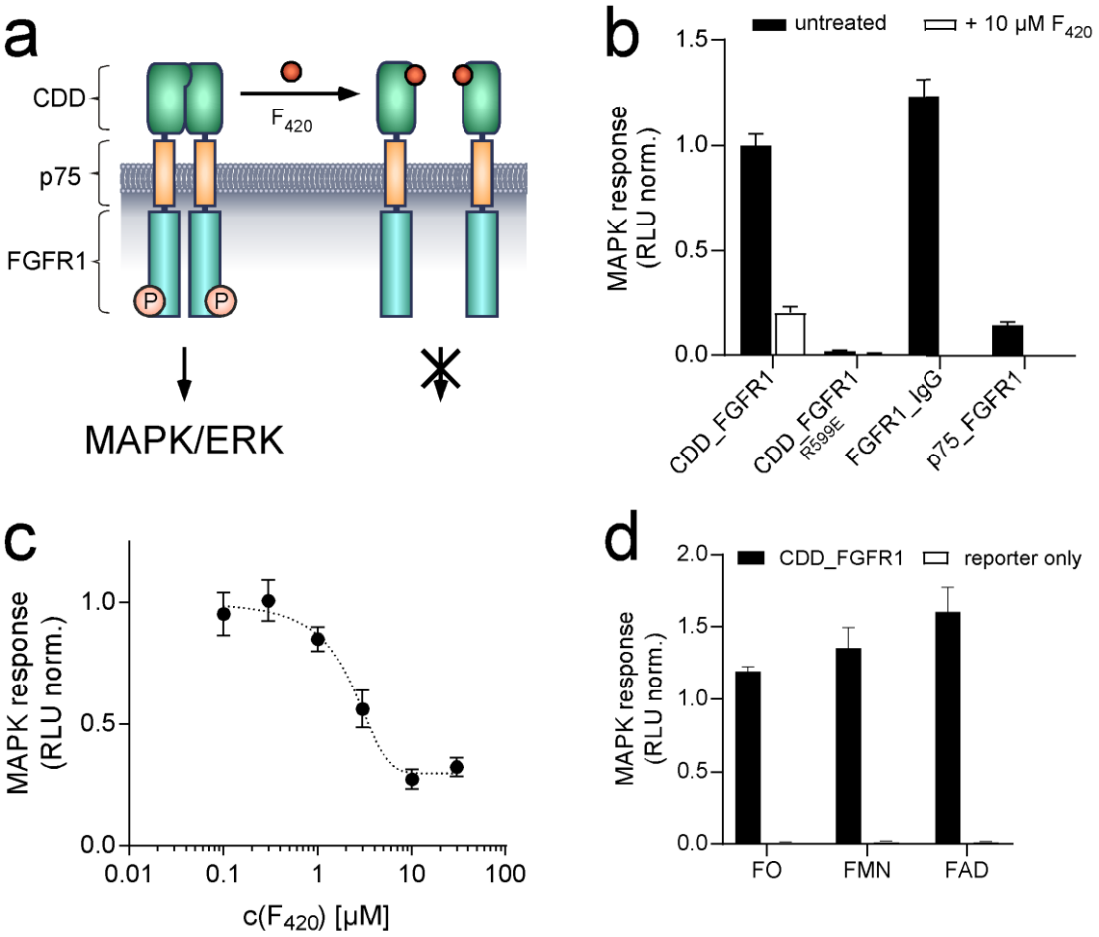

Figure 20: F_{420}-mediated inhibition of a synthetic FGFR1 receptor. a) CDD was fused to p75-FGFR1 to create a synthetic receptor, termed CDD_FGFR1, that is constitutively signalling until inactivated by F_{420} treatment. b) Activation of the MAPK/ERK pathway (RLU = relative luminescence unit, normalized to CDD_FGFR1) by FGFR1 fused to CDD, the Fc domain of IgG1 (IgG), or without fusion, in response to treatment with 10 µM F_{420}. c) MAPK response of CDD_FGFR1 to an increasing dose of F_{420}. d) MAPK response of CDD_FGFR1and reporter only transfected cells to 10 µM FO, FMN and FAD. Data normalized to respective vehicle (Tris-Cl pH 7.5 for FO, H_2O for FMN and FAD). Mean values ± SEM for three to eleven independent experiments, each performed in triplicate, are given.

4.3.4. Validation of F_{420} orthogonality and specificity in mammalian cells

Due to its natural prevalence in bacterial and archaeal metabolism only, F_{420} is suitable as orthogonal stimulus in eukaryotic systems. However, F_{420} is structurally based on a flavin core ring (isoalloxazine), and flavins are metabolic cofactors in many living systems. We tested above that F_{420} does not impact mammalian metabolism or viability, and we next aimed to validate that the observed inhibition of MAPK/ERK signal is a specific effect of both CDD and F_{420}.

When testing a range of F_{420} concentrations on CDD-FGFR1 expressing cells, we observed a dose-dependent reduction in MAPK/ERK pathway activity, where 10 µM proved sufficient to inhibit the MAPK signal to a basal level (Figure 20 c). Cells transfected with MAPK/ERK reporter only did not show any response to F_{420} (Figure 21 a), and cells transfected with FGFR1_IgG or FGFR1_mono did not respond to F_{420} treatment with signalling inhibition (Figure 21 b).

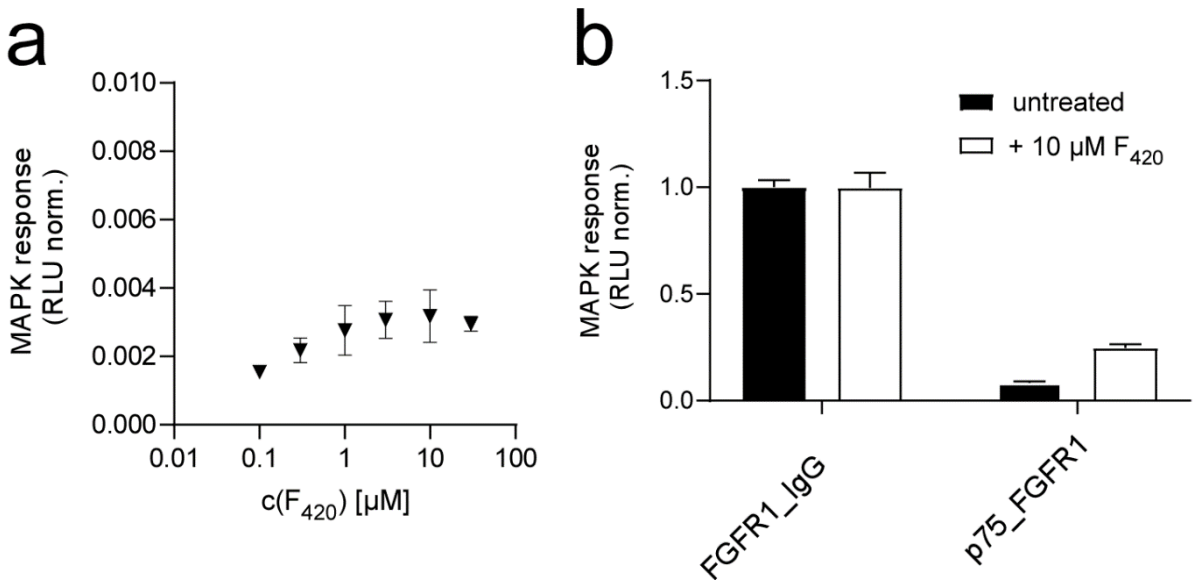

Figure 21: MAPK pathway response to F_{420}. a) MAPK response of reporter only transfected HEK293 cells upon treatment with F_{420}. Data normalized to untreated FGFR1_IgG cells which were used as a maximum signalling control. Mean ± SEM for three independent experiments each performed in triplicate. b) MAPK response of HEK293 cells expressing FGFR_IgG or p75_FGFR, upon treatment with 10 µM F_{420}. Data normalized untreated FGFR1_IgG for each experimental run. Mean ± SEM for three independent experiments each performed in triplicate.

Since the core ring of F_{420} is an isoalloxazine moiety, we tested the response of CDD_FGFR1 to other flavin-based compounds. FMN (flavin mononucleotide) and FAD (flavin adenine dinucleotide) are metabolic cofactors in all living systems. F_0 is a chemical precursor of F_{420} consisting of just the core ring without phosphate, lactyl group and polyglutamate chain, and is structurally similar to FMN. F_0, FMN or FAD showed no inhibition of the MAPK/ERK pathway in CDD-FGFR1 transfected cells (Figure 20 d). Thus, F_{420} acts orthogonally and specifically on breaking the dimerization of the CDD.

4.4. Discussion

Expanding the "synthetic biology toolbox" with a variety of different domains that recognize unique orthogonal cues is a vital prerequisite to delineate the sequence of events and kinetics of complex processes. Here, we showed that the mycobacterial protein MSMEG_2027 can be repurposed as a tool for synthetic biology with a distinct, novel mechanism. Our tool, termed CDD, forms a homodimer that can be disrupted upon addition of the flavin-derivative F_{420}, and combines several highly desirable properties. The cofactor F_{420} is of non-eukaryotic origin, easy to produce and purify, and exhibits no crosstalk or toxicity, making it applicable to a wide range of biological model organisms. Structurally, the binding interface of F_{420} in the pocket of CDD has been resolved, facilitating further design choices.

We show here that CDD expresses well and safely in cells and *in vivo*, and that the structural properties of the domain can be harnessed to regulate PPIs. Upon expression, the CDD forms homo-dimers and can thereby mimic constitutive activity of processes such as cell signalling or apoptosis. Upon addition of sufficient F_{420}, which binds to the domain with high affinity, the interaction can be broken and the process disrupted. The system does not require genetic fusion of target proteins, works independent of enzymatic cleavage, and requires the addition of only one type of molecule to achieve a graded response.

In the rCD1 system, the PPI is disrupted when FK506 displaces rCD1, a hetero-bifurcational fusion of an FKBP and SNAP-tag ligand. The system relies on two different chemical ligands, and the temporal kinetics of the process (dimer induction with rCD1 within 5 to 30 min, and disruption within minutes after addition of FK506)[282] require a distinctly higher affinity of FK506 to FKBP.[283]

In contrast to ubiquitin ligase-based systems, such as PROTACs (hetero-bifurcational molecules targeting E3 ubiquitin ligase to a POI to mark it for degradation)[294] our tool directly mediates interaction of a fused POI and allows its disruption, and does not require the use of different molecules to specifically target different POIs.

Protease-based approaches allow disruption of protein function through induced polypeptide cleavage. In the StaPL system, two POIs are fused via the StaPL module which can be targeted by NS3 protease from Hepatitis C virus. In presence of a drug, catalytic cleavage is inhibited.[295,296] A recently developed system termed PROCISiR allows for multi-input chemical control of several signalling pathways in tandem. Engineered protein interfaces interact with different drug-bound states of NS3 protease to create a platform for multiple input-output control. The system uses clinically approved drugs and is capable of generating proportional and graded control over the transcription and cellular signalling downstream of receptors.[297] However, methods based on proteolytic cleavage do not permit the direct manipulation of PPIs, and instead irreversibly destroy a genetically encoded peptide bond, which can be challenging to design if the POIs are dynamically interacting partners, such as cell surface receptors. Furthermore, breakage of the PPI relies on an enzymatic process, whereas the CDD/F_{420} system functions solely through competitive binding.

Light sensitive derivatives of rapamycin have been developed that can be cleaved[184,298] or isomerized between an active and inactive state[299] upon illumination, providing an additional

level of control over the previously induced PPI. Conversely, the initial interaction in our system is immediate (constitutive), and exclusively mediated by a newly introduced protein domain in a structurally and stoichiometrically defined manner, similar to our previously described optogenetic tool CBD.[287]

In nature, graded responses are prevalent for the formation and regulation of complex processes, but are difficult to achieve through application of conventional synthetic tools. Complex synthetic input platforms have been applied in tandem to precisely regulate antagonistic outputs to achieve graded responses of cellular morphology and transcription[296,297] and Boolean logic in synthetic signalling circuits.[211] These applications highlight the importance of having a range of synthetic tools available to manipulate complex processes in parallel and orthogonally not just from the host system but also with minimal crosstalk to each other. Unlike previous tools to break dimers or higher order oligomers[176,281,282] CDD is not based on any other previously used domain or compound, therefore it can easily be incorporated in tandem experimental designs to manipulate PPIs.

In our system, CDD mimics a ligand binding domain rather than working through enzymatic activity, hence we were able to apply it directly at the top of the signalling cascade, at the receptor level. We were able to achieve a graded inhibition of MAPK signalling upon titrating the amount of F_{420} added. As such, our system enables graded output on a population level, consequently opening up the avenue for spatially controlled signalling gradients, similar to endogenous ligands in embryonic development.[300]

We show that our tool can be used to control PPIs and regulate fundamental processes driving cell survival. By providing a completely novel mechanism and chemistry independent from previously described domains, drugs and interaction modes, CDD and F_{420} complement the existing synthetic biology toolbox and can in the future be combined with existing tools, in cells and *in vivo,* for tandem manipulation of processes driven by PPIs.

Chapter 5: Conclusion and Outlook

This work presents two new protein tools that critically expand the repertoire of synthetic tools to control PPIs. CBDs are light-sensing domains that react to green light, thereby filling a gap in the color spectrum relative to existing optogenetic tools. Notably, they are expressed as non-covalently linked oligomers and their interaction is disrupted upon illumination, which makes them particularly relevant for applications in which a constitutive PPI shall be disrupted. Similarly, CDDs provide a system for disruption of a PPI via a small molecule. Together, CBDs and CDDs present novel means to control PPIs *in vivo* and *in vitro*.

Open questions remain as to the nature of CBD interactions in synthetic fusion proteins. Natively, CarH forms dimer-of-dimer tetramers.[128] While we did not observe significant aggregation in the cytosol upon expression of soluble CBD-mVenus fusions, and application for FGFR1 activation only provides evidence that the domains form at least dimers, it is not entirely clear if the domains form dimers or tetramers, which may be relevant for applications where a tightly control stoichiometry is crucial. A mutation of CBDs has been described that prevents tetramer assembly, and results in formation of mere dimers. However, this also drastically reduced binding of the native CarH protein to its cognate DNA sequence, as measured by transcriptional output.[128] This could be a result of lowered affinity to DNA by the dimeric complex, but whether or not a dimeric mutant CBD can function as a CID in synthetic proteins with sufficient affinity remains to be seen.

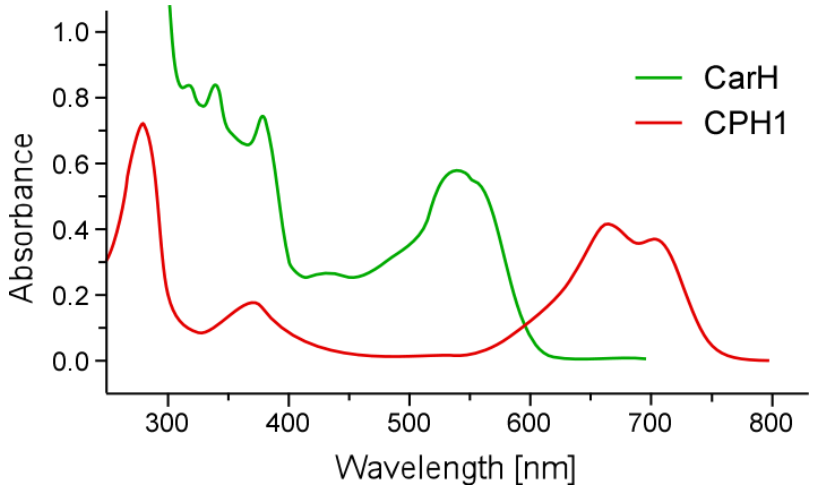

Figure 22: Overlay of absorbance spectra of CarH of *T. thermophilus*[128] and CPH1 of *Synechocystis* sp.[301]

Illumination with green light opens up an avenue for tandem experimental designs with other optogenetic tools, for example the cyanobacterial red-light sensor CPH1 (Figure 22). However, green is also the wavelength of light that is strongest absorbed by mammalian tissue.[302] Consequently, applications *in vivo* might be limited to local delivery of light, e.g. via an implanted light source.[303-305]

The use of a novel cofactor with no toxicity and unique, radical-free photochemistry based on AdoCbl provide the potential for future applications of CBDs in vivo. Notably, while the cofactor must be exogenously supplied for the applications presented here, AdoCbl is generally present in mammalian cells in the mitochondria. Vitamin B12 metabolism within the cell relies on a series of transport proteins and metabolic enzymes.[251] Similar to how the PhyB cofactor PCB was made available in the cytosol by introduction of a synthetic metabolic pathway, engineered transport or metabolic pathways might in the future allow to enrich the cytosol with AdoCbl and circumvent the necessity for supplementation.

CDD presents an exciting addition to the chemogenetic toolbox by providing an unprecedent interaction mechanism that does not rely on any existing chemogenetic system. Structurally, the homo-interaction of CDD is well studied, and evidence from implementation in synthetic FGFR1 illustrates that the interaction is strong enough to mediate dimerization-dependent effects such as cellular signalling. In future experiments, to verify that the N-terminal loop of CDD mediates dimerization, a truncated version of the domain shall act as a negative control, unable to induce MAPK signalling when fused to FGFR1. The crucial role of the N-terminus indicates that CDD fusion to a POI should occur via its C-terminus, however, it remains to be explored if its ability to interact can be sustained by employing linkers of sufficient length.

While the CDD ligand F_{420} has been successfully applied in cell culture with no immediate toxicity, uptake of the molecule is very limited, which hampers potential intracellular applications. One way to improve cellular uptake is esterification. By shielding polar groups, the compound is rendered more membrane permeable. Once inside, cellular esterases cleave the modifications.[306] Improved uptake would allow applications of CDD in the cytosol, for example for transcriptional control or re-constitution of split proteins. While preliminary data *in vivo* shows no toxicity of F_{420} treatment in zebrafish embryos, functional applications of CDD *in vivo* remain to be explored.

Since CDD originates form a bacterial reductase there is a possibility that it exerts its catalytic effect also in mammalian cells. While no negative effect on cellular viability was observed upon expression of CDD fusion proteins, subtle changes in metabolite concentrations might only show upon prolonged expression of CDDs. To avoid any negative impact of CDD expression, targeted mutations to abolish enzymatic activity can be employed. Mutations of the F_{420} binding pocket could abolish F_{420} binding while potentially retaining the ability to dimerize.[290] While these mutants could serve as useful complementary controls for applications of CDD as a synthetic tool, the CDD-FGFR1 fusion receptor itself could additionally serve to interrogate the effect of different mutations of CDD, potentially shining new light on structure-function relationships of the original bacterial protein MSEMG_2027.

An interesting potential application of CDDs *in vivo* is a chemically inhibited Caspase 9 system. The FKBP-based inducible Caspase 9 iCasp9 is activated by treatment with an FKBP ligand to provide a kill switch in T-cell therapy.[189,273,307] CDD and F_{420} could provide an inverse system, in which cells expressing a CDD-Casp9 (dCasp9) fusion are dependent on supplementation with F_{420}. In absence of the cofactor, dCasp9 would be able to dimerize and exert its function as an initiator of apoptosis.

CBDs and CDD both provide a novel interaction mechanism, by mediating a non-covalent PPI that can be disrupted by application of light or a chemical ligand, respectively. They are well-expressed and tolerated *in vitro* and *in vivo*, and their stimuli are orthogonal to endogenous proteins and existing synthetic tools. Future applications of these systems include tandem experimental designs that combine multiple inputs to generate diverse outputs and any applications where a sustained, homomeric PPI requires precise disruption.

References

1 De Las Rivas, J. & Fontanillo, C. Protein-protein interactions essentials: key concepts to building and analyzing interactome networks. *PLoS Comput Biol* **6**, e1000807, doi:10.1371/journal.pcbi.1000807 (2010).

2 Klemm, J. D., Schreiber, S. L. & Crabtree, G. R. Dimerization as a regulatory mechanism in signal transduction. *Annu Rev Immunol* **16**, 569-592, doi:DOI 10.1146/annurev.immunol.16.1.569 (1998).

3 Amoutzias, G. D., Robertson, D. L., Van de Peer, Y. & Oliver, S. G. Choose your partners: dimerization in eukaryotic transcription factors. *Trends Biochem Sci* **33**, 220-229, doi:10.1016/j.tibs.2008.02.002 (2008).

4 Li, P. *et al.* Caspase-9: structure, mechanisms and clinical application. *Oncotarget* **8**, 23996-24008, doi:10.18632/oncotarget.15098 (2017).

5 McLure, K. G. & Lee, P. W. How p53 binds DNA as a tetramer. *The EMBO journal* **17**, 3342-3350, doi:10.1093/emboj/17.12.3342 (1998).

6 Svitkina, T. The Actin Cytoskeleton and Actin-Based Motility. *Cold Spring Harb Perspect Biol* **10**, doi:10.1101/cshperspect.a018267 (2018).

7 Musacchio, A. & Desai, A. A Molecular View of Kinetochore Assembly and Function. *Biology (Basel)* **6**, doi:10.3390/biology6010005 (2017).

8 Liu, Z. *et al.* Programming Bacteria With Light-Sensors and Applications in Synthetic Biology. *Front Microbiol* **9**, 2692, doi:10.3389/fmicb.2018.02692 (2018).

9 Hu, W. *et al.* Optogenetics sheds new light on tissue engineering and regenerative medicine. *Biomaterials* **227**, 119546, doi:10.1016/j.biomaterials.2019.119546 (2020).

10 Mansouri, M., Strittmatter, T. & Fussenegger, M. Light-Controlled Mammalian Cells and Their Therapeutic Applications in Synthetic Biology. *Adv Sci (Weinh)* **6**, 1800952, doi:10.1002/advs.201800952 (2019).

11 Crivat, G. & Taraska, J. W. Imaging proteins inside cells with fluorescent tags. *Trends Biotechnol* **30**, 8-16, doi:10.1016/j.tibtech.2011.08.002 (2012).

12 Thorn, K. Genetically encoded fluorescent tags. *Molecular biology of the cell* **28**, 848-857, doi:10.1091/mbc.E16-07-0504 (2017).

13 Arora, B., Tandon, R., Attri, P. & Bhatia, R. Chemical Crosslinking: Role in Protein and Peptide Science. *Curr Protein Pept Sci* **18**, 946-955, doi:10.2174/1389203717666160724202806 (2017).

14 Guglielmi, G., Falk, H. J. & De Renzis, S. Optogenetic Control of Protein Function: From Intracellular Processes to Tissue Morphogenesis. *Trends Cell Biol* **26**, 864-874, doi:10.1016/j.tcb.2016.09.006 (2016).

15 Rutkowska, A. & Schultz, C. Protein tango: the toolbox to capture interacting partners. *Angew Chem Int Ed Engl* **51**, 8166-8176, doi:10.1002/anie.201201717 (2012).

16 Mathes, T. Natural Resources for Optogenetic Tools. *Methods Mol Biol* **1408**, 19-36, doi:10.1007/978-1-4939-3512-3_2 (2016).

17 Foster, R. G., Hankins, M. W. & Peirson, S. N. Light, photoreceptors, and circadian clocks. *Methods Mol Biol* **362**, 3-28, doi:10.1007/978-1-59745-257-1_1 (2007).

18 Moglich, A., Yang, X., Ayers, R. A. & Moffat, K. Structure and function of plant photoreceptors. *Annu Rev Plant Biol* **61**, 21-47, doi:10.1146/annurev-arplant-042809-112259 (2010).

19 Christie, J. M., Gawthorne, J., Young, G., Fraser, N. J. & Roe, A. J. LOV to BLUF: flavoprotein contributions to the optogenetic toolkit. *Mol Plant* **5**, 533-544, doi:10.1093/mp/sss020 (2012).

20 Conrad, K. S., Manahan, C. C. & Crane, B. R. Photochemistry of flavoprotein light sensors. *Nat Chem Biol* **10**, 801-809, doi:10.1038/nchembio.1633 (2014).

21 Ortiz-Guerrero, J. M., Polanco, M. C., Murillo, F. J., Padmanabhan, S. & Elias-Arnanz, M. Light-dependent gene regulation by a coenzyme B12-based photoreceptor. *Proc Natl Acad Sci U S A* **108**, 7565-7570, doi:10.1073/pnas.1018972108 (2011).
22 Takano, H., Beppu, T. & Ueda, K. The CarA/LitR-family transcriptional regulator: Its possible role as a photosensor and wide distribution in non-phototrophic bacteria. *Bioscience, biotechnology, and biochemistry* **70**, 2320-2324, doi:10.1271/bbb.60230 (2006).
23 Burgie, E. S. & Vierstra, R. D. Phytochromes: an atomic perspective on photoactivation and signaling. *Plant Cell* **26**, 4568-4583, doi:10.1105/tpc.114.131623 (2014).
24 Jenkins, G. I. Structure and function of the UV-B photoreceptor UVR8. *Curr Opin Struct Biol* **29**, 52-57, doi:10.1016/j.sbi.2014.09.004 (2014).
25 Fenno, L., Yizhar, O. & Deisseroth, K. The development and application of optogenetics. *Annu Rev Neurosci* **34**, 389-412, doi:10.1146/annurev-neuro-061010-113817 (2011).
26 Hegemann, P. & Nagel, G. From channelrhodopsins to optogenetics. *EMBO Mol Med* **5**, 173-176, doi:10.1002/emmm.201202387 (2013).
27 Choe, H. W., Park, J. H., Kim, Y. J. & Ernst, O. P. Transmembrane signaling by GPCRs: insight from rhodopsin and opsin structures. *Neuropharmacology* **60**, 52-57, doi:10.1016/j.neuropharm.2010.07.018 (2011).
28 Wu, Y. I., Wang, X., He, L., Montell, D. & Hahn, K. M. Spatiotemporal control of small GTPases with light using the LOV domain. *Methods Enzymol* **497**, 393-407, doi:10.1016/B978-0-12-385075-1.00016-0 (2011).
29 Stierl, M. *et al.* Light modulation of cellular cAMP by a small bacterial photoactivated adenylyl cyclase, bPAC, of the soil bacterium Beggiatoa. *J Biol Chem* **286**, 1181-1188, doi:10.1074/jbc.M110.185496 (2011).
30 Crosson, S., Rajagopal, S. & Moffat, K. The LOV domain family: photoresponsive signaling modules coupled to diverse output domains. *Biochemistry* **42**, 2-10, doi:10.1021/bi026978l (2003).
31 Demarsy, E. & Fankhauser, C. Higher plants use LOV to perceive blue light. *Curr Opin Plant Biol* **12**, 69-74, doi:10.1016/j.pbi.2008.09.002 (2009).
32 Takahashi, F. *et al.* AUREOCHROME, a photoreceptor required for photomorphogenesis in stramenopiles. *Proc Natl Acad Sci U S A* **104**, 19625-19630, doi:10.1073/pnas.0707692104 (2007).
33 Losi, A., Polverini, E., Quest, B. & Gartner, W. First evidence for phototropin-related blue-light receptors in prokaryotes. *Biophys J* **82**, 2627-2634, doi:10.1016/S0006-3495(02)75604-X (2002).
34 Zoltowski, B. D. & Gardner, K. H. Tripping the light fantastic: blue-light photoreceptors as examples of environmentally modulated protein-protein interactions. *Biochemistry* **50**, 4-16, doi:10.1021/bi101665s (2011).
35 Harper, S. M., Christie, J. M. & Gardner, K. H. Disruption of the LOV-Jalpha helix interaction activates phototropin kinase activity. *Biochemistry* **43**, 16184-16192, doi:10.1021/bi048092i (2004).
36 Okajima, K., Matsuoka, D. & Tokutomi, S. LOV2-linker-kinase phosphorylates LOV1-containing N-terminal polypeptide substrate via photoreaction of LOV2 in Arabidopsis phototropin1. *FEBS Lett* **585**, 3391-3395, doi:10.1016/j.febslet.2011.10.003 (2011).
37 Pfeifer, A., Mathes, T., Lu, Y., Hegemann, P. & Kottke, T. Blue light induces global and localized conformational changes in the kinase domain of full-length phototropin. *Biochemistry* **49**, 1024-1032, doi:10.1021/bi9016044 (2010).
38 Moglich, A. & Moffat, K. Structural basis for light-dependent signaling in the dimeric LOV domain of the photosensor YtvA. *J Mol Biol* **373**, 112-126, doi:10.1016/j.jmb.2007.07.039 (2007).
39 Zoltowski, B. D. *et al.* Conformational switching in the fungal light sensor Vivid. *Science* **316**, 1054-1057, doi:10.1126/science.1137128 (2007).

40 Heintz, U. & Schlichting, I. Blue light-induced LOV domain dimerization enhances the affinity of Aureochrome 1a for its target DNA sequence. *Elife* **5**, e11860, doi:10.7554/eLife.11860 (2016).
41 Mitra, D., Yang, X. & Moffat, K. Crystal structures of Aureochrome1 LOV suggest new design strategies for optogenetics. *Structure* **20**, 698-706, doi:10.1016/j.str.2012.02.016 (2012).
42 Zoltowski, B. D., Vaccaro, B. & Crane, B. R. Mechanism-based tuning of a LOV domain photoreceptor. *Nat Chem Biol* **5**, 827-834, doi:10.1038/nchembio.210 (2009).
43 Ma, Z., Du, Z., Chen, X., Wang, X. & Yang, Y. Fine tuning the LightOn light-switchable transgene expression system. *Biochem Biophys Res Commun* **440**, 419-423, doi:10.1016/j.bbrc.2013.09.092 (2013).
44 Wang, X., Chen, X. & Yang, Y. Spatiotemporal control of gene expression by a light-switchable transgene system. *Nature methods* **9**, 266-269, doi:10.1038/nmeth.1892 (2012).
45 Imayoshi, I. *et al.* Oscillatory control of factors determining multipotency and fate in mouse neural progenitors. *Science* **342**, 1203-1208, doi:10.1126/science.1242366 (2013).
46 Isomura, A., Ogushi, F., Kori, H. & Kageyama, R. Optogenetic perturbation and bioluminescence imaging to analyze cell-to-cell transfer of oscillatory information. *Genes Dev* **31**, 524-535, doi:10.1101/gad.294546.116 (2017).
47 Shimojo, H. *et al.* Oscillatory control of Delta-like1 in cell interactions regulates dynamic gene expression and tissue morphogenesis. *Genes Dev* **30**, 102-116, doi:10.1101/gad.270785.115 (2016).
48 Chen, X. *et al.* Synthetic dual-input mammalian genetic circuits enable tunable and stringent transcription control by chemical and light. *Nucleic acids research* **44**, 2677-2690, doi:10.1093/nar/gkv1343 (2016).
49 Liu, L., Huang, W. & Huang, J. D. Synthetic circuits that process multiple light and chemical signal inputs. *BMC Syst Biol* **11**, 5, doi:10.1186/s12918-016-0384-y (2017).
50 Chen, X. *et al.* An extraordinary stringent and sensitive light-switchable gene expression system for bacterial cells. *Cell Res* **26**, 854-857, doi:10.1038/cr.2016.74 (2016).
51 Kawano, F., Suzuki, H., Furuya, A. & Sato, M. Engineered pairs of distinct photoswitches for optogenetic control of cellular proteins. *Nat Commun* **6**, 6256, doi:10.1038/ncomms7256 (2015).
52 Baumschlager, A., Aoki, S. K. & Khammash, M. Dynamic Blue Light-Inducible T7 RNA Polymerases (Opto-T7RNAPs) for Precise Spatiotemporal Gene Expression Control. *ACS Synth Biol* **6**, 2157-2167, doi:10.1021/acssynbio.7b00169 (2017).
53 Yu, G. *et al.* Optical manipulation of the alpha subunits of heterotrimeric G proteins using photoswitchable dimerization systems. *Sci Rep* **6**, 35777, doi:10.1038/srep35777 (2016).
54 Kawano, F., Okazaki, R., Yazawa, M. & Sato, M. A photoactivatable Cre-loxP recombination system for optogenetic genome engineering. *Nat Chem Biol* **12**, 1059-1064, doi:10.1038/nchembio.2205 (2016).
55 Nihongaki, Y., Kawano, F., Nakajima, T. & Sato, M. Photoactivatable CRISPR-Cas9 for optogenetic genome editing. *Nature biotechnology* **33**, 755-760, doi:10.1038/nbt.3245 (2015).
56 Tahara, M. *et al.* Photocontrollable mononegaviruses. *Proc Natl Acad Sci U S A* **116**, 11587-11589, doi:10.1073/pnas.1906531116 (2019).
57 Strickland, D. *et al.* TULIPs: tunable, light-controlled interacting protein tags for cell biology. *Nature methods* **9**, 379-384, doi:10.1038/nmeth.1904 (2012).
58 Conrad, K. S., Bilwes, A. M. & Crane, B. R. Light-induced subunit dissociation by a light-oxygen-voltage domain photoreceptor from Rhodobacter sphaeroides. *Biochemistry* **52**, 378-391, doi:10.1021/bi3015373 (2013).
59 Richter, F. *et al.* Engineering of temperature- and light-switchable Cas9 variants. *Nucleic acids research* **44**, 10003-10014, doi:10.1093/nar/gkw930 (2016).

60 Motta-Mena, L. B. *et al.* An optogenetic gene expression system with rapid activation and deactivation kinetics. *Nat Chem Biol* **10**, 196-202, doi:10.1038/nchembio.1430 (2014).
61 Reade, A. *et al.* TAEL: a zebrafish-optimized optogenetic gene expression system with fine spatial and temporal control. *Development* **144**, 345-355, doi:10.1242/dev.139238 (2017).
62 Grusch, M. *et al.* Spatio-temporally precise activation of engineered receptor tyrosine kinases by light. *The EMBO journal* **33**, 1713-1726, doi:10.15252/embj.201387695 (2014).
63 Sako, K. *et al.* Optogenetic Control of Nodal Signaling Reveals a Temporal Pattern of Nodal Signaling Regulating Cell Fate Specification during Gastrulation. *Cell reports* **16**, 866-877, doi:10.1016/j.celrep.2016.06.036 (2016).
64 Moglich, A., Ayers, R. A. & Moffat, K. Design and signaling mechanism of light-regulated histidine kinases. *J Mol Biol* **385**, 1433-1444, doi:10.1016/j.jmb.2008.12.017 (2009).
65 Ohlendorf, R., Vidavski, R. R., Eldar, A., Moffat, K. & Moglich, A. From dusk till dawn: one-plasmid systems for light-regulated gene expression. *J Mol Biol* **416**, 534-542, doi:10.1016/j.jmb.2012.01.001 (2012).
66 Moon, J., Gam, J., Lee, S. G., Suh, Y. G. & Lee, J. Light-regulated tetracycline binding to the Tet repressor. *Chemistry* **20**, 2508-2514, doi:10.1002/chem.201304027 (2014).
67 Liu, H., Liu, B., Zhao, C., Pepper, M. & Lin, C. The action mechanisms of plant cryptochromes. *Trends Plant Sci* **16**, 684-691, doi:10.1016/j.tplants.2011.09.002 (2011).
68 Chaves, I. *et al.* The cryptochromes: blue light photoreceptors in plants and animals. *Annu Rev Plant Biol* **62**, 335-364, doi:10.1146/annurev-arplant-042110-103759 (2011).
69 Zuo, Z. C. *et al.* A study of the blue-light-dependent phosphorylation, degradation, and photobody formation of Arabidopsis CRY2. *Mol Plant* **5**, 726-733, doi:10.1093/mp/sss007 (2012).
70 Liu, B. *et al.* Signaling mechanisms of plant cryptochromes in Arabidopsis thaliana. *J Plant Res* **129**, 137-148, doi:10.1007/s10265-015-0782-z (2016).
71 Yang, H. Q., Tang, R. H. & Cashmore, A. R. The signaling mechanism of Arabidopsis CRY1 involves direct interaction with COP1. *Plant Cell* **13**, 2573-2587, doi:10.1105/tpc.010367 (2001).
72 Liu, H. *et al.* Photoexcited CRY2 interacts with CIB1 to regulate transcription and floral initiation in Arabidopsis. *Science* **322**, 1535-1539, doi:10.1126/science.1163927 (2008).
73 Mas, P., Devlin, P. F., Panda, S. & Kay, S. A. Functional interaction of phytochrome B and cryptochrome 2. *Nature* **408**, 207-211, doi:10.1038/35041583 (2000).
74 Yu, X. *et al.* Formation of nuclear bodies of Arabidopsis CRY2 in response to blue light is associated with its blue light-dependent degradation. *Plant Cell* **21**, 118-130, doi:10.1105/tpc.108.061663 (2009).
75 Hoang, N., Bouly, J. P. & Ahmad, M. Evidence of a light-sensing role for folate in Arabidopsis cryptochrome blue-light receptors. *Mol Plant* **1**, 68-74, doi:10.1093/mp/ssm008 (2008).
76 Brautigam, C. A. *et al.* Structure of the photolyase-like domain of cryptochrome 1 from Arabidopsis thaliana. *Proc Natl Acad Sci U S A* **101**, 12142-12147, doi:10.1073/pnas.0404851101 (2004).
77 Muller, P. *et al.* ATP binding turns plant cryptochrome into an efficient natural photoswitch. *Sci Rep* **4**, 5175, doi:10.1038/srep05175 (2014).
78 Kennedy, M. J. *et al.* Rapid blue-light-mediated induction of protein interactions in living cells. *Nature methods* **7**, 973-975, doi:10.1038/nmeth.1524 (2010).
79 Polstein, L. R., Juhas, M., Hanna, G., Bursac, N. & Gersbach, C. A. An Engineered Optogenetic Switch for Spatiotemporal Control of Gene Expression, Cell Differentiation, and Tissue Morphogenesis. *ACS Synth Biol* **6**, 2003-2013, doi:10.1021/acssynbio.7b00147 (2017).
80 Hughes, R. M., Bolger, S., Tapadia, H. & Tucker, C. L. Light-mediated control of DNA transcription in yeast. *Methods* **58**, 385-391, doi:10.1016/j.ymeth.2012.08.004 (2012).
81 Liu, H., Gomez, G., Lin, S., Lin, S. & Lin, C. Optogenetic control of transcription in zebrafish. *PLoS One* **7**, e50738, doi:10.1371/journal.pone.0050738 (2012).

82 Chan, Y. B., Alekseyenko, O. V. & Kravitz, E. A. Optogenetic Control of Gene Expression in Drosophila. *PLoS One* **10**, e0138181, doi:10.1371/journal.pone.0138181 (2015).
83 Taslimi, A. *et al.* Optimized second-generation CRY2-CIB dimerizers and photoactivatable Cre recombinase. *Nat Chem Biol* **12**, 425-430, doi:10.1038/nchembio.2063 (2016).
84 Konermann, S. *et al.* Optical control of mammalian endogenous transcription and epigenetic states. *Nature* **500**, 472-476, doi:10.1038/nature12466 (2013).
85 Polstein, L. R. & Gersbach, C. A. A light-inducible CRISPR-Cas9 system for control of endogenous gene activation. *Nat Chem Biol* **11**, 198-200, doi:10.1038/nchembio.1753 (2015).
86 Katsura, Y. *et al.* An optogenetic system for interrogating the temporal dynamics of Akt. *Sci Rep* **5**, 14589, doi:10.1038/srep14589 (2015).
87 Idevall-Hagren, O., Dickson, E. J., Hille, B., Toomre, D. K. & De Camilli, P. Optogenetic control of phosphoinositide metabolism. *Proc Natl Acad Sci U S A* **109**, E2316-2323, doi:10.1073/pnas.1211305109 (2012).
88 Kakumoto, T. & Nakata, T. Optogenetic control of PIP3: PIP3 is sufficient to induce the actin-based active part of growth cones and is regulated via endocytosis. *PLoS One* **8**, e70861, doi:10.1371/journal.pone.0070861 (2013).
89 Zhang, K. *et al.* Light-mediated kinetic control reveals the temporal effect of the Raf/MEK/ERK pathway in PC12 cell neurite outgrowth. *PLoS One* **9**, e92917, doi:10.1371/journal.pone.0092917 (2014).
90 Guglielmi, G., Barry, J. D., Huber, W. & De Renzis, S. An Optogenetic Method to Modulate Cell Contractility during Tissue Morphogenesis. *Dev Cell* **35**, 646-660, doi:10.1016/j.devcel.2015.10.020 (2015).
91 Bugaj, L. J., Choksi, A. T., Mesuda, C. K., Kane, R. S. & Schaffer, D. V. Optogenetic protein clustering and signaling activation in mammalian cells. *Nature methods* **10**, 249-252, doi:10.1038/nmeth.2360 (2013).
92 Che, D. L., Duan, L., Zhang, K. & Cui, B. The Dual Characteristics of Light-Induced Cryptochrome 2, Homo-oligomerization and Heterodimerization, for Optogenetic Manipulation in Mammalian Cells. *ACS Synth Biol* **4**, 1124-1135, doi:10.1021/acssynbio.5b00048 (2015).
93 Chang, K. Y. *et al.* Light-inducible receptor tyrosine kinases that regulate neurotrophin signalling. *Nat Commun* **5**, 4057, doi:10.1038/ncomms5057 (2014).
94 Kim, N. *et al.* Spatiotemporal control of fibroblast growth factor receptor signals by blue light. *Chem Biol* **21**, 903-912, doi:10.1016/j.chembiol.2014.05.013 (2014).
95 Han, K. A. *et al.* Neurotrophin-3 Regulates Synapse Development by Modulating TrkC-PTPsigma Synaptic Adhesion and Intracellular Signaling Pathways. *J Neurosci* **36**, 4816-4831, doi:10.1523/JNEUROSCI.4024-15.2016 (2016).
96 Wend, S. *et al.* Optogenetic Control of Protein Kinase Activity in Mammalian Cells. *ACS Synth. Biol.* **3**, 280-285, doi:10.1021/sb400090s (2014).
97 Bugaj, L. J. *et al.* Regulation of endogenous transmembrane receptors through optogenetic Cry2 clustering. *Nature Communications* **6**, doi:ARTN 6898

10.1038/ncomms7898 (2015).
98 Lee, S. *et al.* Reversible protein inactivation by optogenetic trapping in cells. *Nature methods* **11**, 633-636, doi:10.1038/nmeth.2940 (2014).
99 Taslimi, A. *et al.* An optimized optogenetic clustering tool for probing protein interaction and function. *Nat Commun* **5**, 4925, doi:10.1038/ncomms5925 (2014).
100 Nguyen, N. T. *et al.* CRAC channel-based optogenetics. *Cell Calcium* **75**, 79-88, doi:10.1016/j.ceca.2018.08.007 (2018).
101 Osswald, M., Santos, A. F. & Morais-de-Sa, E. Light-Induced Protein Clustering for Optogenetic Interference and Protein Interaction Analysis in Drosophila S2 Cells. *Biomolecules* **9**, doi:10.3390/biom9020061 (2019).

102 Zhao, E. M. *et al.* Light-based control of metabolic flux through assembly of synthetic organelles. *Nat Chem Biol* **15**, 589-597, doi:10.1038/s41589-019-0284-8 (2019).
103 Wang, L. & Cooper, J. A. Optogenetic control of the Dab1 signaling pathway. *Sci Rep* **7**, 43760, doi:10.1038/srep43760 (2017).
104 Alapin, J. M. *et al.* Activation of EphB2 Forward Signaling Enhances Memory Consolidation. *Cell reports* **23**, 2014-2025, doi:10.1016/j.celrep.2018.04.042 (2018).
105 Rockwell, N. C., Su, Y. S. & Lagarias, J. C. Phytochrome structure and signaling mechanisms. *Annu Rev Plant Biol* **57**, 837-858, doi:10.1146/annurev.arplant.56.032604.144208 (2006).
106 Sharrock, R. A. The phytochrome red/far-red photoreceptor superfamily. *Genome Biol* **9**, 230, doi:10.1186/gb-2008-9-8-230 (2008).
107 Li, J., Li, G., Wang, H. & Wang Deng, X. Phytochrome signaling mechanisms. *Arabidopsis Book* **9**, e0148, doi:10.1199/tab.0148 (2011).
108 Mroginski, M. A., Murgida, D. H. & Hildebrandt, P. The chromophore structural changes during the photocycle of phytochrome: a combined resonance Raman and quantum chemical approach. *Acc Chem Res* **40**, 258-266, doi:10.1021/ar6000523 (2007).
109 Ulijasz, A. T. & Vierstra, R. D. Phytochrome structure and photochemistry: recent advances toward a complete molecular picture. *Curr Opin Plant Biol* **14**, 498-506, doi:10.1016/j.pbi.2011.06.002 (2011).
110 Shimizu-Sato, S., Huq, E., Tepperman, J. M. & Quail, P. H. A light-switchable gene promoter system. *Nature biotechnology* **20**, 1041-1044, doi:10.1038/nbt734 (2002).
111 Tyszkiewicz, A. B. & Muir, T. W. Activation of protein splicing with light in yeast. *Nature methods* **5**, 303-305, doi:10.1038/nmeth.1189 (2008).
112 Leung, D. W., Otomo, C., Chory, J. & Rosen, M. K. Genetically encoded photoswitching of actin assembly through the Cdc42-WASP-Arp2/3 complex pathway. *Proc Natl Acad Sci U S A* **105**, 12797-12802, doi:10.1073/pnas.0801232105 (2008).
113 Beyer, H. M. *et al.* Generic and reversible opto-trapping of biomolecules. *Acta Biomater* **79**, 276-282, doi:10.1016/j.actbio.2018.08.032 (2018).
114 Muller, K., Zurbriggen, M. D. & Weber, W. Control of gene expression using a red- and far-red light-responsive bi-stable toggle switch. *Nat Protoc* **9**, 622-632, doi:10.1038/nprot.2014.038 (2014).
115 Muller, K. *et al.* A red light-controlled synthetic gene expression switch for plant systems. *Molecular bioSystems* **10**, 1679-1688, doi:10.1039/c3mb70579j (2014).
116 Levskaya, A., Weiner, O. D., Lim, W. A. & Voigt, C. A. Spatiotemporal control of cell signalling using a light-switchable protein interaction. *Nature* **461**, 997-1001, doi:10.1038/nature08446 (2009).
117 Toettcher, J. E., Weiner, O. D. & Lim, W. A. Using optogenetics to interrogate the dynamic control of signal transmission by the Ras/Erk module. *Cell* **155**, 1422-1434, doi:10.1016/j.cell.2013.11.004 (2013).
118 Toettcher, J. E., Gong, D., Lim, W. A. & Weiner, O. D. Light-based feedback for controlling intracellular signaling dynamics. *Nature methods* **8**, 837-839, doi:10.1038/nmeth.1700 (2011).
119 Hughes, R. M., Vrana, J. D., Song, J. & Tucker, C. L. Light-dependent, dark-promoted interaction between Arabidopsis cryptochrome 1 and phytochrome B proteins. *J Biol Chem* **287**, 22165-22172, doi:10.1074/jbc.M112.360545 (2012).
120 Wang, Q. *et al.* New insights into the mechanisms of phytochrome-cryptochrome coaction. *New Phytol* **217**, 547-551, doi:10.1111/nph.14886 (2018).
121 Redchuk, T. A., Omelina, E. S., Chernov, K. G. & Verkhusha, V. V. Near-infrared optogenetic pair for protein regulation and spectral multiplexing. *Nat Chem Biol* **13**, 633-639, doi:10.1038/nchembio.2343 (2017).

122 Strauss, H. M., Schmieder, P. & Hughes, J. Light-dependent dimerisation in the N-terminal sensory module of cyanobacterial phytochrome 1. *FEBS Lett* **579**, 3970-3974, doi:10.1016/j.febslet.2005.06.025 (2005).
123 Levskaya, A. *et al.* Synthetic biology: engineering Escherichia coli to see light. *Nature* **438**, 441-442, doi:10.1038/nature04405 (2005).
124 Gasser, C. *et al.* Engineering of a red-light-activated human cAMP/cGMP-specific phosphodiesterase. *Proc Natl Acad Sci U S A* **111**, 8803-8808, doi:10.1073/pnas.1321600111 (2014).
125 Ryu, M. H. *et al.* Engineering adenylate cyclases regulated by near-infrared window light. *Proc Natl Acad Sci U S A* **111**, 10167-10172, doi:10.1073/pnas.1324301111 (2014).
126 Reichhart, E., Ingles-Prieto, A., Tichy, A.-M., McKenzie, C. & Janovjak, H. A Phytochrome Sensory Domain Permits Receptor Activation by Red Light. *Angewandte Chemie International Edition* **55**, 6339-6342, doi:10.1002/anie.201601736 (2016).
127 Kyriakakis, P. *et al.* Biosynthesis of Orthogonal Molecules Using Ferredoxin and Ferredoxin-NADP(+) Reductase Systems Enables Genetically Encoded PhyB Optogenetics. *ACS Synth Biol* **7**, 706-717, doi:10.1021/acssynbio.7b00413 (2018).
128 Jost, M. *et al.* Structural basis for gene regulation by a B12-dependent photoreceptor. *Nature* **526**, 536-541, doi:10.1038/nature14950 (2015).
129 Jost, M., Simpson, J. H. & Drennan, C. L. The Transcription Factor CarH Safeguards Use of Adenosylcobalamin as a Light Sensor by Altering the Photolysis Products. *Biochemistry* **54**, 3231-3234, doi:10.1021/acs.biochem.5b00416 (2015).
130 Warren, M. J., Raux, E., Schubert, H. L. & Escalante-Semerena, J. C. The biosynthesis of adenosylcobalamin (vitamin B12). *Nat Prod Rep* **19**, 390-412, doi:10.1039/b108967f (2002).
131 Perez-Marin, M. C., Padmanabhan, S., Polanco, M. C., Murillo, F. J. & Elias-Arnanz, M. Vitamin B12 partners the CarH repressor to downregulate a photoinducible promoter in Myxococcus xanthus. *Molecular microbiology* **67**, 804-819, doi:10.1111/j.1365-2958.2007.06086.x (2008).
132 Diez, A. I. *et al.* Analytical ultracentrifugation studies of oligomerization and DNA-binding of TtCarH, a Thermus thermophilus coenzyme B12-based photosensory regulator. *European biophysics journal : EBJ* **42**, 463-476, doi:10.1007/s00249-013-0897-x (2013).
133 Kainrath, S., Stadler, M., Reichhart, E., Distel, M. & Janovjak, H. Green-Light-Induced Inactivation of Receptor Signaling Using Cobalamin-Binding Domains. *Angew Chem Int Ed Engl* **56**, 4608-4611, doi:10.1002/anie.201611998 (2017).
134 Chatelle, C. *et al.* A Green-Light-Responsive System for the Control of Transgene Expression in Mammalian and Plant Cells. *ACS Synth Biol* **7**, 1349-1358, doi:10.1021/acssynbio.7b00450 (2018).
135 Wang, R., Yang, Z., Luo, J., Hsing, I. M. & Sun, F. B12-dependent photoresponsive protein hydrogels for controlled stem cell/protein release. *Proc Natl Acad Sci U S A* **114**, 5912-5917, doi:10.1073/pnas.1621350114 (2017).
136 Masuda, S. Light detection and signal transduction in the BLUF photoreceptors. *Plant Cell Physiol* **54**, 171-179, doi:10.1093/pcp/pcs173 (2013).
137 Masuda, S. & Bauer, C. E. AppA is a blue light photoreceptor that antirepresses photosynthesis gene expression in Rhodobacter sphaeroides. *Cell* **110**, 613-623, doi:10.1016/s0092-8674(02)00876-0 (2002).
138 Okajima, K. *et al.* Biochemical and functional characterization of BLUF-type flavin-binding proteins of two species of cyanobacteria. *J Biochem* **137**, 741-750, doi:10.1093/jb/mvi089 (2005).
139 Mussi, M. A. *et al.* The opportunistic human pathogen Acinetobacter baumannii senses and responds to light. *J Bacteriol* **192**, 6336-6345, doi:10.1128/JB.00917-10 (2010).
140 Iseki, M. *et al.* A blue-light-activated adenylyl cyclase mediates photoavoidance in Euglena gracilis. *Nature* **415**, 1047-1051, doi:10.1038/4151047a (2002).

141 Rajagopal, S., Key, J. M., Purcell, E. B., Boerema, D. J. & Moffat, K. Purification and initial characterization of a putative blue light-regulated phosphodiesterase from Escherichia coli. *Photochem Photobiol* **80**, 542-547, doi:10.1562/2004-06-16-RA-203 (2004).
142 Kanazawa, T. *et al.* Biochemical and physiological characterization of a BLUF protein-EAL protein complex involved in blue light-dependent degradation of cyclic diguanylate in the purple bacterium Rhodopseudomonas palustris. *Biochemistry* **49**, 10647-10655, doi:10.1021/bi101448t (2010).
143 Masuda, S., Nakatani, Y., Ren, S. & Tanaka, M. Blue light-mediated manipulation of transcription factor activity in vivo. *ACS Chem Biol* **8**, 2649-2653, doi:10.1021/cb400174d (2013).
144 Zirak, P. *et al.* Photodynamics of the small BLUF protein BlrB from Rhodobacter sphaeroides. *J Photochem Photobiol B* **83**, 180-194, doi:10.1016/j.jphotobiol.2005.12.015 (2006).
145 Masuda, S., Hasegawa, K. & Ono, T. A. Light-induced structural changes of apoprotein and chromophore in the sensor of blue light using FAD (BLUF) domain of AppA for a signaling state. *Biochemistry* **44**, 1215-1224, doi:10.1021/bi047876t (2005).
146 Tanaka, K. *et al.* Time-resolved tracking of interprotein signal transduction: Synechocystis PixD-PixE complex as a sensor of light intensity. *J Am Chem Soc* **134**, 8336-8339, doi:10.1021/ja301540r (2012).
147 Yuan, H. *et al.* Crystal structures of the Synechocystis photoreceptor Slr1694 reveal distinct structural states related to signaling. *Biochemistry* **45**, 12687-12694, doi:10.1021/bi061435n (2006).
148 Tanaka, K. *et al.* Light-induced conformational change and transient dissociation reaction of the BLUF photoreceptor Synechocystis PixD (Slr1694). *J Mol Biol* **409**, 773-785, doi:10.1016/j.jmb.2011.04.032 (2011).
149 Wu, D. *et al.* Structural basis of ultraviolet-B perception by UVR8. *Nature* **484**, 214-219, doi:10.1038/nature10931 (2012).
150 Favory, J. J. *et al.* Interaction of COP1 and UVR8 regulates UV-B-induced photomorphogenesis and stress acclimation in Arabidopsis. *The EMBO journal* **28**, 591-601, doi:10.1038/emboj.2009.4 (2009).
151 Brown, B. A. *et al.* A UV-B-specific signaling component orchestrates plant UV protection. *Proc Natl Acad Sci U S A* **102**, 18225-18230, doi:10.1073/pnas.0507187102 (2005).
152 Huang, X., Yang, P., Ouyang, X., Chen, L. & Deng, X. W. Photoactivated UVR8-COP1 module determines photomorphogenic UV-B signaling output in Arabidopsis. *PLoS Genet* **10**, e1004218, doi:10.1371/journal.pgen.1004218 (2014).
153 Heijde, M. & Ulm, R. Reversion of the Arabidopsis UV-B photoreceptor UVR8 to the homodimeric ground state. *Proc Natl Acad Sci U S A* **110**, 1113-1118, doi:10.1073/pnas.1214237110 (2013).
154 O'Hara, A. & Jenkins, G. I. In vivo function of tryptophans in the Arabidopsis UV-B photoreceptor UVR8. *Plant Cell* **24**, 3755-3766, doi:10.1105/tpc.112.101451 (2012).
155 Cloix, C. *et al.* C-terminal region of the UV-B photoreceptor UVR8 initiates signaling through interaction with the COP1 protein. *Proc Natl Acad Sci U S A* **109**, 16366-16370, doi:10.1073/pnas.1210898109 (2012).
156 Crefcoeur, R. P., Yin, R., Ulm, R. & Halazonetis, T. D. Ultraviolet-B-mediated induction of protein-protein interactions in mammalian cells. *Nat Commun* **4**, 1779, doi:10.1038/ncomms2800 (2013).
157 Chen, D., Gibson, E. S. & Kennedy, M. J. A light-triggered protein secretion system. *J Cell Biol* **201**, 631-640, doi:10.1083/jcb.201210119 (2013).
158 Vlasov, K., Van Dort, C. J. & Solt, K. Optogenetics and Chemogenetics. *Methods Enzymol* **603**, 181-196, doi:10.1016/bs.mie.2018.01.022 (2018).
159 Roth, B. L. DREADDs for Neuroscientists. *Neuron* **89**, 683-694, doi:10.1016/j.neuron.2016.01.040 (2016).

160 Sternson, S. M. & Roth, B. L. Chemogenetic tools to interrogate brain functions. *Annu Rev Neurosci* **37**, 387-407, doi:10.1146/annurev-neuro-071013-014048 (2014).
161 Jung, D., Min, K., Jung, J., Jang, W. & Kwon, Y. Chemical biology-based approaches on fluorescent labeling of proteins in live cells. *Molecular bioSystems* **9**, 862-872, doi:10.1039/c2mb25422k (2013).
162 Haring, D. & Distefano, M. D. Enzymes by design: chemogenetic assembly of transamination active sites containing lysine residues for covalent catalysis. *Bioconjug Chem* **12**, 385-390, doi:10.1021/bc000117c (2001).
163 Fegan, A., White, B., Carlson, J. C. & Wagner, C. R. Chemically controlled protein assembly: techniques and applications. *Chem Rev* **110**, 3315-3336, doi:10.1021/cr8002888 (2010).
164 Siekierka, J. J., Hung, S. H., Poe, M., Lin, C. S. & Sigal, N. H. A cytosolic binding protein for the immunosuppressant FK506 has peptidyl-prolyl isomerase activity but is distinct from cyclophilin. *Nature* **341**, 755-757, doi:10.1038/341755a0 (1989).
165 Schreiber, S. L. & Crabtree, G. R. The mechanism of action of cyclosporin A and FK506. *Immunol Today* **13**, 136-142, doi:10.1016/0167-5699(92)90111-J (1992).
166 Lyson, T. *et al.* Cyclosporine- and FK506-induced sympathetic activation correlates with calcineurin-mediated inhibition of T-cell signaling. *Circ Res* **73**, 596-602, doi:10.1161/01.res.73.3.596 (1993).
167 Spencer, D. M., Wandless, T. J., Schreiber, S. L. & Crabtree, G. R. Controlling signal transduction with synthetic ligands. *Science* **262**, 1019-1024, doi:10.1126/science.7694365 (1993).
168 Diver, S. T. & Schreiber, S. L. Single-step synthesis of cell-permeable protein dimerizers that activate signal transduction and gene expression. *Journal of the American Chemical Society* **119**, 5106-5109, doi:DOI 10.1021/ja963891c (1997).
169 Holt, D. A. *et al.* Design, Synthesis, and Kinetic Evaluation of High-Affinity Fkbp Ligands and the X-Ray Crystal-Structures of Their Complexes with Fkbp12. *Journal of the American Chemical Society* **115**, 9925-9938, doi:DOI 10.1021/ja00075a008 (1993).
170 Keenan, T. *et al.* Synthesis and activity of bivalent FKBP12 ligands for the regulated dimerization of proteins. *Bioorgan Med Chem* **6**, 1309-1335, doi:Doi 10.1016/S0968-0896(98)00125-4 (1998).
171 Amara, J. F. *et al.* A versatile synthetic dimerizer for the regulation of protein-protein interactions. *Proc Natl Acad Sci U S A* **94**, 10618-10623, doi:10.1073/pnas.94.20.10618 (1997).
172 Clackson, T. *et al.* Redesigning an FKBP-ligand interface to generate chemical dimerizers with novel specificity. *Proc Natl Acad Sci U S A* **95**, 10437-10442, doi:10.1073/pnas.95.18.10437 (1998).
173 Spencer, D. M. *et al.* Functional analysis of Fas signaling in vivo using synthetic inducers of dimerization. *Curr Biol* **6**, 839-847, doi:10.1016/s0960-9822(02)00607-3 (1996).
174 Spencer, D. M., Graef, I., Austin, D. J., Schreiber, S. L. & Crabtree, G. R. A general strategy for producing conditional alleles of Src-like tyrosine kinases. *Proc Natl Acad Sci U S A* **92**, 9805-9809, doi:10.1073/pnas.92.21.9805 (1995).
175 Holsinger, L. J., Spencer, D. M., Austin, D. J., Schreiber, S. L. & Crabtree, G. R. Signal transduction in T lymphocytes using a conditional allele of Sos. *Proc Natl Acad Sci U S A* **92**, 9810-9814, doi:10.1073/pnas.92.21.9810 (1995).
176 Rollins, C. T. *et al.* A ligand-reversible dimerization system for controlling protein-protein interactions. *Proc Natl Acad Sci U S A* **97**, 7096-7101, doi:10.1073/pnas.100101997 (2000).
177 Sabatini, D. M., Erdjument-Bromage, H., Lui, M., Tempst, P. & Snyder, S. H. RAFT1: a mammalian protein that binds to FKBP12 in a rapamycin-dependent fashion and is homologous to yeast TORs. *Cell* **78**, 35-43, doi:10.1016/0092-8674(94)90570-3 (1994).

178 Pecot, M. Y. & Malhotra, V. Golgi membranes remain segregated from the endoplasmic reticulum during mitosis in mammalian cells. *Cell* **116**, 99-107, doi:10.1016/s0092-8674(03)01068-7 (2004).
179 Rivera, V. M. *et al.* A humanized system for pharmacologic control of gene expression. *Nat Med* **2**, 1028-1032, doi:10.1038/nm0996-1028 (1996).
180 Hay, N. & Sonenberg, N. Upstream and downstream of mTOR. *Genes Dev* **18**, 1926-1945, doi:10.1101/gad.1212704 (2004).
181 Liberles, S. D., Diver, S. T., Austin, D. J. & Schreiber, S. L. Inducible gene expression and protein translocation using nontoxic ligands identified by a mammalian three-hybrid screen. *Proc Natl Acad Sci U S A* **94**, 7825-7830, doi:10.1073/pnas.94.15.7825 (1997).
182 Stockwell, B. R. & Schreiber, S. L. Probing the role of homomeric and heteromeric receptor interactions in TGF-beta signaling using small molecule dimerizers. *Curr Biol* **8**, 761-770, doi:10.1016/s0960-9822(98)70299-4 (1998).
183 Bayle, J. H. *et al.* Rapamycin analogs with differential binding specificity permit orthogonal control of protein activity. *Chem Biol* **13**, 99-107, doi:10.1016/j.chembiol.2005.10.017 (2006).
184 Karginov, A. V. *et al.* Light regulation of protein dimerization and kinase activity in living cells using photocaged rapamycin and engineered FKBP. *J Am Chem Soc* **133**, 420-423, doi:10.1021/ja109630v (2011).
185 Stankunas, K. *et al.* Conditional protein alleles using knockin mice and a chemical inducer of dimerization. *Mol Cell* **12**, 1615-1624, doi:10.1016/s1097-2765(03)00491-x (2003).
186 Licitra, E. J. & Liu, J. O. A three-hybrid system for detecting small ligand-protein receptor interactions. *Proc Natl Acad Sci U S A* **93**, 12817-12821, doi:10.1073/pnas.93.23.12817 (1996).
187 Baker, K. *et al.* Chemical complementation: a reaction-independent genetic assay for enzyme catalysis. *Proc Natl Acad Sci U S A* **99**, 16537-16542, doi:10.1073/pnas.262420099 (2002).
188 Zhou, X., Di Stasi, A. & Brenner, M. K. iCaspase 9 Suicide Gene System. *Methods Mol Biol* **1317**, 87-105, doi:10.1007/978-1-4939-2727-2_6 (2015).
189 Straathof, K. C. *et al.* An inducible caspase 9 safety switch for T-cell therapy. *Blood* **105**, 4247-4254, doi:10.1182/blood-2004-11-4564 (2005).
190 Goodsell, D. S. The molecular perspective: methotrexate. *Oncologist* **4**, 340-341 (1999).
191 Kopytek, S. J., Standaert, R. F., Dyer, J. C. & Hu, J. C. Chemically induced dimerization of dihydrofolate reductase by a homobifunctional dimer of methotrexate. *Chem Biol* **7**, 313-321, doi:10.1016/s1074-5521(00)00109-5 (2000).
192 Althoff, E. A. & Cornish, V. W. A bacterial small-molecule three-hybrid system. *Angew Chem Int Ed Engl* **41**, 2327-2330, doi:10.1002/1521-3773(20020703)41:13<2327::AID-ANIE2327>3.0.CO;2-U (2002).
193 de Felipe, K. S., Carter, B. T., Althoff, E. A. & Cornish, V. W. Correlation between ligand-receptor affinity and the transcription readout in a yeast three-hybrid system. *Biochemistry* **43**, 10353-10363, doi:10.1021/bi049716n (2004).
194 Gallagher, S. S., Miller, L. W. & Cornish, V. W. An orthogonal dexamethasone-trimethoprim yeast three-hybrid system. *Anal Biochem* **363**, 160-162, doi:10.1016/j.ab.2006.12.013 (2007).
195 Baker, K., Sengupta, D., Salazar-Jimenez, G. & Cornish, V. W. An optimized dexamethasone-methotrexate yeast 3-hybrid system for high-throughput screening of small molecule-protein interactions. *Anal Biochem* **315**, 134-137, doi:10.1016/s0003-2697(02)00698-x (2003).
196 Abida, W. M., Carter, B. T., Althoff, E. A., Lin, H. & Cornish, V. W. Receptor-dependence of the transcription read-out in a small-molecule three-hybrid system. *Chembiochem* **3**, 887-895, doi:10.1002/1439-7633(20020902)3:9<887::AID-CBIC887>3.0.CO;2-F (2002).

197 Lin, H. N., Abida, W. M., Sauer, R. T. & Cornish, V. W. Dexamethasone-methotrexate: An efficient chemical inducer of protein dimerization in vivo. *Journal of the American Chemical Society* **122**, 4247-4248, doi:DOI 10.1021/ja9941532 (2000).
198 Gendreizig, S., Kindermann, M. & Johnsson, K. Induced protein dimerization in vivo through covalent labeling. *J Am Chem Soc* **125**, 14970-14971, doi:10.1021/ja037883p (2003).
199 Howard, S. C., McCormick, J., Pui, C. H., Buddington, R. K. & Harvey, R. D. Preventing and Managing Toxicities of High-Dose Methotrexate. *Oncologist* **21**, 1471-1482, doi:10.1634/theoncologist.2015-0164 (2016).
200 Czlapinski, J. L. *et al.* Conditional glycosylation in eukaryotic cells using a biocompatible chemical inducer of dimerization. *J Am Chem Soc* **130**, 13186-13187, doi:10.1021/ja8037728 (2008).
201 Lymperopoulos, P., Msanne, J. & Rabara, R. Phytochrome and Phytohormones: Working in Tandem for Plant Growth and Development. *Front Plant Sci* **9**, 1037, doi:10.3389/fpls.2018.01037 (2018).
202 Cutler, S. R., Rodriguez, P. L., Finkelstein, R. R. & Abrams, S. R. Abscisic acid: emergence of a core signaling network. *Annu Rev Plant Biol* **61**, 651-679, doi:10.1146/annurev-arplant-042809-112122 (2010).
203 Liang, F. S., Ho, W. Q. & Crabtree, G. R. Engineering the ABA plant stress pathway for regulation of induced proximity. *Sci Signal* **4**, rs2, doi:10.1126/scisignal.2001449 (2011).
204 Wright, C. W., Guo, Z. F. & Liang, F. S. Light control of cellular processes by using photocaged abscisic acid. *Chembiochem* **16**, 254-261, doi:10.1002/cbic.201402576 (2015).
205 Rademacher, W. Gibberellin Formation in Microorganisms. *Plant Growth Regul* **15**, 303-314, doi:Doi 10.1007/Bf00029903 (1994).
206 Daviere, J. M. & Achard, P. Gibberellin signaling in plants. *Development* **140**, 1147-1151, doi:10.1242/dev.087650 (2013).
207 Yamaguchi, S. Gibberellin metabolism and its regulation. *Annu Rev Plant Biol* **59**, 225-251, doi:10.1146/annurev.arplant.59.032607.092804 (2008).
208 Hirano, K., Ueguchi-Tanaka, M. & Matsuoka, M. GID1-mediated gibberellin signaling in plants. *Trends Plant Sci* **13**, 192-199, doi:10.1016/j.tplants.2008.02.005 (2008).
209 Ueguchi-Tanaka, M. *et al.* GIBBERELLIN INSENSITIVE DWARF1 encodes a soluble receptor for gibberellin. *Nature* **437**, 693-698, doi:10.1038/nature04028 (2005).
210 Miyamoto, T. *et al.* Rapid and orthogonal logic gating with a gibberellin-induced dimerization system. *Nat Chem Biol* **8**, 465-470, doi:10.1038/nchembio.922 (2012).
211 Razavi, S., Su, S. & Inoue, T. Cellular signaling circuits interfaced with synthetic, post-translational, negating Boolean logic devices. *ACS Synth Biol* **3**, 676-685, doi:10.1021/sb500222z (2014).
212 Weinberg, B. H. *et al.* High-performance chemical- and light-inducible recombinases in mammalian cells and mice. *Nat Commun* **10**, 4845, doi:10.1038/s41467-019-12800-7 (2019).
213 Gronemeyer, T., Chidley, C., Juillerat, A., Heinis, C. & Johnsson, K. Directed evolution of O6-alkylguanine-DNA alkyltransferase for applications in protein labeling. *Protein Eng Des Sel* **19**, 309-316, doi:10.1093/protein/gzl014 (2006).
214 Mie, M., Naoki, T., Uchida, K. & Kobatake, E. Development of a split SNAP-tag protein complementation assay for visualization of protein-protein interactions in living cells. *Analyst* **137**, 4760-4765, doi:10.1039/c2an35762c (2012).
215 Gautier, A. *et al.* An engineered protein tag for multiprotein labeling in living cells. *Chem Biol* **15**, 128-136, doi:10.1016/j.chembiol.2008.01.007 (2008).
216 Erhart, D. *et al.* Chemical development of intracellular protein heterodimerizers. *Chem Biol* **20**, 549-557, doi:10.1016/j.chembiol.2013.03.010 (2013).
217 Belshaw, P. J., Spencer, D. M., Crabtree, G. R. & Schreiber, S. L. Controlling programmed cell death with a cyclophilin-cyclosporin-based chemical inducer of dimerization. *Chem Biol* **3**, 731-738, doi:10.1016/s1074-5521(96)90249-5 (1996).

218 Berens, C. & Hillen, W. Gene regulation by tetracyclines. Constraints of resistance regulation in bacteria shape TetR for application in eukaryotes. *Eur J Biochem* **270**, 3109-3121, doi:10.1046/j.1432-1033.2003.03694.x (2003).
219 Zeng, Y. *et al.* A Split Transcriptional Repressor That Links Protein Solubility to an Orthogonal Genetic Circuit. *ACS Synth Biol* **7**, 2126-2138, doi:10.1021/acssynbio.8b00129 (2018).
220 Hill, Z. B., Martinko, A. J., Nguyen, D. P. & Wells, J. A. Human antibody-based chemically induced dimerizers for cell therapeutic applications. *Nat Chem Biol* **14**, 112-117, doi:10.1038/nchembio.2529 (2018).
221 Zhao, H. F., Boyd, J., Jolicoeur, N. & Shen, S. H. A coumermycin/novobiocin-regulated gene expression system. *Hum Gene Ther* **14**, 1619-1629, doi:10.1089/104303403322542266 (2003).
222 Sako, K. *et al.* Optogenetic Control of Nodal Signaling Reveals a Temporal Pattern of Nodal Signaling Regulating Cell Fate Specification during Gastrulation. *Cell reports* **16**, 866-877, doi:10.1016/j.celrep.2016.06.036 (2016).
223 Pathak, G. P., Strickland, D., Vrana, J. D. & Tucker, C. L. Benchmarking of optical dimerizer systems. *ACS Synth Biol* **3**, 832-838, doi:10.1021/sb500291r (2014).
224 Kaminer, I., Nemirovsky, J. & Segev, M. Optimizing 3D multiphoton fluorescence microscopy. *Opt Lett* **38**, 3945-3948, doi:10.1364/OL.38.003945 (2013).
225 Lemmon, M. A. & Schlessinger, J. Cell Signaling by Receptor Tyrosine Kinases. *Cell* **141**, 1117-1134, doi:10.1016/j.cell.2010.06.011 (2010).
226 Neben, C. L., Lo, M., Jura, N. & Klein, O. D. Feedback regulation of RTK signaling in development. *Developmental Biology* **447**, 71-89, doi:10.1016/j.ydbio.2017.10.017 (2019).
227 Simi, A. & Ibáñez, C. F. Assembly and activation of neurotrophic factor receptor complexes. *Developmental Neurobiology* **70**, 323-331, doi:10.1002/dneu.20773 (2010).
228 Casaletto, J. B. & McClatchey, A. I. Spatial regulation of receptor tyrosine kinases in development and cancer. *Nature Reviews Cancer* **12**, 387-400, doi:10.1038/nrc3277 (2012).
229 Robertson, S. C., Tynan, J. A. & Donoghue, D. J. RTK mutations and human syndromes: when good receptors turn bad. *Trends in Genetics* **16**, 265-271, doi:10.1016/S0168-9525(00)02021-7 (2000).
230 Goglia, A. G. & Toettcher, J. E. A bright future: optogenetics to dissect the spatiotemporal control of cell behavior. *Current Opinion in Chemical Biology* **48**, 106-113, doi:10.1016/j.cbpa.2018.11.010 (2019).
231 Grusch, M. *et al.* Spatio-temporally precise activation of engineered receptor tyrosine kinases by light. *The EMBO journal* **33**, 1713-1726, doi:10.15252/embj.201387695 (2014).
232 Kim, N. *et al.* Spatiotemporal Control of Fibroblast Growth Factor Receptor Signals by Blue Light. *Chemistry & Biology* **21**, 903-912, doi:10.1016/j.chembiol.2014.05.013 (2014).
233 Bugaj, L. J. *et al.* Regulation of endogenous transmembrane receptors through optogenetic Cry2 clustering. *Nature Communications* **6**, 6898, doi:10.1038/ncomms7898 (2015).
234 Duan, L. *et al.* Optical Activation of TrkA Signaling. *ACS Synth. Biol.* **7**, 1685-1693, doi:10.1021/acssynbio.8b00126 (2018).
235 Li, Y. *et al.* Spatiotemporal Control of TGF-β Signaling with Light. *ACS Synth. Biol.* **7**, 443-451, doi:10.1021/acssynbio.7b00225 (2018).
236 Ramachandran, A. *et al.* TGF-β uses a novel mode of receptor activation to phosphorylate SMAD1/5 and induce epithelial-to-mesenchymal transition. *eLife* **7**, e31756, doi:10.7554/eLife.31756 (2018).
237 Muthuswamy, S. K., Gilman, M. & Brugge, J. S. Controlled Dimerization of ErbB Receptors Provides Evidence for Differential Signaling by Homo- and Heterodimers. *Molecular and Cellular Biology* **19**, 6845-6857, doi:10.1128/MCB.19.10.6845 (1999).
238 Welm, B. E. *et al.* Inducible dimerization of FGFR1: development of a mouse model to analyze progressive transformation of the mammary gland. *J Cell Biol* **157**, 703-714, doi:10.1083/jcb.200107119 (2002).

239 Bae, J. H. *et al.* Asymmetric receptor contact is required for tyrosine autophosphorylation of fibroblast growth factor receptor in living cells. *Proc Natl Acad Sci U S A* **107**, 2866-2871, doi:10.1073/pnas.0914157107 (2010).
240 Mohammadi, M. *et al.* Identification of six novel autophosphorylation sites on fibroblast growth factor receptor 1 and elucidation of their importance in receptor activation and signal transduction. *Mol Cell Biol* **16**, 977-989 (1996).
241 Polyethylenimine (PEI), linear (1 mg/mL). *Cold Spring Harb Protoc* **2008**, pdb.rec11323, doi:10.1101/pdb.rec11323 (2008).
242 Baker, J. M. & Boyce, F. M. High-throughput Functional Screening using a Homemade Dual-glow Luciferase Assay. *Journal of visualized experiments : JoVE*, doi:10.3791/50282 (2014).
243 Watanabe, N. & Mitchison, T. J. Single-Molecule Speckle Analysis of Actin Filament Turnover in Lamellipodia. *Science* **295**, 1083-1086, doi:10.1126/science.1067470 (2002).
244 Ingles-Prieto, A. *et al.* Light-assisted small-molecule screening against protein kinases. *Nat Chem Biol* **11**, 952-954, doi:10.1038/nchembio.1933 (2015).
245 Muller, K. & Weber, W. Optogenetic tools for mammalian systems. *Molecular bioSystems* **9**, 596-608, doi:10.1039/c3mb25590e (2013).
246 Reichhart, E., Ingles-Prieto, A., Tichy, A. M., McKenzie, C. & Janovjak, H. A Phytochrome Sensory Domain Permits Receptor Activation by Red Light. *Angew Chem Int Ed Engl* **55**, 6339-6342, doi:10.1002/anie.201601736 (2016).
247 Wang, H. *et al.* LOVTRAP: an optogenetic system for photoinduced protein dissociation. *Nature methods* **13**, 755-758, doi:10.1038/nmeth.3926 (2016).
248 Zhou, X. X., Chung, H. K., Lam, A. J. & Lin, M. Z. Optical control of protein activity by fluorescent protein domains. *Science* **338**, 810-814, doi:10.1126/science.1226854 (2012).
249 Kutta, R. J. *et al.* The photochemical mechanism of a B12-dependent photoreceptor protein. *Nat Commun* **6**, 7907, doi:10.1038/ncomms8907 (2015).
250 Takano, H., Obitsu, S., Beppu, T. & Ueda, K. Light-induced carotenogenesis in Streptomyces coelicolor A3(2): identification of an extracytoplasmic function sigma factor that directs photodependent transcription of the carotenoid biosynthesis gene cluster. *J Bacteriol* **187**, 1825-1832, doi:10.1128/JB.187.5.1825-1832.2005 (2005).
251 Banerjee, R. B12 trafficking in mammals: A for coenzyme escort service. *ACS Chem Biol* **1**, 149-159, doi:10.1021/cb6001174 (2006).
252 in *Dietary Reference Intakes for Thiamin, Riboflavin, Niacin, Vitamin B6, Folate, Vitamin B12, Pantothenic Acid, Biotin, and Choline The National Academies Collection: Reports funded by National Institutes of Health* (1998).
253 Carmel, R. Current concepts in cobalamin deficiency. *Annual review of medicine* **51**, 357-375, doi:10.1146/annurev.med.51.1.357 (2000).
254 Zittoun, J. & Zittoun, R. Modern clinical testing strategies in cobalamin and folate deficiency. *Seminars in hematology* **36**, 35-46 (1999).
255 Watanabe, N. & Mitchison, T. J. Single-molecule speckle analysis of actin filament turnover in lamellipodia. *Science* **295**, 1083-1086, doi:10.1126/science.1067470 (2002).
256 Schneider, Z. & Stroiński, A. *Comprehensive B12 : chemistry, biochemistry, nutrition, ecology, medicine*. 58 (De Gruyter, 1987).
257 Baker, J. M. & Boyce, F. M. High-throughput functional screening using a homemade dual-glow luciferase assay. *Journal of visualized experiments : JoVE*, doi:10.3791/50282 (2014).
258 Nagai, T. *et al.* A variant of yellow fluorescent protein with fast and efficient maturation for cell-biological applications. *Nature biotechnology* **20**, 87-90, doi:10.1038/nbt0102-87 (2002).
259 Kimmel, C. B., Ballard, W. W., Kimmel, S. R., Ullmann, B. & Schilling, T. F. Stages of embryonic development of the zebrafish. *Developmental dynamics : an official publication of the American Association of Anatomists* **203**, 253-310, doi:10.1002/aja.1002030302 (1995).
260 Westerfield, M. *The zebrafish book. A guide for the laboratory use of zebrafish (Danio rerio)*. 4th edn, (Univ. of Oregon Press, 2000).

261 Schlessinger, J. Cell signaling by receptor tyrosine kinases. *Cell* **103**, 211-225 (2000).
262 Bryant, D. M., Wylie, F. G. & Stow, J. L. Regulation of endocytosis, nuclear translocation, and signaling of fibroblast growth factor receptor 1 by E-cadherin. *Molecular biology of the cell* **16**, 14-23, doi:10.1091/mbc.E04-09-0845 (2005).
263 Ota, S., Tonou-Fujimori, N. & Yamasu, K. The roles of the FGF signal in zebrafish embryos analyzed using constitutive activation and dominant-negative suppression of different FGF receptors. *Mechanisms of development* **126**, 1-17, doi:10.1016/j.mod.2008.10.008 (2009).
264 Turner, N. & Grose, R. Fibroblast growth factor signalling: from development to cancer. *Nature reviews. Cancer* **10**, 116-129, doi:10.1038/nrc2780 (2010).
265 Marianayagam, N. J., Sunde, M. & Matthews, J. M. The power of two: protein dimerization in biology. *Trends Biochem Sci* **29**, 618-625, doi:10.1016/j.tibs.2004.09.006 (2004).
266 Chen, J., Zheng, X. F., Brown, E. J. & Schreiber, S. L. Identification of an 11-kDa FKBP12-rapamycin-binding domain within the 289-kDa FKBP12-rapamycin-associated protein and characterization of a critical serine residue. *Proc Natl Acad Sci U S A* **92**, 4947-4951, doi:10.1073/pnas.92.11.4947 (1995).
267 Kolos, J. M., Voll, A. M., Bauder, M. & Hausch, F. FKBP Ligands-Where We Are and Where to Go? *Front Pharmacol* **9**, 1425, doi:10.3389/fphar.2018.01425 (2018).
268 Keenan, T. *et al.* Synthesis and activity of bivalent FKBP12 ligands for the regulated dimerization of proteins. *Bioorg Med Chem* **6**, 1309-1335, doi:10.1016/s0968-0896(98)00125-4 (1998).
269 Yang, W. *et al.* Investigating protein-ligand interactions with a mutant FKBP possessing a designed specificity pocket. *J Med Chem* **43**, 1135-1142, doi:10.1021/jm9904396 (2000).
270 Braun, P. D. *et al.* A bifunctional molecule that displays context-dependent cellular activity. *J Am Chem Soc* **125**, 7575-7580, doi:10.1021/ja035176q (2003).
271 Sellmyer, M. A., Stankunas, K., Briesewitz, R., Crabtree, G. R. & Wandless, T. J. Engineering small molecule specificity in nearly identical cellular environments. *Bioorg Med Chem Lett* **17**, 2703-2705, doi:10.1016/j.bmcl.2007.03.012 (2007).
272 Gestwicki, J. E., Crabtree, G. R. & Graef, I. A. Harnessing chaperones to generate small-molecule inhibitors of amyloid beta aggregation. *Science* **306**, 865-869, doi:10.1126/science.1101262 (2004).
273 Gargett, T. & Brown, M. P. The inducible caspase-9 suicide gene system as a "safety switch" to limit on-target, off-tumor toxicities of chimeric antigen receptor T cells. *Front Pharmacol* **5**, 235, doi:10.3389/fphar.2014.00235 (2014).
274 Hathaway, N. A. *et al.* Dynamics and memory of heterochromatin in living cells. *Cell* **149**, 1447-1460, doi:10.1016/j.cell.2012.03.052 (2012).
275 Inoue, T., Heo, W. D., Grimley, J. S., Wandless, T. J. & Meyer, T. An inducible translocation strategy to rapidly activate and inhibit small GTPase signaling pathways. *Nature methods* **2**, 415-418, doi:10.1038/nmeth763 (2005).
276 Putyrski, M. & Schultz, C. Switching heterotrimeric G protein subunits with a chemical dimerizer. *Chem Biol* **18**, 1126-1133, doi:10.1016/j.chembiol.2011.07.013 (2011).
277 Szentpetery, Z., Varnai, P. & Balla, T. Acute manipulation of Golgi phosphoinositides to assess their importance in cellular trafficking and signaling. *Proc Natl Acad Sci U S A* **107**, 8225-8230, doi:10.1073/pnas.1000157107 (2010).
278 Johnston, J. *et al.* Regulated expression of erythropoietin from an AAV vector safely improves the anemia of beta-thalassemia in a mouse model. *Mol Ther* **7**, 493-497, doi:10.1016/s1525-0016(03)00043-1 (2003).
279 Matsumoto, D., Tamamura, H. & Nomura, W. TALEN-Based Chemically Inducible, Dimerization-Dependent, Sequence-Specific Nucleases. *Biochemistry*, doi:10.1021/acs.biochem.9b00798 (2019).
280 Tebo, A. G. & Gautier, A. A split fluorescent reporter with rapid and reversible complementation. *Nat Commun* **10**, 2822, doi:10.1038/s41467-019-10855-0 (2019).

281 Barrero, J. J., Papanikou, E., Casler, J. C., Day, K. J. & Glick, B. S. An improved reversibly dimerizing mutant of the FK506-binding protein FKBP. *Cell Logist* **6**, e1204848, doi:10.1080/21592799.2016.1204848 (2016).
282 Feng, S. *et al.* A rapidly reversible chemical dimerizer system to study lipid signaling in living cells. *Angew Chem Int Ed Engl* **53**, 6720-6723, doi:10.1002/anie.201402294 (2014).
283 Schifferer, M., Feng, S., Stein, F. & Schultz, C. Reversible Chemical Dimerization by rCD1. *Methods Enzymol* **583**, 173-195, doi:10.1016/bs.mie.2016.10.035 (2017).
284 Ahmed, F. H. *et al.* Sequence-Structure-Function Classification of a Catalytically Diverse Oxidoreductase Superfamily in Mycobacteria. *J Mol Biol* **427**, 3554-3571, doi:10.1016/j.jmb.2015.09.021 (2015).
285 Ney, B. *et al.* The methanogenic redox cofactor F420 is widely synthesized by aerobic soil bacteria. *ISME J* **11**, 125-137, doi:10.1038/ismej.2016.100 (2017).
286 Taylor, M., Scott, C. & Grogan, G. F420-dependent enzymes - potential for applications in biotechnology. *Trends Biotechnol* **31**, 63-64, doi:10.1016/j.tibtech.2012.09.003 (2013).
287 Kainrath, S., Stadler, M., Reichhart, E., Distel, M. & Janovjak, H. Green-Light-Induced Inactivation of Receptor Signaling Using Cobalamin-Binding Domains. *Angewandte Chemie International Edition* **56**, 4608-4611, doi:10.1002/anie.201611998 (2017).
288 Riss, T. L. *et al.* in *Assay Guidance Manual* (eds G. S. Sittampalam *et al.*) (2004).
289 Dietmair, S. *et al.* A multi-omics analysis of recombinant protein production in Hek293 cells. *PLoS One* **7**, e43394, doi:10.1371/journal.pone.0043394 (2012).
290 Antoney, J. & Jackson, C. J. (Australian National University Research School of Chemistry, Acton, Australia, 2019).
291 Huhner, J., Ingles-Prieto, A., Neususs, C., Lammerhofer, M. & Janovjak, H. Quantification of riboflavin, flavin mononucleotide, and flavin adenine dinucleotide in mammalian model cells by CE with LED-induced fluorescence detection. *Electrophoresis* **36**, 518-525, doi:10.1002/elps.201400451 (2015).
292 Ornitz, D. M. & Itoh, N. The Fibroblast Growth Factor signaling pathway. *Wiley Interdiscip Rev Dev Biol* **4**, 215-266, doi:10.1002/wdev.176 (2015).
293 Muthuswamy, S. K., Gilman, M. & Brugge, J. S. Controlled dimerization of ErbB receptors provides evidence for differential signaling by homo- and heterodimers. *Mol Cell Biol* **19**, 6845-6857, doi:10.1128/mcb.19.10.6845 (1999).
294 An, S. & Fu, L. Small-molecule PROTACs: An emerging and promising approach for the development of targeted therapy drugs. *EBioMedicine* **36**, 553-562, doi:10.1016/j.ebiom.2018.09.005 (2018).
295 Jacobs, C. L., Badiee, R. K. & Lin, M. Z. StaPLs: versatile genetically encoded modules for engineering drug-inducible proteins. *Nature methods* **15**, 523-526, doi:10.1038/s41592-018-0041-z (2018).
296 Tague, E. P., Dotson, H. L., Tunney, S. N., Sloas, D. C. & Ngo, J. T. Chemogenetic control of gene expression and cell signaling with antiviral drugs. *Nature methods* **15**, 519-522, doi:10.1038/s41592-018-0042-y (2018).
297 Foight, G. W. *et al.* Multi-input chemical control of protein dimerization for programming graded cellular responses. *Nature biotechnology* **37**, 1209-1216, doi:10.1038/s41587-019-0242-8 (2019).
298 Umeda, N., Ueno, T., Pohlmeyer, C., Nagano, T. & Inoue, T. A photocleavable rapamycin conjugate for spatiotemporal control of small GTPase activity. *J Am Chem Soc* **133**, 12-14, doi:10.1021/ja108258d (2011).
299 Courtney, T. M., Horst, T. J., Hankinson, C. P. & Deiters, A. Synthesis and application of light-switchable arylazopyrazole rapamycin analogs. *Org Biomol Chem* **17**, 8348-8353, doi:10.1039/c9ob01719d (2019).

300 Makarenkova, H. P. *et al.* Differential interactions of FGFs with heparan sulfate control gradient formation and branching morphogenesis. *Sci Signal* **2**, ra55, doi:10.1126/scisignal.2000304 (2009).
301 Lamparter, T., Esteban, B. & Hughes, J. Phytochrome Cph1 from the cyanobacterium Synechocystis PCC6803. Purification, assembly, and quaternary structure. *Eur J Biochem* **268**, 4720-4730, doi:10.1046/j.1432-1327.2001.02395.x (2001).
302 Jacques, S. L. Optical properties of biological tissues: a review. *Phys Med Biol* **58**, R37-61, doi:10.1088/0031-9155/58/11/R37 (2013).
303 Kravitz, A. V. & Kreitzer, A. C. Optogenetic manipulation of neural circuitry in vivo. *Curr Opin Neurobiol* **21**, 433-439, doi:10.1016/j.conb.2011.02.010 (2011).
304 Sidor, M. M. *et al.* In vivo optogenetic stimulation of the rodent central nervous system. *Journal of visualized experiments : JoVE*, 51483, doi:10.3791/51483 (2015).
305 Montgomery, K. L. *et al.* Wirelessly powered, fully internal optogenetics for brain, spinal and peripheral circuits in mice. *Nature methods* **12**, 969-974, doi:10.1038/nmeth.3536 (2015).
306 Tsien, R. Y. A non-disruptive technique for loading calcium buffers and indicators into cells. *Nature* **290**, 527-528, doi:10.1038/290527a0 (1981).
307 Esensten, J. H., Bluestone, J. A. & Lim, W. A. Engineering Therapeutic T Cells: From Synthetic Biology to Clinical Trials. *Annu Rev Pathol* **12**, 305-330, doi:10.1146/annurev-pathol-052016-100304 (2017).

Appendix

Table 3: Codon-optimized sequences of CBDs and 2027.

Name	Sequence
MxCBD	CCACACGCAGAGACTTGGAGGGAATCTATGCTTGCCGCCACACAAGCCTACGACCAGCCTAGAG TATCAGATGTACTGGATGAGGTCCTTGCGGCTCTGCCCCCTCTGAAGGCCTTCGATGAAGTGCTG GCCCCTTTGCTGTGCGATGTCGGAGAGCGGTGGGAGAGCGGAACCCTGACAGTTGCGCAGGAA CATCTGGTCTCACAGATGGTGCGCGCCCGGCTGGTGAGTCTGCTGCACGCGGCACCATTGGGAC GCCACAGACATGGCGTTCTCGCCTGTTTCCCAGAGGAGGAGCATGAGATGGGCTTGCTTGGTGC CGCCTTGAGACTCCGCCATCTCGGCGTTAGAGTAACCCTGCTCGGCCAGCGAGTGCCAGCCGAG GACCTCGGGCGAGCAGTGTTGGCCCTGCGCCCGGACTTCGTGGGCCTGTCAACAGTTGCAAGCA GGAGCGCAGAGGACTTCGAGGATACCTTGACCCGACTCCGCCAGGCCCTGCCAAGGGGCCTCCC TGTATGGGTGGGCGGGGCAGCCGCAAGGTCTCATCAGGCCGTGTGCGAGCGCCTGGCAGTCCA TGTTTTTCAGGGCGAAGAAGATTGGGATAGACTTGCCGGAACA
TtCBD	CCCGAGGACCTCGGCACCGGACTCCTCGAAGCACTCTTGAGAGGAGATTTGGCCGGCGCCGAG GCTCTCTTTCGACGGGGGCTTAGGTTTTGGGGACCCGAGGGTATTCTGGAGCACCTGCTCCTGC CTGTGCTTCGGGAGGTGGGAGAAGCCTGGCATCGCGGCGAGATCGGTGTGGCCGAGGAGCAT CTGGCATCCACATTTCTGCGCGCGAGACTGCAGGAGCTGCTCGACCTCGCCGGGTTCCCACCTG GCCCCCCCGTGCTGGTAACCACGCCACCAGGGGAGAGGCACGAGATCGGCGCAATGTTGGCTG CCTATCACCTGCGAAGGAAGGGCGTGCCAGCGCTGTACTTGGGACCAGACACCCCCCTCCCCGA TCTCAGAGCACTTGCGAGACGGCTCGGAGCCGGAGCGGTGGTTCTGTCAGCTTTGCTTTCCGAG CCTCTCAGGGCGTTGCCAGACGGCGCACTGAAAGACTTGGCACCTCGGGTGTTCCTGGGAGGG CAAGGAGCCGGCCCTGAAGAGGCCCGACGGCTCGGGGCCGAGTACATGGAAGATCTGAAGGG ATTGGCCGAAGCACTGTGGCTTCCAAGAGGACCAGAGAAAGAAGCAATC
CDD	ACAGATGCGGAACTTTCCCCTACTGACTGGGTGCGCGAGCAGACGGAGAGAATCCTTGAACAA GGCACAACTGATGGGGTGCATGTCCTTGATCGGCCCATAGTACTTTTCACGACGACGGGAGCCA AAAGCGGTAAGAAACGCTATGTGCCTTTGATGCGGGTAGAGGAGAACGGCAAGTACGCTATGG TCGCTTCTAAGGGAGGCGACCCCAAGCACCCCTCCTGGTACTTCAATGTTAAAGCTAACCCTACA GTGTCCGTTCAGGATGGGGACAAAGTTCTCCCCGATAGGACTGCCCGAGAGTTGGAAGGCGAG GAGAGAGAGCACTGGTGGAAGTTGGCTGTAGAGGCGTACCCTCCCTATGCTGAATATCAAACCA AAACTGACCGCCTGATTCCAGTTTTCATAGTTGAG

Table 4: Oligonucleotides utilized for PCR. Restriction sites are underlined.

	Name	**Sequence**
1	MxCBD_F	GATCATACCGGTCCACACGCA
2	MxCBD_R	GATCATCCCGGGTGTTCCGGCA
3	TtCBD_F	GATCATACCGGTCCCGAGGACCT
4	TtCBD_R	GATCATCCCGGGGATTGCTTCTTT
5	IgG_F	GACGACCGGTGAGCCCAAATCTTCTGACAAAACTCAC
6	IgG_R	GATCACCGGTTTTACCCGGAGACAGGGAGAG
7	truncated CMV_pcDNA3.1(-)_F	TGGGAGGTCTATATAAGCAGAGC
8	truncated CMV_pcDNA3.1(-)_R	GGCGGGCCATTTACCGTAAG
9	mFGFR1_R195E_F	TACAGGCCCGGGAGCCTCCTGGGCTGGAGTACTGCTATAA
10	mFGFR1_R195E_R	TTATAGCAGTACTCCAGCCCAGGAGGCTCCCGGGCCTGTA
11	mFGFR1-TtCBD_H497A_F	GAGAAGCCTGGGCTCGCGGCGAGAT
12	mFGFR1-TtCBD_H497A_R	ATCTCGCCGCGAGCCCAGGCTTCTC
13	mFGFR1-MxCBD_E499H_F	GAGAGCGGTGGCACAGCGGAACCCT
14	mFGFR1-MxCBD_E499H_R	AGGGTTCCGCTGTGCCACCGCTCTC
15	2027_ClaI_F	GATCATATCGATACAGATGCGGAACTTTCCCCTACTGACT
16	2027_ClaI_R	GATCATATCGATCTCAACTATGAAAACTGGAATCAGGCGGTCAGT
17	2027_AgeI_F	GATCATACCGGTACAGATGCGGAACTTTCCCCTACTGACT
18	2027_XmaI_R	GATCATCCCGGGTCAACTATGAAAACTGGAATCAGGCGGTCAGT
19	P75_ClaI_F	GATCATATCGATAAAGAAGCATGCCCAACTGGACTCTACAC
20	Sp_ClaI_R	GATCATATCGATTGCTCCACCCAGGGACACT
21	mFGFR1_R599E_ F	GTATCTACAGGCCCGGGAGCCTCCTGGGCTGGAG
22	mFGFR1_R599E_R	CTCCAGCCCAGGAGGCTCCCGGGCCTGTAGATAC
23	IgG_AgeI_F	GATCATACCGGTGAGCCCAAATCTTCTGACAAAACTCACACAT
24	IgG_AgeI_R	GATCATACCGGTTTTACCCGGAGACAGGGAGAGG
25	2027_HindIII_F	AGTCAAGCTTACCATGGCCACCGGTACA
26	FKBP_HindIII_F	AGTCAAGCTTACCATGGCCACCGGTAAAC

Table 5: Protein sequences of full length proteins (NCBI Reference Sequence given in brackets), CBDs, receptors, and fluorescent fusion proteins

Name	**Sequence**
MxCarH (CAA79965.2)	MAERTYRINIAAELAGVRVELIRAWERRYGVLTPRRTPAGYRAYTDRDVAVLKQLKRLT DEGVAISEAAKLLPQLMEGLEAEVAGRGASQDARPHAETWRESMLAATQAYDQPRVS DVLDEVLAALPPLKAFDEVLAPLLCDVGERWESGTLTVAQEHLVSQMVRARLVSLLHAA PLGRHRHGVLACFPEEEHEMGLLGAALRLRHLGVRVTLLGQRVPAEDLGRAVLALRPDF VGLSTVASRSAEDFEDTLTRLRQALPRGLPVWVGGAAARSHQAVCERLAVHVFQGEED WDRLAGT
MxCBD	HAETWRESMLAATQAYDQPRVSDVLDEVLAALPPLKAFDEVLAPLLCDVGERWESGTL TVAQEHLVSQMVRARLVSLLHAAPLGRHRHGVLACFPEEEHEMGLLGAALRLRHLGVR VTLLGQRVPAEDLGRAVLALRPDFVGLSTVASRSAEDFEDTLTRLRQALPRGLPVWVGG AAARSHQAVCERLAVHVFQGEEDWDRLAGT
TtCarH (WP_038030370.1)	MTSSGVYTIAEVEAMTGLSAEALRQWERRYGFPKPRRTPGGHRLYSAEDVEALKTIKR WLEEGATPKAAIRRYLAQGVRPEDLGTGLLEALLRGDLAGAEALFRRGLRFWGPEGILE HLLLPVLREVGEAWHRGEIGVAEEHLASTFLRARLQELLDLAGFPPGPPVLVTTPPGERH EIGAMLAAYHLRRKGVPALYLGPDTPLPDLRALARRLGAGAVVLSALLSEPLRALPDGAL KDLAPRVFLGGQGAGPEEARRLGAEYMEDLKGLAEALWLPRGPEKEAI
TtCBD	PEDLGTGLLEALLRGDLAGAEALFRRGLRFWGPEGILEHLLLPVLREVGEAWHRGEIGVA EEHLASTFLRARLQELLDLAGFPPGPPVLVTTPPGERHEIGAMLAAYHLRRKGVPALYLG PDTPLPDLRALARRLGAGAVVLSALLSEPLRALPDGALKDLAPRVFLGGQGAGPEEARRL GAEYMEDLKGLAEALWLPRGPEKEAI
mFGFR1-MxCBD	MGSSKSKPKDPSQRLDMKSGTKKSDFHSQMAVHKLAKSIPLRRQVTVSADSSASMNS GVLLVRPSRLSSSGTPMLAGVSEYELPEDPRWELPRDRLVLGKPLGEGCFGQVVLAEAIG LDKDKPNRVTKVAVKMLKSDATEKDLSDLISEMEMMKMIGKHKNIINLLGACTQDGPL YVIVEYASKGNLREYLQARRPPGLEYCYNPSHNPEEQLSSKDLVSCAYQVARGMEYLASK KCIHRDLAARNVLVTEDNVMKIADFGLARDIHHIDYYKKTTNGRLPVKWMAPEALFDRI YTHQSDVWSFGVLLWEIFTLGGSPYPGVPVEELFKLLKEGHRMDKPSNCTNELYMMMM RDCWHAVPSQRPTFKQLVEDLDRIVALTSNQEYLDLSIPLDQYSPSFPDTRSSTCSSGED SVFSHEPLPEEPCLPRHPTQLANSGLKRRVETGPHAETWRESMLAATQAYDQPRVSDV LDEVLAALPPLKAFDEVLAPLLCDVGERWESGTLTVAQEHLVSQMVRARLVSLLHAAPL GRHRHGVLACFPEEEHEMGLLGAALRLRHLGVRVTLLGQRVPAEDLGRAVLALRPDFV GLSTVASRSAEDFEDTLTRLRQALPRGLPVWVGGAAARSHQAVCERLAVHVFQGEED WDRLAGTPGGSGVDYPYDVPDYALD

mFGFR1-TtCBD	MGSSKSKPKDPSQRLDMKSGTKKSDFHSQMAVHKLAKSIPLRRQVTVSADSSASMNS GVLLVRPSRLSSSGTPMLAGVSEYELPEDPRWELPRDRLVLGKPLGEGCFGQVVLAEAIG LDKDKPNRVTKVAVKMLKSDATEKDLSDLISEMEMMKMIGKHKNIINLLGACTQDGPL YVIVEYASKGNLREYLQARRPPGLEYCYNPSHNPEEQLSSKDLVSCAYQVARGMEYLASK KCIHRDLAARNVLVTEDNVMKIADFGLARDIHHIDYYKKTTNGRLPVKWMAPEALFDRI YTHQSDVWSFGVLLWEIFTLGGSPYPGVPVEELFKLLKEGHRMDKPSNCTNELYMMM RDCWHAVPSQRPTFKQLVEDLDRIVALTSNQEYLDLSIPLDQYSPSFPDTRSSTCSSGED SVFSHEPLPEEPCLPRHPTQLANSGLKRRVETGPEDLGTGLLEALLRGDLAGAEALFRRGL RFWGPEGILEHLLLPVLREVGEAWHRGEIGVAEEHLASTFLRARLQELLDLAGFPPGPPV LVTTPPGERHEIGAMLAAYHLRRKGVPALYLGPDTPLPDLRALARRLGAGAVVLSALLSE PLRALPDGALKDLAPRVFLGGQGAGPEEARRLGAEYMEDLKGLAEALWLPRGPEKEAIP GGSGVDYPYDVPDYALD
mFGFR1-IgG	MGSSKSKPKDPSQRLDMKSGTKKSDFHSQMAVHKLAKSIPLRRQVTVSADSSASMNS GVLLVRPSRLSSSGTPMLAGVSEYELPEDPRWELPRDRLVLGKPLGEGCFGQVVLAEAIG LDKDKPNRVTKVAVKMLKSDATEKDLSDLISEMEMMKMIGKHKNIINLLGACTQDGPL YVIVEYASKGNLREYLQARRPPGLEYCYNPSHNPEEQLSSKDLVSCAYQVARGMEYLASK KCIHRDLAARNVLVTEDNVMKIADFGLARDIHHIDYYKKTTNGRLPVKWMAPEALFDRI YTHQSDVWSFGVLLWEIFTLGGSPYPGVPVEELFKLLKEGHRMDKPSNCTNELYMMM RDCWHAVPSQRPTFKQLVEDLDRIVALTSNQEYLDLSIPLDQYSPSFPDTRSSTCSSGED SVFSHEPLPEEPCLPRHPTQLANSGLKRRVETGEPKSSDKTHTCPPCPAPELLGGPSVFLF PPKPKDTLMISRTPEVTCVVVDVSHEDPEVKFNWYVDGVEVHNAKTKPREEQYNSTYR VVSVLTVLHQDWLNGKEYKCKVSNKALPAPIEKTISKAKGQPREPQVYTLPPSRDELTKN QVSLTCLVKGFYPSDIAVEWESNGQPENNYKTTPPVLDSDGSFFLYSKLTVDKSRWQQG NVFSCSVMHEALHNHYTQKSLSLSPGKTGGSGVDYPYDVPDYALD
mV-MxCBD	MVSKGEELFTGVVPILVELDGDVNGHKFSVSGEGEGDATYGKLTLKLICTTGKLPVPWPT LVTTLGYGLQCFARYPDHMKQHDFFKSAMPEGYVQERTIFFKDDGNYKTRAEVKFEGD TLVNRIELKGIDFKEDGNILGHKLEYNYNSHNVYITADKQKNGIKANFKIRHNIEDGGVQL ADHYQQNTPIGDGPVLLPDNHYLSYQSKLSKDPNEKRDHMVLLEFVTAAGITLGMDEL YKGSSGSSGPHAETWRESMLAATQAYDQPRVSDVLDEVLAALPPLKAFDEVLAPLLCDV GERWESGTLTVAQEHLVSQMVRARLVSLLHAAPLGRHRHGVLACFPEEEHEMGLLGA ALRLRHLGVRVTLLGQRVPAEDLGRAVLALRPDFVGLSTVASRSAEDFEDTLTRLRQALP RGLPVWVGGAAARSHQAVCERLAVHVFQGEEDWDRLAGTPG
mV-TtCBD	MVSKGEELFTGVVPILVELDGDVNGHKFSVSGEGEGDATYGKLTLKLICTTGKLPVPWPT LVTTLGYGLQCFARYPDHMKQHDFFKSAMPEGYVQERTIFFKDDGNYKTRAEVKFEGD

	TLVNRIELKGIDFKEDGNILGHKLEYNYNSHNVYITADKQKNGIKANFKIRHNIEDGGVQL ADHYQQNTPIGDGPVLLPDNHYLSYQSKLSKDPNEKRDHMVLLEFVTAAGITLGMDEL YKGSSGSSGPEDLGTGLLEALLRGDLAGAEALFRRGLRFWGPEGILEHLLLPVLREVGEA WHRGEIGVAEEHLASTFLRARLQELLDLAGFPPGPPVLVTTPPGERHEIGAMLAAYHLR RKGVPALYLGPDTPLPDLRALARRLGAGAVVLSALLSEPLRALPDGALKDLAPRVFLGGQ GAGPEEARRLGAEYMEDLKGLAEALWLPRGPEKEAIPG
MSMEG_2027 (UniProt A0QU01) / CDD	TDAELSPTDWVREQTERILEQGTTDGVHVLDRPIVLFTTTGAKSGKKRYVPLMRVEENG KYAMVASKGGDPKHPSWYFNVKANPTVSVQDGDKVLPDRTARELEGEEREHWWKLA VEAYPPYAEYQTKTDRLIPVFIVE
CDD_mV	MSGTDAELSPTDWVREQTERILEQGTTDGVHVLDRPIVLFTTTGAKSGKKRYVPLMRVE ENGKYAMVASKGGDPKHPSWYFNVKANPTVSVQDGDKVLPDRTARELEGEEREHW WKLAVEAYPPYAEYQTKTDRLIPVFIVEPGGSSGSVSKGEELFTGVVPILVELDGDVNGH KFSVSGEGEGDATYGKLTLKLICTTGKLPVPWPTLVTTLGYGLQCFARYPDHMKQHDFF KSAMPEGYVQERTIFFKDDGNYKTRAEVKFEGDTLVNRIELKGIDFKEDGNILGHKLEYN YNSHNVYITADKQKNGIKANFKIRHNIEDGGVQLADHYQQNTPIGDGPVLLPDNHYLSY QSKLSKDPNEKRDHMVLLEFVTAAGITLGMDELYK
mV_CDD	MVSKGEELFTGVVPILVELDGDVNGHKFSVSGEGEGDATYGKLTLKLICTTGKLPVPWPT LVTTLGYGLQCFARYPDHMKQHDFFKSAMPEGYVQERTIFFKDDGNYKTRAEVKFEGD TLVNRIELKGIDFKEDGNILGHKLEYNYNSHNVYITADKQKNGIKANFKIRHNIEDGGVQL ADHYQQNTPIGDGPVLLPDNHYLSYQSKLSKDPNEKRDHMVLLEFVTAAGITLGMDEL YKGSSGSSGTDAELSPTDWVREQTERILEQGTTDGVHVLDRPIVLFTTTGAKSGKKRYVP LMRVEENGKYAMVASKGGDPKHPSWYFNVKANPTVSVQDGDKVLPDRTARELEGEE REHWWKLAVEAYPPYAEYQTKTDRLIPVFIVEPG
p75_FGFR1	MGAGATGRAMDGPRLLLLLLLGVSLGGAIDKEACPTGLYTHSGECCKACNLGEGVAQP CGANQTVCEPCLDSVTFSDVVSATEPCKPCTECVGLQSMSAPCVEADDAVCRCAYGYY QDETTGRCEACRVCEAGSGLVFSCQDKQNTVCEECPDGTYSDEANHVDPCLPCTVCED TERQLRECTRWADAECEEIPGRWITRSTPPEGSDSTAPSTQEPEAPPEQDLIASTVAGVV TTVMGSSQPVVTRGTTDNLIPVYCSILAAVVVGLVAYIAFKRGRAMKSGTKKSDFHSQM AVHKLAKSIPLRRQVTVSADSSASMNSGVLLVRPSRLSSSGTPMLAGVSEYELPEDPRW ELPRDRLVLGKPLGEGCFGQVVLAEAIGLDKDKPNRVTKVAVKMLKSDATEKDLSDLISE MEMMKMIGKHKNIINLLGACTQDGPLYVIVEYASKGNLREYLQARRPPGLEYCYNPSH NPEEQLSSKDLVSCAYQVARGMEYLASKKCIHRDLAARNVLVTEDNVMKIADFGLARDI HHIDYYKKTTNGRLPVKWMAPEALFDRIYTHQSDVWSFGVLLWEIFTLGGSPYPGVPV EELFKLLKEGHRMDKPSNCTNELYMMMRDCWHAVPSQRPTFKQLVEDLDRIVALTSN

	QEYLDLSIPLDQYSPSFPDTRSSTCSSGEDSVFSHEPLPEEPCLPRHPTQLANSGLKRRVET GGSGVDYPYDVPDYALD
CDD_FGFR1	MGAGATGRAMDGPRLLLLLLLGVSLGGAIDTDAELSPTDWVREQTERILEQGTTDGVH VLDRPIVLFTTTGAKSGKKRYVPLMRVEENGKYAMVASKGGDPKHPSWYFNVKANPTV SVQDGDKVLPDRTARELEGEEREHWWKLAVEAYPPYAEYQTKTDRLIPVFIVEIDKEACP TGLYTHSGECCKACNLGEGVAQPCGANQTVCEPCLDSVTFSDVVSATEPCKPCTECVGL QSMSAPCVEADDAVCRCAYGYYQDETTGRCEACRVCEAGSGLVFSCQDKQNTVCEEC PDGTYSDEANHVDPCLPCTVCEDTERQLRECTRWADAECEEIPGRWITRSTPPEGSDST APSTQEPEAPPEQDLIASTVAGVVTTVMGSSQPVVTRGTTDNLIPVYCSILAAVVVGLVA YIAFKRGRAMKSGTKKSDFHSQMAVHKLAKSIPLRRQVTVSADSSASMNSGVLLVRPSR LSSSGTPMLAGVSEYELPEDPRWELPRDRLVLGKPLGEGCFGQVVLAEAIGLDKDKPNR VTKVAVKMLKSDATEKDLSDLISEMEMMKMIGKHKNIINLLGACTQDGPLYVIVEYASK GNLREYLQARRPPGLEYCYNPSHNPEEQLSSKDLVSCAYQVARGMEYLASKKCIHRDLA ARNVLVTEDNVMKIADFGLARDIHHIDYYKKTTNGRLPVKWMAPEALFDRIYTHQSDV WSFGVLLWEIFTLGGSPYPGVPVEELFKLLKEGHRMDKPSNCTNELYMMMRDCWHA VPSQRPTFKQLVEDLDRIVALTSNQEYLDLSIPLDQYSPSFPDTRSSTCSSGEDSVFSHEPL PEEPCLPRHPTQLANSGLKRRVETGGSGVDYPYDVPDYALD
CDD_FGFR1_R599E	MGAGATGRAMDGPRLLLLLLLGVSLGGAIDTDAELSPTDWVREQTERILEQGTTDGVH VLDRPIVLFTTTGAKSGKKRYVPLMRVEENGKYAMVASKGGDPKHPSWYFNVKANPTV SVQDGDKVLPDRTARELEGEEREHWWKLAVEAYPPYAEYQTKTDRLIPVFIVEIDKEACP TGLYTHSGECCKACNLGEGVAQPCGANQTVCEPCLDSVTFSDVVSATEPCKPCTECVGL QSMSAPCVEADDAVCRCAYGYYQDETTGRCEACRVCEAGSGLVFSCQDKQNTVCEEC PDGTYSDEANHVDPCLPCTVCEDTERQLRECTRWADAECEEIPGRWITRSTPPEGSDST APSTQEPEAPPEQDLIASTVAGVVTTVMGSSQPVVTRGTTDNLIPVYCSILAAVVVGLVA YIAFKRGRAMKSGTKKSDFHSQMAVHKLAKSIPLRRQVTVSADSSASMNSGVLLVRPSR LSSSGTPMLAGVSEYELPEDPRWELPRDRLVLGKPLGEGCFGQVVLAEAIGLDKDKPNR VTKVAVKMLKSDATEKDLSDLISEMEMMKMIGKHKNIINLLGACTQDGPLYVIVEYASK GNLREYLQAREPPGLEYCYNPSHNPEEQLSSKDLVSCAYQVARGMEYLASKKCIHRDLA ARNVLVTEDNVMKIADFGLARDIHHIDYYKKTTNGRLPVKWMAPEALFDRIYTHQSDV WSFGVLLWEIFTLGGSPYPGVPVEELFKLLKEGHRMDKPSNCTNELYMMMRDCWHA VPSQRPTFKQLVEDLDRIVALTSNQEYLDLSIPLDQYSPSFPDTRSSTCSSGEDSVFSHEPL PEEPCLPRHPTQLANSGLKRRVETGGSGVDYPYDVPDYALD
FGFR1_IgG	MGAGATGRAMDGPRLLLLLLLGVSLGGAIDKEACPTGLYTHSGECCKACNLGEGVAQP CGANQTVCEPCLDSVTFSDVVSATEPCKPCTECVGLQSMSAPCVEADDAVCRCAYGYY

	QDETTGRCEACRVCEAGSGLVFSCQDKQNTVCEECPDGTYSDEANHVDPCLPCTVCED TERQLRECTRWADAECEEIPGRWITRSTPPEGSDSTAPSTQEPEAPPEQDLIASTVAGVV TTVMGSSQPVVTRGTTDNLIPVYCSILAAVVVGLVAYIAFKRGRAMKSGTKKSDFHSQM AVHKLAKSIPLRRQVTVSADSSASMNSGVLLVRPSRLSSSGTPMLAGVSEYELPEDPRW ELPRDRLVLGKPLGEGCFGQVVLAEAIGLDKDKPNRVTKVAVKMLKSDATEKDLSDLISE MEMMKMIGKHKNIINLLGACTQDGPLYVIVEYASKGNLREYLQARRPPGLEYCYNPSH NPEEQLSSKDLVSCAYQVARGMEYLASKKCIHRDLAARNVLVTEDNVMKIADFGLARDI HHIDYYKKTTNGRLPVKWMAPEALFDRIYTHQSDVWSFGVLLWEIFTLGGSPYPGVPV EELFKLLKEGHRMDKPSNCTNELYMMMRDCWHAVPSQRPTFKQLVEDLDRIVALTSN QEYLDLSIPLDQYSPSFPDTRSSTCSSGEDSVFSHEPLPEEPCLPRHPTQLANSGLKRRVET GEPKSSDKTHTCPPCPAPELLGGPSVFLFPPKPKDTLMISRTPEVTCVVVDVSHEDPEVK FNWYVDGVEVHNAKTKPREEQYNSTYRVVSVLTVLHQDWLNGKEYKCKVSNKALPAPI EKTISKAKGQPREPQVYTLPPSRDELTKNQVSLTCLVKGFYPSDIAVEWESNGQPENNYK TTPPVLDSDGSFFLYSKLTVDKSRWQQGNVFSCSVMHEALHNHYTQKSLSLSPGKTGGS GVDYPYDVPDYALD